Glycogen metabolism influences embryonic segmentation and appendages outgrowth during *Tribolium castaneum* embryogenesis

Dissertation

for the award of the degree

"Doctor rerum naturalium" (Dr.rer.nat.)

of the Georg-August-Universität Göttingen

within the doctoral program biology

of the Georg-August University School of Science (GAUSS)

submitted by

Xuebin Wan

from Liaoning, China

Göttingen, 2021

Thesis Committee

Prof. Dr. Gregor Bucher (advisor)
Department of Evolutionary Developmental Genetics, Johann-Friedrich-Blumenbach-Institute of Zoology and Anthropology, Georg-August-University Göttingen

Prof. Dr. Jörg Großhans
Institute for Developmental Biochemistry, Medical School, Georg-August-University Göttingen

Dr. Gerd Vorbrüggen
Department of Molecular Cell Dynamics, Max-Planck-Institute for biophysical Chemistry, Georg-August-University Göttingen

Members of the Examination Board

First reviewer: Prof. Dr. Gregor Bucher
Department of Evolutionary Developmental Genetics, Johann-Friedrich-Blumenbach-Institute of Zoology and Anthropology, Georg-August-University Göttingen

Second reviewer: Dr. Gerd Vorbrüggen
Department of Molecular Cell Dynamics, Max-Planck-Institute for biophysical Chemistry, Georg-August-University Göttingen

Further members of the Examination Board

Prof. Dr. Ralf Heinrich
Department of Cellular Neurobiology, Schwann-Schleiden Research Center, Georg-August-University Göttingen

Prof. Dr. Ernst A. Wimmer
Department of Developmental Biology, Johann-Friedrich-Blumenbach-Institute of Zoology and Anthropology, Georg-August-University Göttingen

Prof. Dr. Jörg Großhans
Institute for Developmental Biochemistry, Medical School, Georg-August-University Göttingen

Prof. Dr. Daniel J. Jackson
Department of Geobiology, Courant Research Center, Georg-August-University Göttingen

Date of Oral Examination: 19.01.2022

Declaration

Herewith I declare, that I prepared the Dissertation

"Glycogen metabolism mediates embryonic segmentation and appendages outgrowth during *Tribolium castaneum* embryogenesis" has been written independently and with no other sources and aids than quoted.

_____ Göttingen, 22.12.2021

Xuebin Wan

To my Family

Acknowledgement

The PhD journey in Germany was an amazing and joyful experience in my life and it would not have been possible without the support and guidance of many wonderful people.

Firstly, I would like to express my sincere gratitude to my supervisor Prof. Dr. Gregor Bucher for his continuous guidance, encouragement, motivation, support and an endless supply of fascinating ideas. His levels of patience, immense knowledge, and ingenuity was something I will always keep aspiring to. He motivated me to come up with new insights and always provided helpful feedback. I truly enjoyed every moment we spent together for not only scientific discussions but also sharing many interesting aspects in history, culture and society.

I would like to thank the rest of my thesis committee, Prof. Dr. Jörg Großhans and Dr. Gerd Vorbrüggen for their insightful comments and encouraging words and thoughtful, but also for the hard questions which incented me to widen my research from various perspectives.

My sincere thanks also to Dr. Daniela Grossmann who introduced me into this project and constantly helped and guided my work. She was a good teacher who raised many precious points about my screening project.

I greatly acknowledge scientific help and support by Dominik Mühlen for being such a good lab colleague and friend. He took time out of his schedules to help me whenever I had questions.

I would like to thank all lab members of both departments for making me feel welcome in the lab and for their support throughout the project. I was grateful to Prof. Ernst A. Wimmer, Dr. Nico Posnien, Dr. Bicheng He, Dr. Salim Ansari, Dr. Vera Terblanche, Dr. Musa Dan'azumi Isah, Dr. Bibi Atika, Dr. Constanza Tapia Contreras, Dr. Hassan M.

M. Ahmed, Georg Christian, Bullinger, Ting Hsuan Lu, Xiaojuan Li, Dr. Jürgen Dönitz and many lab interns. I really enjoyed the time we had in the lab.

My heartfelt thanks and gratitude go to Elke Küster, Claudia Hinners, Beate Preitz, Birgit Rossi and Merle Eggers, for their technical assistance and support throughout the project. Particularly, Beate Preitz was kindly to teach me microscope operation and solve all microscope issues.

Outside the lab, very special thanks to my friends Wenjun Guo, Xiaoyan Zhang, Fangzheng Xu, Shuwen Shan, Jiaojiao Feng, Shoukun Zhang, Wanping Chen and Li Liu for providing me continuous support at all times, for bringing me so much fun.

I was also conveying my heartfelt thanks to China Scholarship Council (CSC), Georg-August-University School of Science (GAUSS), Göttingen University for the financial and project support.

Last and most importantly, I was extremely thankful to my parents whose constant love and support keep me motivated and confident. Deepest thanks to my wife, Dan Wang, for the unconditional love and support throughout the entire master, PhD time and every day.

Contents

1 Summary

Embryonic segmentation of arthropods is a dynamic biological process that produces an organism by pattern formation, morphogenesis and specification of corresponding cells. The involved genes have mostly been identified by their phenotypes in systematic mutagenesis screens in few model systems, such as *Drosophila melanogaster*. The candidate gene approach based on RNAi was used to compare the function of those genes in other arthropods but was not able to detect novel and unsuspected functions. The detection of novel gene functions by a hypothesis independent screen has been a major endeavor to fill this gap.

In this work, a large collection of knock-down experiments was analyzed for cuticle phenotypes indicating a function in embryogenesis and a subset was re-screened to confirm the phenotypes. However, respective systematic searches may have remained incomplete, because interference of some patterning genes caused embryonic death before cuticle formation. Therefore, such "empty egg phenotypes" without any recognizable cuticle structures had been screened for defects in red flour beetle *Tribolium castaneum* embryogenesis and two glycogen metabolism genes had been shown to produce patterning defects. Here, I showed that RNAi targeting two genes involved in glucose synthesis *Tc-GlyS* and *Tc-AGBE* led to segmentation and appendage defects ultimately leading to empty egg phenotypes. Indeed, loss of *Tc-GlyS* and *Tc-AGBE* resulted in malformed and asymmetrically absent stripes of segment polarity genes indicating issues with maintaining segmental boundaries. More specifically, the defects first affected posterior abdominal segments but later extended to the entire trunk while the growth zone and pair-rule gene expression appeared to remain intact. *Tc-dac* and *Tc-Sp8* expression marked medial portions of the appendages and were strongly affected while *Tc-Dll* and *Tc-Sp8* expression marked distal parts and remained intact in RNAi phenotypes. I tested the hypothesis that this effect of glycogen metabolism enzymes was via the *Glycogen synthase kinase 3* (*GSK-3*), which is known to be required for Wnt, Hh and Notch pathways, as well. I found that the effect was not

exclusively by one of these pathways. Taken together, I found that *Tc-GlyS* and *Tc-AGBE* functions were required for segmental boundary maintenance, axis elongation and appendages outgrowth thereby linking metabolism and patterning formation.

2 Introduction

2.1 Segment patterning in long germ-band and short germ-band insects

It is well known that segmentation and associated appendages of arthropods play multiple roles in insects to enable diverse functions such as feeding, movement, and reproduction (Hannibal and Patel, 2013). During growth and development of arthropods, serially reiterated segmental units are set up bearing a diversity of appendages, leading to the subdivision into morphologically distinct structures along anterior-posterior (A-P) and dorsal-ventral (D-V) axes. Establishment of early embryonic axes originate from maternal activities by different developmental strategies in different insects and vertebrates (Kimelman and Martin, 2012). In the long germ-band insect *Drosophila melanogaster*, the patterning of the A-P axis is determined simultaneously within syncytial blastoderm, depending on morphogenetic gradients of Bicoid (Bcd) and other regulatory factors such as Hunchback (Hb), Nanos (Nos), and Caudal (Cad) (Dahanukar and Wharton, 1996; Driever and Nüsslein-Volhard, 1988; Hülskamp et al., 1990; Macdonald and Struhl, 1986). The segments are patterned through interaction among a cascade of maternal and zygotic factors, representing a hierarchical regulation along the A-P axis at the blastoderm stage (Fig 2.1). Maternal effect genes form gradients, establishing initial polarity and positional information to subsequently regulate the spatially aperiodic expression of downstream zygotic genes including gap genes, and the periodic pair-rule and segment polarity genes, which finally form segment boundaries (Johnston and Nüsslein-Volhard, 1992; Pankratz et al., 1992; Shvartsman et al., 2008). In contrast, the short germ-band insect *Tribolium castaneum* is thought to represent the ancestral model of axis patterning, in which segments are added sequentially from anterior to posterior during embryogenesis (Copf et al., 2004; Davis and Patel, 2002). In fact, embryos in the syncytial blastoderm only develop the anlage of head, thoracic segments and the segment addition zone (SAZ,

growth zone), from which the abdominal segments form (Liu and Kaufman, 2005; Rosenberg et al., 2009). Instead of relying on a morphogen gradient mechanism of a transcription factor such as Bcd, Wnt signaling represses maternal and zygotic gene activities for anterior specification in *Tribolium* (Ansari et al., 2018). The posterior *cad* concentration gradient is triggered by Wnt activity, contributing to sequential A-P patterning through regulatory interactions of a segmentation clock analogous to vertebrates (El-Sherif et al., 2014; Ozbudak and Pourquié, 2008). Remarkably, position information by gap genes in *Tribolium* is not fully coincident with that in *Drosophila*. They emanate sequentially from anterior to posterior and act to regionalize the trunk but are not required to directly regulate the expression of pair-rule genes (Rudolf et al., 2020). Specifically, the pair-rule gene expression emanates from the posterior pole by cyclical wave-like patterns, similar to the temporal periodicity of expression in vertebrates, relying on a mechanism of clock and wavefront during A-P elongation (Clark and Peel, 2018; Palmeirim et al., 1997; Sarrazin et al., 2012). Accordingly, expression of segment polarity genes in each parasegment compartment are specified directly by specific pair-rule genes in a periodic pattern during elongation stages (Choe et al., 2006; Jaynes and Fujioka, 2004).

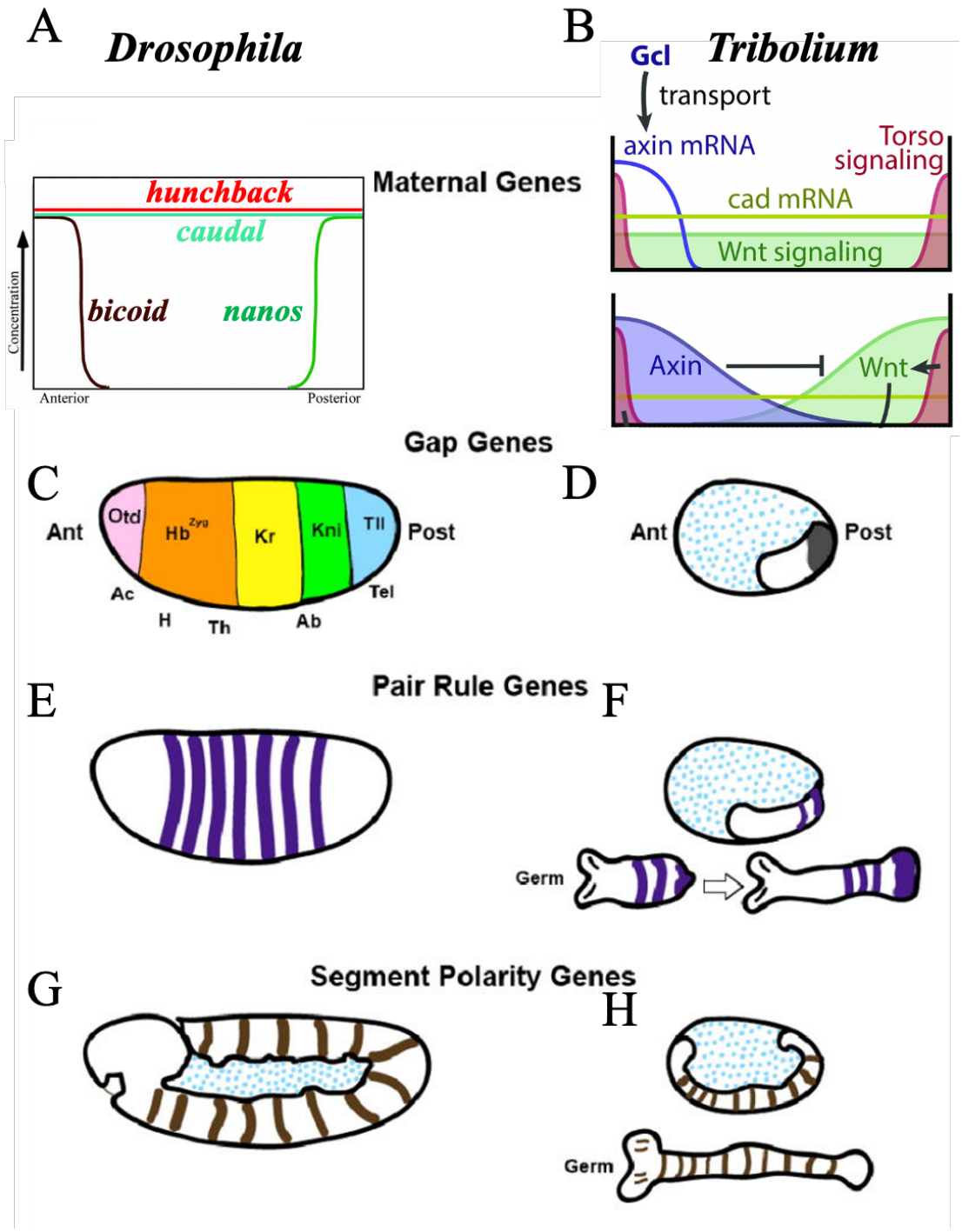

Figure 2.1 Specification of *Drosophila* and *Tribolium* segmentation pattern along the A-P axis

(A & B) Maternal morphogen gradients are utilized to establish A-P axis pattern in long germ-band embryos of *Drosophila* and short germ-band embryos of *Tribolium*, respectively. Bcd and Hb protein specify anterior structures and Nos together with Cad protein regulate the posterior region of *Drosophila* embryos. Wnt and Torso signaling together with maternal *Tc-cad* promote posterior zygotic genes expression and establish embryonic polarity in *Tribolium*. (C) Expression of gap

genes divides early embryos into different domains. (D) Gap genes are expressed in head, thorax, and anterior abdomen. (E) Pair-rule genes are expressed in seven stripes in insects. (F) After cellularization, transcription of pair-rule genes is activated in wave-like stripes. (G & H) Segment polarity genes are expressed in stripes determined by pair-rule genes. Modified from (Ansari et al., 2018; Gilbert, 2006; Rosenberg et al., 2009).

2.1.1 Interactions between segment polarity genes define boundary formation

During the development of arthropods, cells and their descendants are separated into compartments, the cells of which do not intermingle. Particularly, cells develop independently within compartments, whose boundaries prevent cell movement and restrict in compartments (Dahmann et al., 1999). The formation of segment boundaries between populations of adjacent cells exerts pivotal roles in establishing functional units to control future growth and patterning in well-organized cell compartments along the A-P embryonic axis (Lawrence and Struhl, 1996). Moreover, the *Drosophila* imaginal discs are one of the best examples to illustrate features of segment boundaries whose function as the morphogen organizing centers between neighboring compartments by regulating activation or repression of transcription. The segment boundary subdivides the developing wings into A-P compartments, while D-V compartments are formed by other mechanisms (Diaz-Benjumea and Cohen, 1993; Garcia-Bellido et al., 1973). In fact, primary clonal parasegment borders are established after *Drosophila* embryos undergo cellularization. Boundaries are defined by repeated stripes of segment polarity genes *wingless* (*wg*)*, hedgehog* (*hh*) and *engrailed* (*en*) expressed on either side of the parasegment boundary after being activated by pair-rule genes (Larsen et al., 2003). Wg is a secreted glycoprotein and belongs to the Wnt ligand family, whose functions are conserved in providing position information and to initiate signal transduction in cell-cell communication (Nusse and Varmus, 1992).

In general, the expression of segment polarity genes defines the anterior (*wg*) and posterior (*en* and *hh*) compartment boundaries, respectively, and their interaction

maintains stability of segment boundaries. Mutual transmission between neighboring compartments requires Wnt and Hh signaling, forming a genetic regulatory circuit to control transcription (Fig 2.2). Wg and Hh are involved in segment boundary formation, they are signaling molecules and excellent markers for forming segments (Neumann and Cohen, 1997; Swarup and Verheyen, 2012). Similar phenotypes are observed for a series of other segment polarity genes such as *cubitus interruptus* (*ci*), *smoothened* (*smo*), *fused* (*fu*), *armadillo* (*arm*), *disheveled* (*dsh*) and *porcupine* (*proc*). Knock-down embryos resemble the phenotypes observed in *wg* or *hh,* respectively, indicating their involvement in Wg or Hh receptor signaling pathways (Perrimon and Mahowald, 1987). Highly conserved functions of *wg*, *en* and *hh* are found in *Tribolium* segmentation. The expression is strongly disorganized in the head and trunk region after depletion of one of them. Knockdown of *wg* and *hh* both produce compact embryos with fused *en* stripes and shortened axis after germ-band retraction, suggesting that formation of A-P axis and segment boundaries are strictly controlled by the segment polarity gene circuit (Farzana and Brown, 2008; Lim and Choe, 2020; Ober and Jockusch, 2006). The *Drosophila shaggy* gene (*sgg*, also called *zeste-white 3*), is the homolog of *GSK-3*. It is an important downstream component of Wnt/Wg signaling pathway (He et al., 1995; Siegfried et al., 1992). *Sgg* is not only an inhibitory component of Wnt pathway but also antagonizes Hh signaling through regulating c*i* in *Drosophila* (Jia et al., 2002). During *Drosophila* segmentation, the inactivation of *sgg* triggered by Wg ligand binding leads to expression of *en*, determining cell fates during embryonic segmentation (Siegfried et al., 1992). *Sgg* is essential for establishing body pattern along A-P axis in *Tribolium* and vertebrates (Fu et al., 2012; Heslip et al., 1997; Ruel et al., 1993). This conclusion is further supported by a study in *Oncopeltus*, where RNAi of *sgg* severely disrupts segment boundaries (Lev and Chipman, 2021). Thus, the regulatory mechanism of segment polarity genes seems to be highly conserved based on interaction between Hh and Wnt signaling pathways affecting all boundaries from head to abdominal segments. Recent research has pointed out pre-gnathal (ocular, antennal, and intercalary) and trunk segments are different in that they show modifications of the segment polarity gene regulatory network, while gnathal and

thoracic segment stripes appear to form in the same way simultaneously in the insect *Oncopeltus* (Lev and Chipman, 2021).

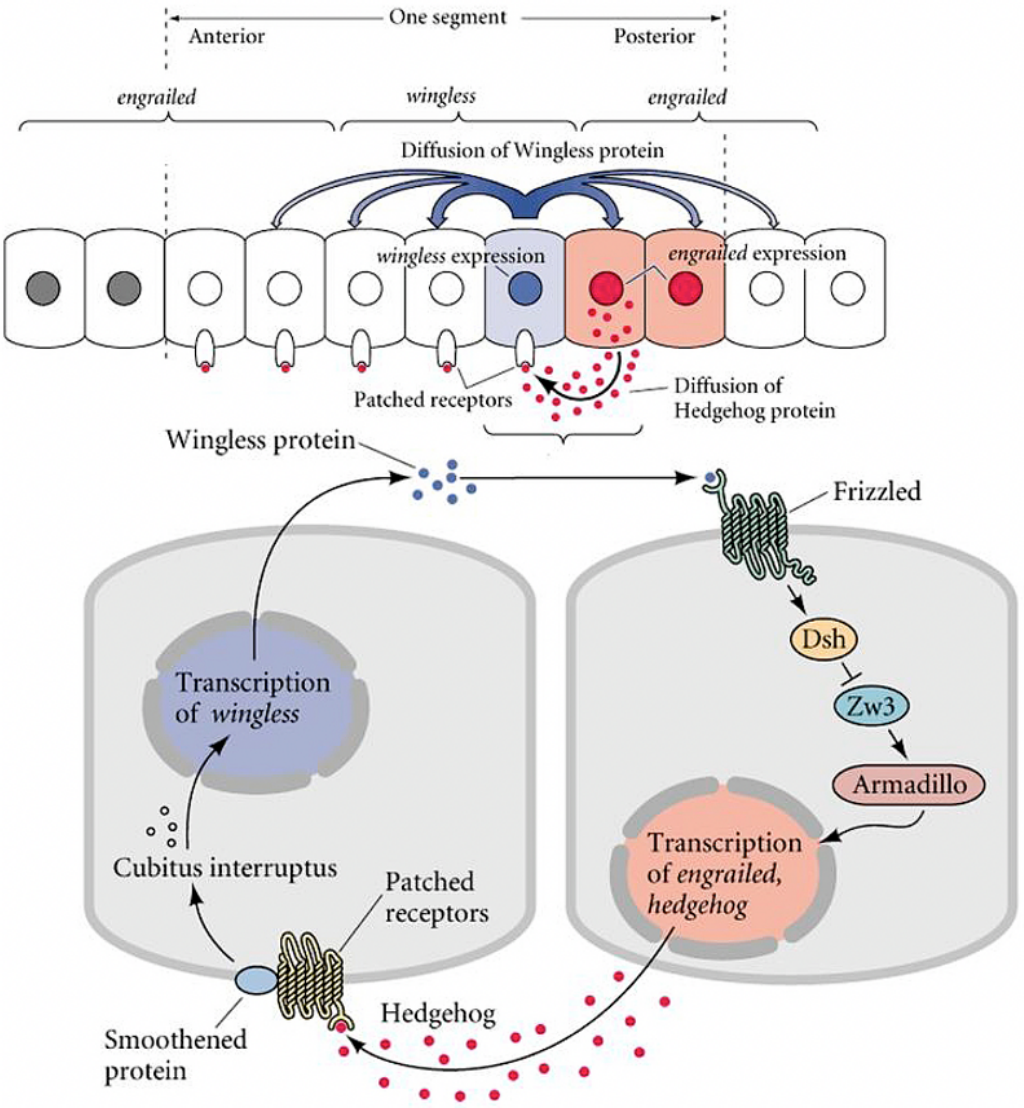

Figure 2.2 Segment boundaries are established by *wg* and *en*

wg is expressed in the anterior compartment of every segment. *en* and *hh* are transcribed in the same posterior cells. Diffusion of Hh is responsible for transmitting signal to *wg* expressing cells through binding to the Patched (Ptc) receptor, maintaining transcription of *wg* in adjacent cells. Stability of *en* expression is depending on Wg activity. The circuit between neighboring cells is specified by Wg and Hh signaling pathways. Diffused Wg protein binds to Frizzled receptor on the surface of *en* expressing cell to promote transcription of *en* and to secrete the Hh ligand. Taken from (Gilbert, 2003).

2.1.2 Functions of Wnt and Hh signaling in A-P axis formation

In *Drosophila*, there is no evidence for Wnt signaling functions in A-P axis formation, although establishment of segment boundaries requires *wg* (Bejsovec and Arias, 1991). Data from most short germ-band arthropods reveals that Wnt signaling is involved in the specification of the posterior pole, contributing to axis elongation and abdominal formation. However, depletion of the ligand Wg causes segment boundary and appendage defects in arthropods (Angelini and Kaufman, 2005a; Miyawaki et al., 2004). *Tribolium* has the typical axis patterning features of short germ embryogenesis, where the body plan is elongated progressively dependent on the function of the growth zone (Davis and Patel, 2002). Knockdown of multiple Wnt family genes produce truncated phenotypes with absence of a certain number of abdominal segments. Additionally, cuticles with depletion of the Wnt receptor *Tc-Arrow* (*Tc-Arr*) and the *Tc-Pan* resemble the truncated phenotypes, which suggests that canonical Wnt signaling participates in segmentation and elongation of the posterior growth zone (Bolognesi et al., 2008; Bolognesi et al., 2009). Data from *Tribolium* embryogenesis indicates that Wnt signaling has a crucial role in early axis formation as well. The mRNA of the Wnt-signaling antagonist *Tc-axin* is maternally localized at the anterior pole of the egg and RNAi targeting *Tc-axin* activates Wnt activity in anterior development. Interestingly, *Tc-axin* RNAi results in anteriorly truncated phenotypes showing that *Tc-axin* function to suppress Wnt signaling is required for anterior patterning in *Tribolium* (Fu et al., 2012; Prühs et al., 2017). Interestingly, the principle of axis formation based on Wnt polarity is first demonstrated in vertebrate embryogenesis (Petersen and Reddien, 2009) , and such a role is found in *Tribolium* (Ansari et al., 2018) and other animals (Fu et al., 2012; Yoon et al., 2019) – but not *Drosophila*.

The Hh signaling pathway is also determined through dynamic interaction with Wnt signaling affecting specific target genes in anterior head and posterior growth zone, respectively. Apparently, cross-regulatory relationships between the Wnt and Hh pathways are not conserved in the *Drosophila* head, in which *wg* seems to weakly

regulate *hh* expression (Gallitano-Mendel and Finkelstein, 1997; Oberhofer et al., 2014). The functions of the Hh signaling pathway have been shown to be highly conserved in insect development among others in maintaining formation of segmental boundaries (Lee et al., 1992; Varjosalo et al., 2006). In *Tribolium*, loss of key components such as *Tc-hh*, *Tc-smo* and *Tc-ci* lead to small spherical cuticles resulting from compact germ-bands in the strongest affected embryos. These phenotypes resemble those of *Tc-wg* and *Tc-wntless* (*Tc-wls*) RNAi, suggesting *Tc-hh* could be involved in multiple roles during A-P axis formation similar to the Wnt pathway (Bolognesi et al., 2008; Farzana and Brown, 2008). Functional interaction of Wnt and Hh signaling is not only apparent in insects but also in vertebrates, where analysis of Hh–Smo signaling supports that Hh mediates Wnt mediated cell polarity signaling along that A-P axis through *wls* in mouse embryos (Onishi and Zou, 2017).

2.2 Appendages development on P-D axis

Appendages are external projections of the body plan and play fundamental roles in maintaining movement, feeding, or environment exploration. A key aspect is that the diverse modifications and innovations of appendages give rise to diverse functions (Angelini and Kaufman, 2005b). Several molecular and genetic studies appear to confirm that multiple appendages retain common evolutionary origin and are generally considered serially homologous in arthropods (Boxshall, 2004; Panganiban et al., 1997). The basic development of limb appendage primordia is based on the same genetic processes but using specific position information along the body axis in order to develop into distinct types of appendages. Limb development is suppressed in posterior abdominal segments (Shubin et al., 1997). Appendage development is thought to require an additional embryonic axis system, the proximal-distal (P-D) axis. So far, the best-understood P-D axis formation is the one of the limb and gnathal structures derived from imaginal discs developing during larval stages in the holometabolous insect, *Drosophila* (Cohen, 1990). The invagination and growth of groups of epithelial imaginal cells in the ventrolateral region give rise to limb and gnathal appendages.

These imaginal cells are able to proliferate at larval stage and initiate differentiation to develop adult structures such as legs, mouthparts and wings (Simcox et al., 1987). Further studies in *Drosophila* have proposed that antenna and legs are considered to have evolved from ancestral appendages, supporting their homology (Cummins et al., 2003).

2.2.1 Wnt and Hh signaling mediate appendage outgrowth

The Wg protein has been shown to provide the positional information affecting cell fate not only for proper specification of segment boundaries but also in the leg imaginal disc (González et al., 1991; Kubota et al., 2003; Tabata and Takei, 2004). Studies of *wg* mutants show the importance of *wg* in patterning of embryonic leg allocation (Cohen, 1990). Moreover, both proximal and distal parts of the legs require Wnt signaling, and depletion of Wg activity produces strongly shortened limb along the P-D axis accompanied by absence of ventral structures (Couso and González-Gaitán, 1993). In general, the defects of limbs both in D-V and P-D axes are depending on interaction between *wg* and *dpp*, because these two signaling molecules are activated in the dorsal and ventral part of the leg disc through response to secreted Hh signaling emerging from the posterior compartment (Brook and Cohen, 1996; Johnston and Schubiger, 1996). Hh proteins activate transcription of *wg* and *dpp* both in D-V and P-D axis of limb through signaling transduction mechanism that induces expression of key components of Hh pathway such as *ptc*, *smo* and *ci* (Basler and Struhl, 1994; Méthot and Basler, 1999). In knock-down embryos, segment boundaries and limb deformities are found after *ptc* RNAi in *Drosophila* and *Oncopeltus* (Capdevila et al., 1994; Lev and Chipman, 2021). Dpp and Wg signaling are essential for the determination of the distal and medial parts of the limbs in the forming leg imaginal discs, respectively (Estella and Mann, 2008). The function of *wg* is essential for the ventral fate of legs, whereas expression of *dpp* is required to specify the dorsal portion (Couso and González-Gaitán, 1993; Morimura et al., 1996). A series of target genes expressed in limbs subdividing the P-D axis such as *Distalless* (*Dll*) and *dachshund* (*dac*) are

induced by integration of the Dpp and Wg morphogens in *Drosophila* (Fig 2.3) (Lecuit and Cohen, 1997). *Dll* functions in the distal outgrowth of limbs and *dac* expression contributes to proximal and intermediate limbs patterns. This has been shown for *Drosophila* and *Tribolium* mutants, and in *Oncopeltus* and the spider *Cupiennius salei* through RNAi experiments, revealing a highly conserved feature (Abzhanov and Kaufman, 2000; Angelini and Kaufman, 2004; Beermann et al., 2001; Schoppmeier and Damen, 2001). In *Tribolium*, the function of *dpp* does not seem to play a conserved role in limb outgrowth, although *dpp* retains a similar expression at the tip of the legs as observed in *Drosophila* (Ober and Jockusch, 2006). Further research has shown that loss of *sgg* or *dsh* functions generate similar limb defects as the *wg* mutants, being response to regulation of *wg* in leg development (Diaz-Benjumen and Cohen, 1994; Theisen et al., 1994). Subsequent research reveals that *dsh* and *sgg* could mediate the antagonism between *wg* and *dpp* in the anterior compartment through affecting *wg* and *dpp* transcription, which are involved in leg and eye-antennal development in *Drosophila* (Heslip et al., 1997). In *Tribolium*, knockdown of Wnt receptors *Tc-Arr* and *Tc-frizzled-1*(*Tc-fz1*) produce incomplete limb structure with retained proximal part and absent distal parts, indicating that Wnt signaling is essential for appendage patterning (Beermann et al., 2011). Additionally, *Tc-Sp8* (ortholog of *Sp1*, *Drosophila*) is required for the appendage outgrowth including gnathal and limbs shown by depletion of *Tc-Sp8* expression during *Tribolium* embryogenesis (Beermann et al., 2004; Ing et al., 2013). Importantly, the conserved functions of *Tc-Sp8*, *Tc-dac* and *Tc-Dll* are also found in gnathal appendages, the antennae and the labrum, which might be regulated hierarchically by *Tc-wg* in appendage outgrowth. Interestingly, antenna and labrum present normal development in *wg* mutants or RNAi embryos, whereas *Tc-Sp8*, *Tc-Dll*, or *Tc-dac* RNAi or mutant embryos obviously lack distal part of labrum in *Tribolium* (Ober and Jockusch, 2006; Prpic et al., 2001). Recently, some results have indicated that *Tc-wg* is directly regulating *Tc-Dll* during labrum patterning (Siemanowski et al., 2015). Extensive research has shown that Wnt signaling has abundant functions involved in multiple developing stages throughout limb morphogenesis in vertebrates as well (Church and Francis-West, 2004; Geetha-Loganathan et al., 2008). The

expression of some Wnt family members is found in the two signaling centers in early formation of limb bud, which are apical ectodermal ridge (AER) and the dorsal ectoderm (Church and Francis-West, 2004). The AER forms at the distal tip of the limb bud, controlling limb outgrowth along P-D axis through continuous communication between the AER and mesenchyme (Niswander, 2004). *Wls* has been found with fundamental function to transport various of Wnts for secretion, involved in regulation of distal vertebrate limb patterning (Zhu et al., 2012).

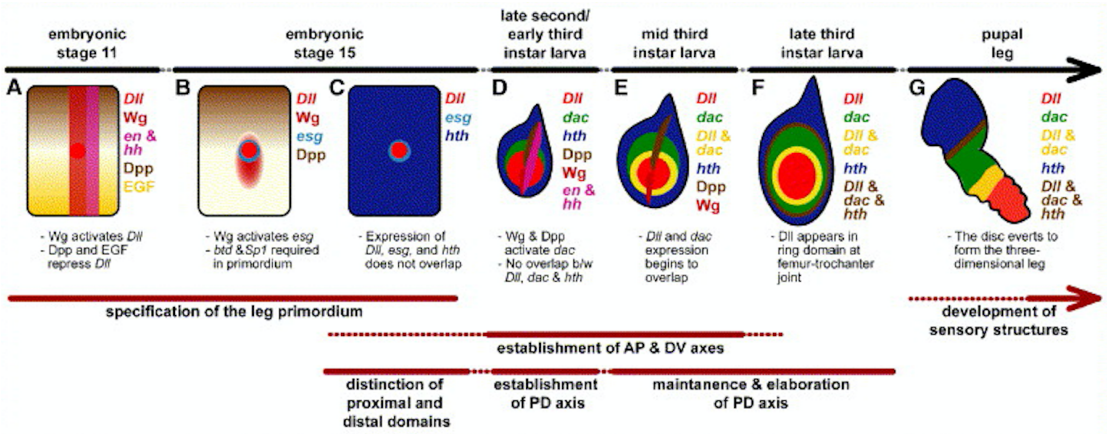

Figure 2.3 Specification of limb primordia in the leg development

(A-C) Wg and Dpp morphogens contribute to early development of the thoracic segment. *wg* is essential for establishment of the segment boundary and activates *Dll* expression which is inhibited by Dpp and EGF signaling in the dorsal and ventral ectoderm, respectively. At embryonic stage 15, expression of *wg* in the primordium is able to specify the proximal domain and to affect *esg* expression. (D-F) In the third instar larva stage, P-D and D-V axes are formed in the leg disc and some specific target genes are expressed along the P-D axis. (G) At the pupal stage, *Dll* expression distributes in the sensory bristles region, and circular disc stretches outward to form leg structure. Taken from (Angelini and Kaufman, 2005b).

2.2.2 Roles of EGFR and Notch signaling on limb development

It has previously been shown that a number of predominant signaling pathways and transcription factors are integrated and cross-talk participating in formation and development of appendages in arthropods and vertebrates. The similarities in

appendage development are carried out by recruiting homologous genes with similar functions (Pueyo and Couso, 2005). Besides Wg and Dpp morphogens, the Epidermal Growth Factor Receptor (EGFR) cascade exerts a crucial role in limb formation as well, whose function is restricted to a distal domain of limbs in *Drosophila* (Fig 2.4). Simultaneously, the activation of distal to proximal patterning genes such as *aristaless* (*al*), *Bar* (*B*), and *rotund* (*rn*) depends on EGFR-Ras gradient on P-D axis regulated by specific ligand Vein (Vn) (Galindo et al., 2002). Most strikingly, *B*, *al* and *rn* expression resemble to expression of *Dll* with similar expression in appendages, antenna and labrum in *G. marginate*, suggesting that EGFR signaling is required for distal development of gnathal appendages. Analogously, conserved functions of EGFR are strongly supported in *Tribolium* and other insects in that loss of EGFR functions cause distal appendage defects (Angelini et al., 2012; Gotoh et al., 2017). The expression of Vein is in response to signaling Wg and Dpp morphogens, and subsequent inhibition occurs in tarsal and pretarsal regions. Whereas in *Tribolium*, EGFR receptor and another ligand Spitz (Spi) are confirmed to be involved in medial and distal outgrowth of limbs, where RNAi results in downregulated expression of *Dll* and upregulated *dac* expression (Grossmann and Prpic, 2012). When the corresponding genes in the EGFR pathway are activated, *btd* and *Sp1* are co-opted to control growth and patterning of appendages through regulation in Notch signaling pathway in *Drosophila* (Córdoba et al., 2016; Estella and Mann, 2010). Additionally, two transmembrane Notch ligands Delta (Dl) and Serrate (Ser) mediate segmentation to direct formation of leg joints and affect leg imaginal disc development (Parody and Muskavitch, 1993). While Ser as the target of *Sp1* is involved in the mechanism of leg growth controlled by *Sp1* whose functions are conserved at the upstream of *Dll* (Córdoba et al., 2016). The Notch signaling pathway is also essential for limb development and generating segment boundaries along P-D axis in vertebrates, suggesting that Notch signaling is regulated upstream of *wg* (Conlon et al., 1995). Equally, Ser and its ubiquitin ligase Mind bomb1 RNAi cuticles display absent joints between adjacent segments and extremely shortened limbs in *Tribolium*, supporting conserved function of Notch signaling in limb development (Siemanowski et al., 2015). Of note, the Notch pathway is clarified

contributing to labrum formation from these data, which is in line with the function of *Sp8*, *Dll* and *dac*, indicating limb mediated gene regulatory networks also might be applied to labrum development (Ober and Jockusch, 2006; Prpic et al., 2001).

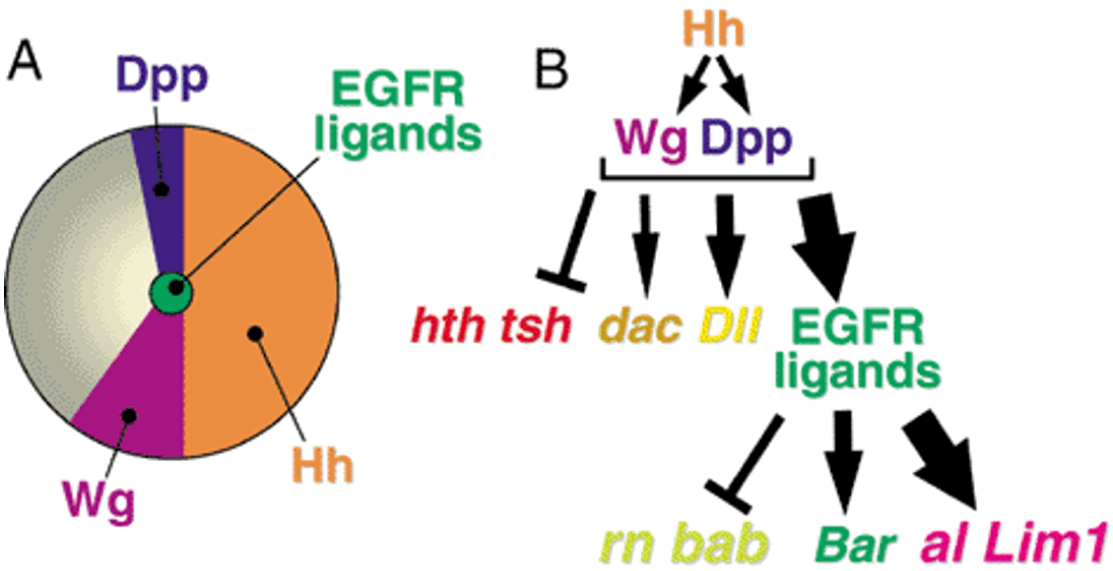

Figure 2.4 EGFR morphogens are involved in gene regulatory network of leg patterning.

(A) Morphogens such as Wg, Dpp, Hh and EGFR establish early position information of leg development. *hh* is expressed in the posterior compartment, inducing *dpp* and *wg* expression neighboring boundary. Initially, EGFR ligand is activated in the center of leg imaginal disc. (B) Schematic of genes regulatory network along P-D axis. Arrows and T-bars represent activation and repression, respectively. *hh* is secreted by posterior compartment induces expression of *wg* and *dpp* regulating downstream target genes expression from proximal to distal axis domains. Images taken from (Kojima, 2004).

2.3 The functions of glycogen synthesis enzymes

Glycogen synthase (*GlyS*) is evolutionarily conserved in vertebrates and invertebrates, and plays an important role in glycogen biosynthesis and metabolism (Ruel et al., 1993; Woodgett and Cohen, 1984). In *Drosophila*, *GlyS* is proposed to contribute to larval survival and adult fitness. *GlyS* mutants displays distinct metabolic defects affecting the storage of circulating sugar or lipid, which leads to growth defects and larval lethality (Yamada et al., 2019). Further, genetic intervention in mouse and *Drosophila*

brains reveal the reduction of neuronal *GlyS* prevents accumulation of glycogen clusters by improving neurological function with age and extends lifespan. Knockdown of *GlyS* reduces the storage of polyglucosan in brain cells and increases lifespan, with a sexual dimorphism, with strong effects observed only in males (Sinadinos et al., 2014). 1,4-alpha-glucan-branching enzyme (AGBE) is utilized to add branches to the glycogen molecule involved in glycogen synthesis in liver and muscle cells (Greene et al., 1988). Loss of AGBE causes a fatal human disorder including glycogen storage disease and adult polyglucosan body porphyria disease (Cappellini et al., 2010; Li et al., 2010). Some studies of *Drosophila* AGBE functions indicate an effect on the regulation of iron homeostasis and lifespan (Huynh et al., 2019; Paik et al., 2012). Thus, both genes might be an important link between development and glycogen synthesis. However, to our knowledge, no previous research has investigated *GlyS* or *AGBE* functions in insect embryogenesis.

2.4 The extensive roles of GSK-3 in multiple signaling pathways

GlyS is regulated by a serine (S)/threonine (T) protein kinase, GSK-3, that is originally purified and isolated from rabbit skeletal muscles (Embi et al., 1980). Additionally, GSK-3 participates in glycogen synthesis and glucose storage by directly inducing GlyS phosphorylation and inactivation (Frame and Cohen, 2001; Wu and Pan, 2010). Mammal tissues ubiquitously express GSK-3 isoforms, GSK-3α and GSK-3β. Both α and β types exhibit kinase activity, but GSK-3α has a higher molecular weight (51KDa) than GSK-3β (47KDa) (Woodgett, 1990). Despite the fact that these two GSK-3 family members share the same substrates, different physiological functions have been demonstrated affecting zebrafish heart positioning and sgg/GSK-3 is downstream of the Notch pathway in *Drosophila* neurogenesis (Lee et al., 2007; Ruel et al., 1993). Besides its role in glycogen metabolism, several pieces of evidence support that *GSK-3* functions in multiple transduction signaling pathways: Wnt/β-catenin, Hh, and Notch signaling pathways (Foltz et al., 2002; He et al., 1995; Jiang and Struhl, 1996). GSK-3 is an inhibitor of Wnt signaling (Fraga et al., 2013; He et al., 1995). Specifically, it is

involved in the phosphorylation of the Wnt pathway component β-catenin affecting its stability (Fig 2.5) (Da Rocha Fernandes et al., 2014). Wnt ligand binding disrupts the activity of GSK-3 through translocating GSK-3 and scaffold protein Axin away from β-catenin destruction complex. Additionally, different levels of Hh may induce partial or complete dephosphorylation of the transcription factor Ci, while the *Drosophila* Sgg protein acts as a negative regulator of Hh signaling through conjunction with PKA to promote hyperphosphorylation of Ci (Jia et al., 2002). Similarly, GSK3β is a key linker between extracellular signaling and Notch1 endosomal transport, where inactivation of GSK3β leads to changes in localization and enhance activity of Notch signaling (Zheng and Conner, 2018). In summary, *GSK-3* provides a link between glycogen metabolism and multiple signaling pathways such as Wnt, Hh and Notch involved in embryonic development.

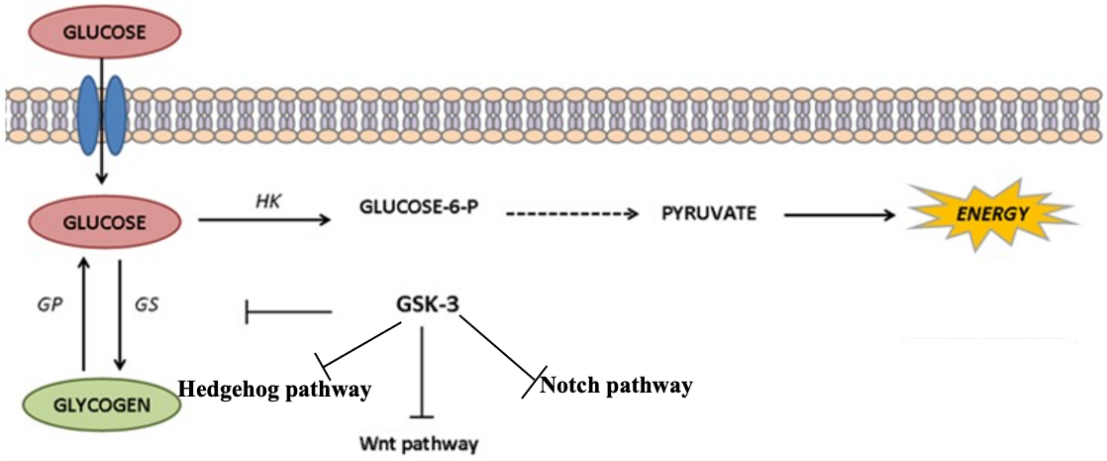

Figure 2.5 *GSK*-3 is involved in Wnt signaling pathway and glycogen synthesis process.

GSK-3 functions are in Wnt pathway and phosphorylate *GS* (also called *GlyS*) required for glycogen synthesis. Glucose is converted into pyruvate leading to generation of ATP through Hexokinase (HK) mediates glycolytic pathway. Modified after (Da Rocha Fernandes et al., 2014).

2.5 Aims of the study

Overall aim: Most genes known to be involved in *Drosophila* segmentation and head development have been tested in *Tribolium*. However, this extensive candidate gene approach cannot reveal patterning genes required in *Tribolium* but not *Drosophila*. Therefore, my aim was to identify and to study for novel genes involved in *Tribolium* head development and segmentation by a hypothesis independent screen.

Objective 1:

The RNAi phenotypes generated in the third phase of the *iBeetle* screen should be annotated for any phenotypes in the first instar cuticle. Next, genes involved in head development and segmentation should be identified and re-screened in order to confirm the phenotypes and to exclude off-target effects.

Objective 2:

The function of selected genes should be analyzed in more detail by extensive expression analysis and RNAi experiments. Specifically, the embryonic phenotypes of the glucose metabolism genes *Tc-GlyS* and *Tc-AGBE* should be studied in detail and the hypothesis should be tested, that they act via Wnt and/or Hh signaling.

3 Material and Methods

3.1 Animals

The strains of *Tribolium castaneum* beetles were reared and processed under standard conditions with full grain flour at 32°C (fast development) or 25°C (Brown et al., 2009). The wild type strain *San Berndardino* (*SB*) was used for all experiments apart from the primary screening phase. There, the female pupae of transgenic line *Pig-19* (*pBA-19*) strain (marked with an EGFP muscle enhancer trap) (Lorenzen et al., 2003) were used for crossing with adult males from the *Black* strain (Sokoloff et al., 1960) for injection in the *iBeetle* screen.

3.2 The screening procedure

Here, the screening procedure was described, which was performed by Mohammad Al Heshan, Claudia Hinners and Elke Küster. My part was to annotate and analyze the cuticle preparations. The pupal injection of the third phase of the *iBeetle* screening was performed and analyzed as described in (Schmitt-Engel et al., 2015). Male and female were identified and collected by using a fine brush or flexible forceps at a stereo-microscope. Pupae at 75-90% were used for injection. Templates and dsRNA were provided by Eupheria Biotech Dresden, Germany.

3.2.1 Screening and re-screening schedule

Detailed schedule of pupal injection was used in the screening and re-screening as seen below (Fig 3.1). Muscle phenotypes and ovary analysis were not performed in the third phase screening.

Day 0: Per gene with 10 female pupae were fixed on a microscope-slide for injection. dsRNA solution was thawed and kept on ice and centrifuged before use. Injection pressure was controlled between 400-900hPa taking at least 5sec/pupae. Buffer injection was injected as control.

Day 3: The hatched beetles and flour were transferred to the block system with a funnel. The hatch and lethality rate were documented. 4 males were added into each vial for mating and kept it at 32°C incubator at 40% humidity.

Day 9: First egg lay. The eggs were put on 300 µm meshes to allow WT larvae to pass through the sunflower oil. The number of surviving females was documented.

Day 11: Second egg lay. Eggs were collected and incubated in 180 µm preparation blocks together with flour allowing larvae to feed.

Day 13: Cuticle preparations. Hatched larvae were kept at 4°C until phenotypes were analyzed. The eggs were transferred from 300 µm to 180 µm mesh-block for dechorionzation. The block was placed into a petri dish with 50% bleach and washed twice for 3 min to remove the flour and chorion of the eggs. The eggs were washed with water before embedding and in a drop of Hoyers medium-lactic acid on a microscope slide. 65°C incubation overnight dissolved all soft tissues.

Day 14-15: The cuticle phenotypes were observed with fluorescent microscope (Zeiss Axioplan 2) set as cy3 filter, darkfield and 8-bit mono. Amounts of empty eggs and morphological defects were analyzed and annotated (see below).

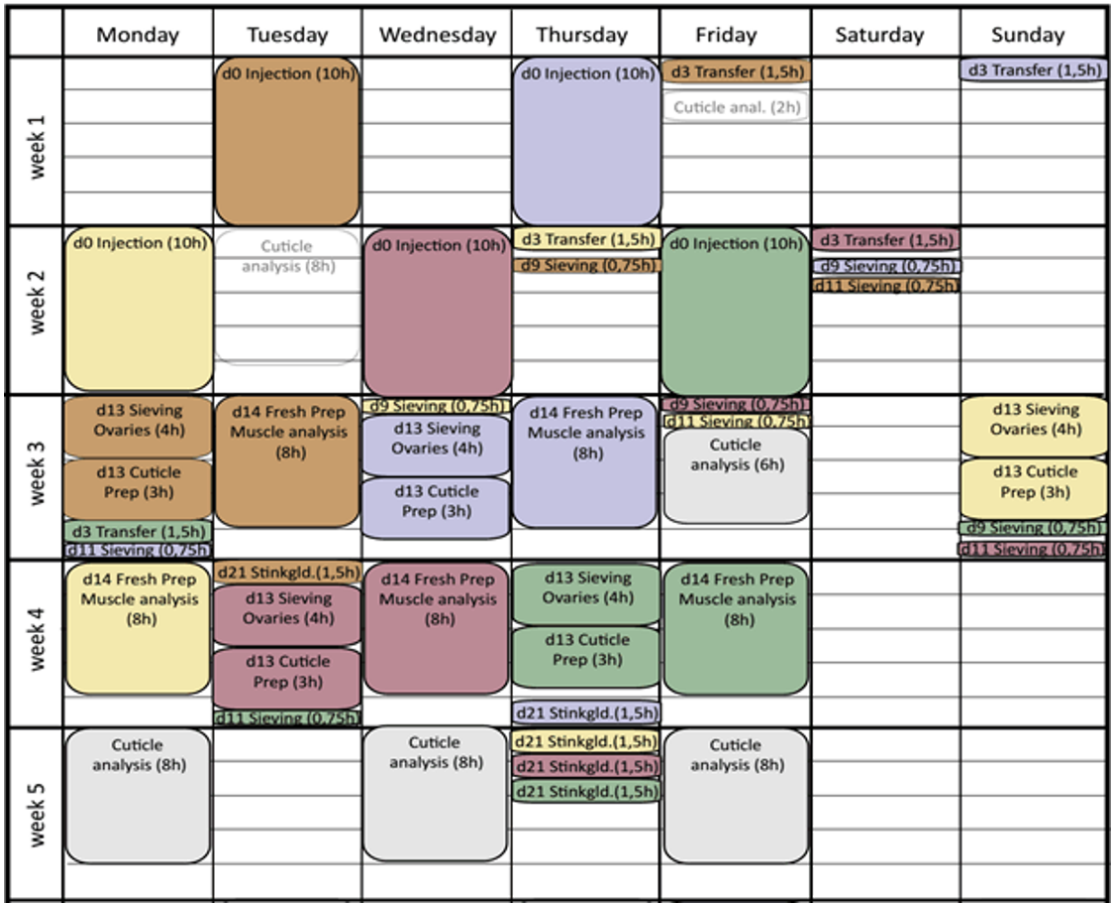

Figure 3.1 Injection schedule of multiple repetitions.

Each repetition (represented with same color) contained the same set of analysis steps at specific timepoints, which was represented with same color.

3.2.2 Database annotation

All phenotypes with specific head, thoracic, abdominal segments or stronger defects were annotated in an online database (http://ibeetle-base.uni-goettingen.de). At least five pictures were uploaded to document a phenotype. The database provided many parameters such as penetrance and number of cuticles on the slide to characterize phenotypes in detail. Standard annotations were defined by entity (pupal or larval), quality (complete or partial), and modifier (abnormal or missing) system. The cuticles were observed from left to right side of slide in turn. The total number of eggs and corresponding phenotypes were counted if only few cuticles appeared on the slide. In case there were a large number of animals on same slide, 30-50 cuticles were analyzed and the penetrance of different phenotypes were estimated and annotated on the

database. The defects of head, thorax and abdomen structures were systematically screened and documented in the third phase *iBeetle* screening. (Fig 3.2).

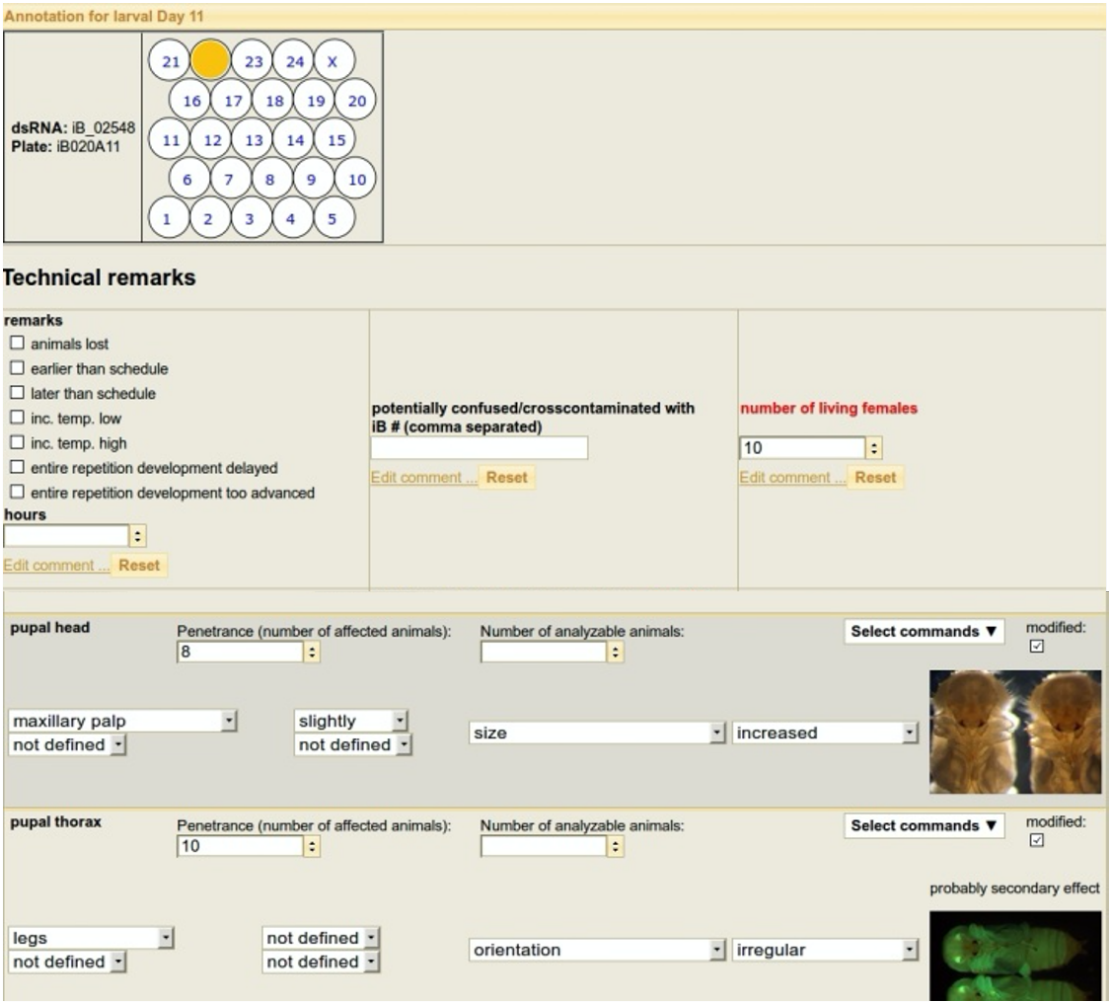

Figure 3.2 Detailed description of phenotypes were annotated on database.

The screenshot of the annotation database shows multiple annotated items to describe clearly phenotypes based on standardized EQM (entity, quality, and modifier). The penetrance of the corresponding phenotype was estimated and annotated for selection of candidate genes later.

3.3 Phylogenetic analysis

Protein sequences of orthologous genes of different species were obtained from *Tribolium* blast browser (http://bioinf.uni-greifswald.de/blast/tribolium/blast.php) and NCBI database (http://blast.ncbi.nlm.nih.gov/Blast.cgi). The multiple sequence alignment was performed with the ClustalW algorithm of MEGA 6 (Tamura et al., 2013) through eliminating positions gaps in one of the sequences on both sides. Phylogenetic

trees were constructed basing on neighbor-joining method (Demoulin, 1979) with a bootstraps value calculated by 1000 repetitions (Felsenstein, 1985).

3.4 Molecular cloning

The specific primers of non-overlapping double-stranded RNA (dsRNA) fragments were designed via Primer3 (https://bioinfo.ut.ee/primer3-0.4.0/) and Geneious11.0.5 software (https://www.geneious.com), and generated by Eurofins MWG Operon (Ebersberg, Germany). Cloning was carried out after standard PCR reaction by using complementary DNA (cDNA) of 0-72 hours embryos as template. cDNA was synthesized by the SMART PCR cDNA kit (ClonTech). The gene fragments were cloned into the appropriate vectors through using the TA Cloning® Kit (Life Technologies, Carlsbad, CA, USA). Plasmids were sequenced by Macrogen (Seoul, Korea and Amsterdam, Netherlands) with standard forward or reverse primers. Gene specific primers and vector maps were showed in the appendix.

3.5 DsRNA synthesis and injection

DsRNA with the length of 500-1000bp was used for RNA interference. Template plasmids for *in vitro* transcription were amplified and produced with Ambion® MEGAscript® T7 kit (Life Technologies, Carlsbad, CA, USA). Non-overlapping fragments were generated and injected in the *SB* strain instead of *pBA-19* strain testing for off-target effects and for strain specific effects. DsRNA with concentration of 1 µg/µl was injected in the *iBeetle* screening and my re-screening, and the concentration was adjusted between 0.15 to 3 µg/µl for other functional knockdown experiments (see results). The dsRNAs with *iBeetle* fragments were ordered from Eupheria BioTech. Pupal injection was performed by using a FemtoJet® express device (Eppendorf, Hamburg, Germany) with a flexible injection pressure regulated by flow velocity of dsRNA solution. Injection puffer (IP) and dsRNA of the exogenous gene *dsRed* (same concentration) were performed as negative controls in the pupal injection and double RNAi experiments, respectively.

3.6 Embryo fixation

Embryos were collected of an age of 0-48 hours from flour and transferred to a washing basket (150 µm). The embryos were dechorionated in 50% bleach and washed with dd-H_2O for 2-3 min. Embryos were transferred into scintillation vial with 2 mL PEMS, 6 mL Heptane and 300 µl formaldehyde (37%). Embryos were agitated for 25-40 min at 220-230 rpm for fixation. Methanol was added to break the embryos from the vitelline membrane. The embryos on the bottom without vitelline membrane were collected for staining (Schinko et al., 2009).

3.7 Immunostaining

3.7.1 Antibody staining

The embryos were blocked in 3% BSA (Fraction V) for 1 hour and incubated with the primary antibody cleaved *Drosophila* Dcp-1 (Asp216, detects endogenous levels of the fragment of cleaved *Dcp-1*) (dilution 1:100) (Cell Signaling Technology, Germany) overnight on the wheel. Embryos were washed with PBT for several steps and added the appropriate secondary fluorescence-coupled antibody (Alexa Fluor 555, 1:1000). DAPI was added together with PBT during washing steps to stain nuclei. Afterwards, the supernatant was removed and VECTASHIELD® (Vector Laboratories) was added for storage.

3.7.2 Statistical analysis

Cell counting was performed with “Count tool” from Adobe photoshop 2020 software. The apoptotic cells were counted in three specific counting regions: head, germ-band and growth zone. Data analysis of counted cells was visualized in box plots generated by the GraphPad Prism 8.2.0 software and significant test was conducted with t-test between the groups.

3.8 Whole mount *in situ* hybridization (ISH)

3.8.1 RNA probes

Sense or anti-sense ISH probes were synthesized by T7 polymerase with DIG (Digoxegenin-UTP, ^{DIG}) and FLU (Fluorescin-UTP, ^{FLUO}) labeling kits (Roche, Germany). 0.5 and 1 µl of probes were diluted in 30 µl Hybe-AT for test staining.

3.8.2 Staining

NBT+BCIP staining:

Nitro blue tetrazolium (NBT) staining was performed in conjunction with 5-Bromo-4-chloro-3-indolyl phosphate (BCIP) reaction to detect activity of alkaline phosphatase as described previously (Oberhofer et al., 2014; Schinko et al., 2009). Staining was done in 1 ml NB-buffer, 4.5 µl NBT and 3.5 µl BCIP solution in hybridization blocks.

Double ISH (NBT/BCIP+TSA) staining:

Fluorescent color staining was conducted in Tyramide signal amplification (TSA) solution containing 250 µl MAB-Tween, 2,5 µl 4-iodophenol, 2.5 µl 0.3% H_2O_2 and 1 µl Dylight (conjugate 555 red or 488 green) for 30 min. The embryos were washed in MABT and stained with NBT/BCIP reaction. Anti-Dig-AP antibody (Roche) was used for the NBT/BCIP staining and anti-Fluorescein-POD (Roche) antibody was to do the TSA reaction (Siemanowski et al., 2015).

Double Fluorescent ISH:

After the first color had been incubated in TSA solution, 10 mM HCL was used to inactivate the peroxidase. Then fresh TSA reaction was prepared on day 4 and stained with another Tyramide conjugate.

DAPI staining:

Embryos were fixed at 0-72 hours and washed with 75%, 50%, 25% Methanol/PBT. Embryonic nuclei were detected with DAPI (1:1000 µl) in PBT for 1 hour on the wheel.

3.9 Quantitative real-time PCR (qRT-PCR)

3.9.1 RNA extraction

0-5, 11-24, 24-48 and 48-72 hours of embryos were collected and total RNA was isolated by using Trizol (Ambion) according to the protocol. The tissue of embryos was homogenized with a pestle in Trizol Reagent. Subsequently, the chloroform and isopropanol were added for extraction of RNA pellet. The pellet was washed with 75% ethanol and stored in RNase-free water.

3.9.2 cDNA synthesis

cDNA was generated by using First-Strand cDNA synthesis Kit (SuperScript® III Reverse Transcriptase, Thermo Fisher Scientific, USA) in accordance with manufacturer's instructions. The cDNA was used as a template for amplification in PCR.

3.9.3 qRT-PCR assay and data analysis

All qRT-PCR reactions were done in triplicate (three biological and three technical replicates) by using CFX96™ Real-Time PCR System (Bio-Rad laboratories, CA, USA) with 5x HOT FIREPol® EvaGreen® qPCR Mix Plus (ROX) (Solis Biodyne, Tartu, Estland). Relative quantification was performed by the $2^{-(\Delta\Delta Ct)}$ method and normalized by reference genes *GAPDH* and *RPS3* (Schmittgen and Livak, 2008).

3.10 Embryonic injection

The beetles of *SB* strain were transferred onto white flour to lay eggs. Fresh eggs were collected every hour and incubated them at room temperature for another hour. The eggs were washed with 1% Klorix and water for several minutes, and kept in water bath waiting for injection. Embryonic injection was conducted according to standard protocol (Berghammer et al., 1999; Schinko et al., 2012). The injection solution was mixed with 1 µl phenol red to visually follow the injection. The posterior end of eggs was injected and the slides were put on apple agar plates incubating at 32°C for 3-4

days. The number of injected embryos and surviving larvae were documented.

3.11 Microscopy and image processing

Cuticle phenotypes of screening, single, double RNAi experiments and glucose injection were imaged with a Zeiss Axioplan 2 Microscope (Wohlfrom et al., 2006). Images of embryos in single ISH and ISH combined with TSA staining were observed with Zeiss Axio Observer Z1 microscope and taken by using Image-Pro Plus software (Media Cybernetics, Rockville, USA). Documentation of immunostaining, double fluorescent ISH and DAPI staining were done with the Zeiss laser scanning microscope (LSM510). All of figures were level-adjusted and assembled in Adobe Photoshop 2020.

4 Results

4.1 *iBeetle* screen and phenotype annotation

The aim of this project was to discover novel genes required for embryonic head pattern formation, and other gene functions, which had not been described in *Drosophila* before, but which had novel functions in development. To that end I joined the third phase of the *iBeetle* genome-wide RNAi screen in the red flour beetle *Tribolium castaneum* (Schmitt-Engel et al., 2015). In order to finalize the screening for regulatory genes, all structures of the L1 cuticle phenotypes were analyzed with a focus on head, thorax and abdominal defects.

Cuticle phenotypes were generated in the ongoing RNAi screen by Mohamad Al Heshan while Dr. Großmann and I did the phenotype analyses. All observed phenotypes were annotated in the online *iBeetle* database like in the previous phases of the *iBeetle* screen (https://ibeetle-base.uni-goettingen.de/ibAnno/home.seam) (Dönitz et al., 2015). During the third screening phase of *iBeetle*, RNAi experiments knocking down 3360 genes of the pupal injection screen from the repetitions no.60 to 200 were screened for phenotypes by me (no.1-60 repetitions screened by Dr. Daniela Großmann). Six repetitions including 144 genes were analyzed and annotated per week. The first two screening phases included analyses of genes required for sterility and muscle and stink gland development. However, in the third phase, we were not be able to annotate muscle phenotypes and sterility, and therefore focused on embryonic patterning genes in the pupal injection screen. All annotations from this and the other parts of the screen were documented and accessible at the *iBeetle* database (http://ibeetle-base.uni-goettingen.de). These datasets offer data that include detailed annotation of the specific phenotypes, related pictures, and the information of corresponding dsRNA along with gene information such as sequences, genomic location and *Drosophila* homologs (Hakeemi et al., 2022).

4.1.1 Criteria for detecting candidate genes from the *iBeetle*-Base

From the entire dataset generated by me and Dr. Daniela Großmann, I looked for candidate genes with interesting phenotypes. In order to obtain interesting phenotypes, I searched broadly all L1 cuticle annotations from pupal injection on screen day 15, which corresponds to the criterion on the database: "pd15". For my purpose, four features with respect to the head were used as search terms:

Larval head, labrum

Larval head, head capsule

Larval head, vertex triplet

Larval head, procephalic head

In addition, I also looked for other two features for interesting genes:

Larval thorax

Larval abdomen

Further criteria were that the phenotype had to be annotated with more than 50-80% penetrance and that the annotation was after 01.01.2016, because the previously annotated genes had already been screened. With the objective to avoid overlooking interesting genes, 30-50% penetrance was also added for searching despite the fact that phenotypes with higher penetrance were more frequently reproduced. Finally, the datasets were looked at manually at *iBeetle* base for further information and to discard genes that led to unspecific phenotypes. For instance, we looked at the GO terms of those candidate genes (transcription factor, function, signaling pathway, etc) on the *iBeetle*-Base (http://ibeetle-base.uni-goettingen.de/) and the closest fly homologs, sequence and location in the genome as well for previous reports on the functions of the genes. The primary search revealed 29 candidate genes involved in head development and 38 candidate genes with other interesting phenotypes. In total, 67 original candidate genes with interesting phenotypes were found covering head, thorax and abdomen (Fig 4.1).

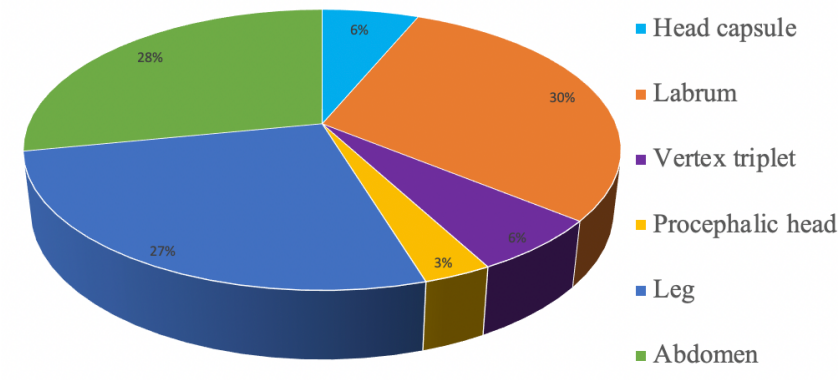

Figure 4.1 Selection of original candidate genes from *iBeetle* database.

Head, labrum, legs, and abdomen phenotypes were obtained based on our screening criteria. These phenotypes with high penetrance defects were interesting and good candidate genes for a rescreen.

4.1.2 More detailed analysis of candidate genes

Of the 29 candidate genes related to head phenotypes, 10 genes were selected in addition to 4 genes with abdominal phenotypes. Quantification of phenotypes based on available slides from the *iBeetle* screen was performed with specificity criteria (Table 4.1 & 4.2): Specific and highly penetrant phenotype (>50%) but low penetrance of the following phenotypes: “empty egg” or “strong” phenotype (the latter two indicating an essential role in basic cell biology rather than in specific patterning); pantagmatic phenotypes (defects not specific to the head but also affecting thorax and abdomen).

We determined the gene’s orthologs in other species and obtained function information from Flybase (http://flybase.org), that helped excluding genes for which a similar function had been described before. For sake of focus, the phenotypes with strong leg or thoracic defects were not analyzed further in this project. Nevertheless, I made an annotation list of these interesting genes and phenotypes which might provide a basis for future research.

Summaries of the cuticle analyses of these 14 candidate genes were shown in Fig 4.2 & 3. Strong defects (i.e. un-identifiable segments or cuticles), cuticle everted (i.e. inside-out) and empty eggs phenotypes (i.e. without any cuticles inside the eggs) were observed as well but with lower frequency compared with main phenotypes (head or abdominal defects).

Table 4.1 Annotation and function information of head specific genes.

Given were *iBeetle* numbers, the annotation for head defects as documented in the database, closest fly homologs names, and the corresponding protein function which had been reported or predicted.

IB-number	Screen annotation	FlyBase gene name	Function in FlyBase
IB_13007	Labrum transformed to maxilla, number of maxillae increased, mandible not present (>80%), (n<50)	*Maf-S*	DNA-binding transcription factor activity; protein heterodimerization activity
IB_13206	Antenna/labrum not present (>80%), size of labium decreased (<30%), (n>50)	*Gustatory receptor 64a*	sweet taste receptor activity
IB_13619	Labrum not present (30-50%), head appendages not present (30-50%), labrum irregular (30-50%), antenna not present (30-50%), (n<50)	*Convoluted (conv)*	-
IB_14403	Labrum/antenna not present (50-80%), head appendages not present (50-80%), size of head capsule decreased (50-80%), Head thorax, abdomen not present (<30%), (n>50)	-	-
IB_14792	Labrum not present (50-80), labrum irregular (<30%), empty eggs (30-50%), (n<50)	-	-
IB_15102	antenna and labrum not present (50-80%), number of abdominal segments decreased and constrict (50-80%), (n<50)	*Accessory gland protein 62F (Acp62F)*	serine-type endopeptidase inhibitor activity
IB_15172	Labrum not present (30-50%), empty eggs (30-50%), un-identify segments (<30%), number of legs decreased (<30%), (<50)	-	-
IB_15175	Labrum and antenna not present (50-80%), number of legs decreased (<30%), head capsule not present (<30%), (<50)	-	-
IB_15350	Labrum and antenna not present (50-80%), head, thorax, and abdomen not present (30-50%), head appendages not present (30-50%), (n>50)	-	-
IB_15365	Labrum and antenna not present (50-80%), vertex triplet not present (50-80%), head and thorax not present (30-50%), number of legs decreased (30-50%), (n>50)	-	-

Table 4.2 Annotation of cuticles and function for four abdominal/leg genes.

IB-number	Screen annotation	FlyBase gene name	Function in FlyBase
IB_15557	femur and tibiotarsus of legs not present (>80%), number of abdominal segments decreased (50-80%), empty eggs (30-50%), (n<50)	-	-
IB_13310	Number of abdominal segments decreased (50-80%), number of thoracic segments decreased (30-50%), empty eggs (30-50%) (n>50)	-	-
IB_14257	Number of abdominal segments decreased (50-80%), empty eggs (30-50%) (n<50)	CG7231	-
IB_14288	thoracic & abdominal segments bent (50-80%), legs tibiotarsus fused (50-80%), empty eggs (30-50%) (n>50)	CG13531	-

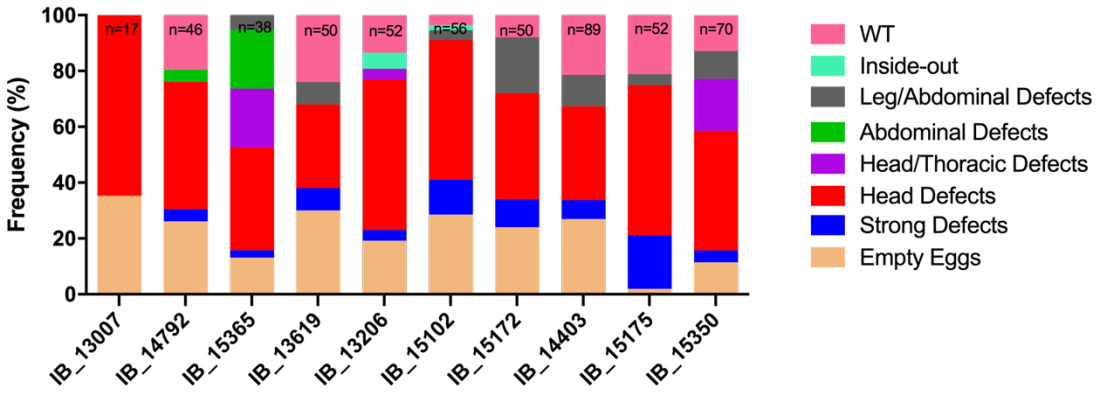

Figure 4.2 Phenotypic aspects of the head specific genes-detailed analysis.

Colors represented specific types of cuticle phenotypes. The analysis of the ten head candidate genes showed strong head defects phenotypes (red and purple) with higher frequency but also varying degree of other phenotypes. The fewer non-specific phenotypes were present, the more interesting the phenotypes were. For example, *IB_13007* presented 65% head defects and 35% empty egg phenotypes but no other phenotype, indicating that phenotype of this gene was very specific and strong for the rescreen. Number of analyzed cuticles was shown in the upper part of each bar.

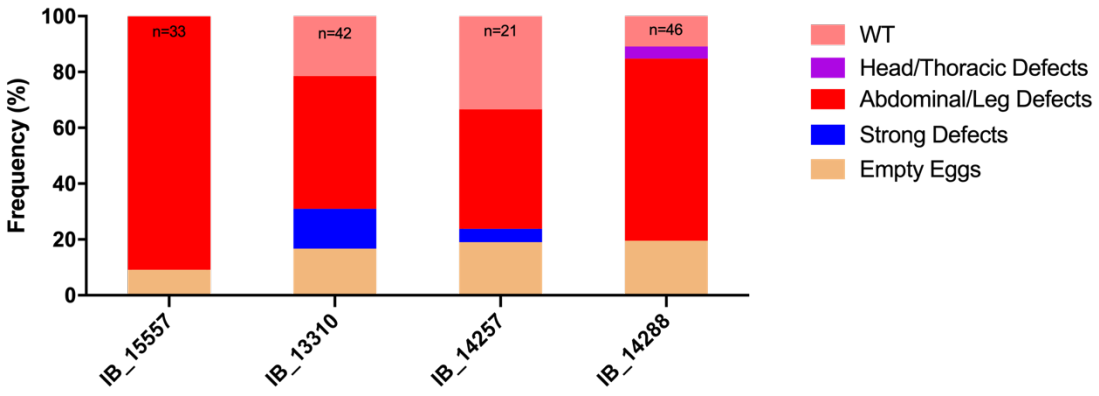

Figure 4.3 Four abdominal/leg specific genes original detailed analysis.

Cuticle phenotypes represented with corresponding color were listed on the right. Each gene with high penetrance abdominal/leg defects or irregular was observed and analyzed after day13 in the screen.

In order to get a more quantitative view on these genes, I analyzed more cuticles from the preparations generated in the *iBeetle* screen in more detail. Excluding other unspecific phenotypes such as empty egg and wild-type, I analyzed about 30 larval cuticles per gene. An overview on the portion of regions affected and broad phenotypes were given in Fig 4.4 & 4.5 (same data as summarized in Fig. 4.2 and 4.3).

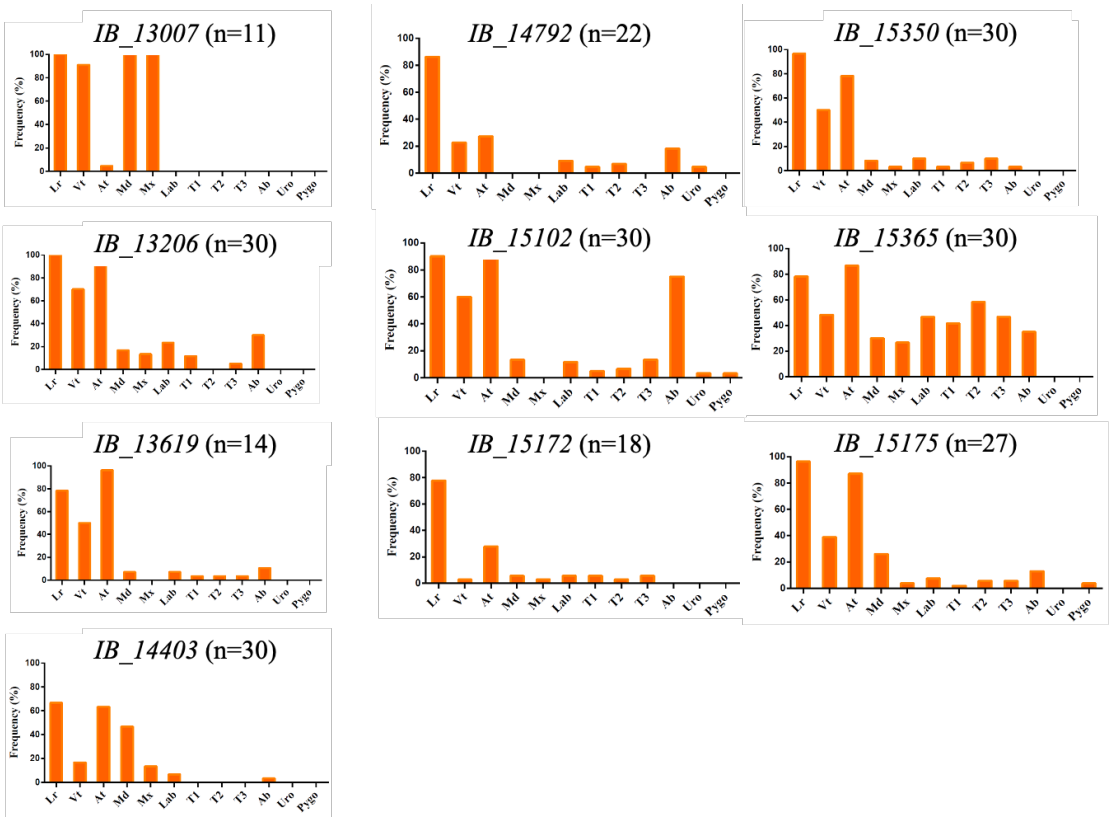

Figure 4.4 Cuticle phenotypes for each gene were recorded from head to pygopods.

First-instar larva cuticle consists of following parts, head, three thoracic segments (T1–T3), eight abdominal segments (A1–A8), and terminal structures. Lr (labrum); Vt (vertex triplet marking the dorsal head); Ant (antenna); Md (mandible); Mx (maxillae); Lab (labium); Ab (abdomen); Uro (urogomphi); Pygo (pygopods).

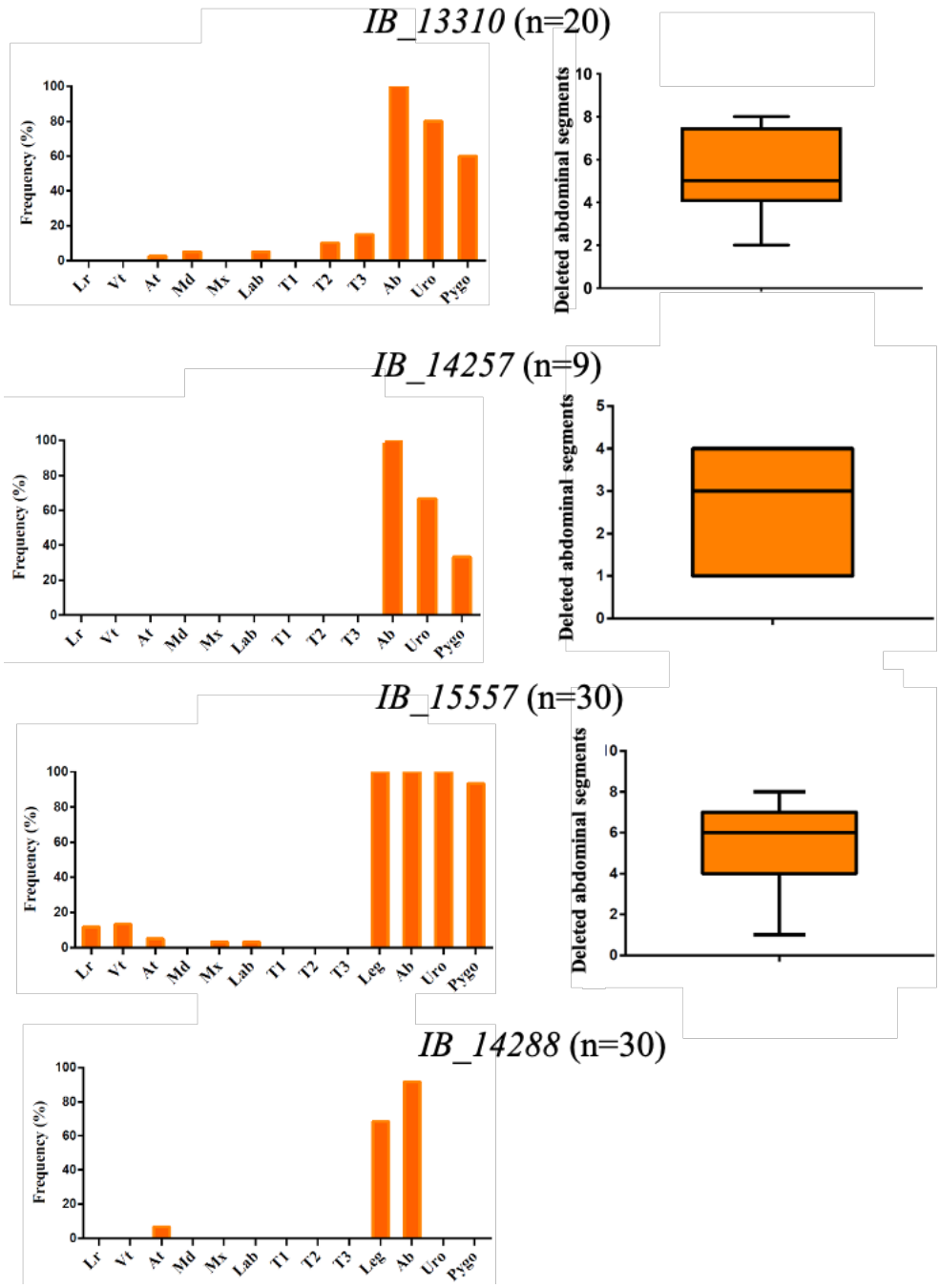

Figure 4.5 Detailed cuticle analysis for these four abdominal/ leg genes.

The histograms showed the defects of the abdomen (Ab) along with other posterior defects in those cuticles. Box plots of remaining abdominal segments were given for *IB_15557*, *IB_14257*, *IB_13310*. For *IB_14288*, the number of abdominal segments was not changed, but the abdomen was bent dorsally.

4.1.3 Rescreen of selected genes

For all 14 specific genes, dsRNA of non-overlapping fragments was ordered (Eupheria GmbH) and injected at a concentration of 1 µg/µl in the wt strain (*San Bernardino*, *SB*) to test for off-target effects and for strain specific effects. In the following, the results of the re-screen were compared to the primary screen and both phenotypes and information on gene orthologs were discussed. The phenotypes of four genes can be reproduced in the re-screen, *IB_13007* and *IB_15350* were related to head phenotype, *IB_14288* and *IB_15557* were involved in abdominal and leg patterning (Table 4.3).

Table 4.3 Injection with non-overlapping fragments of 14 specific genes.

-Not reproduced ; √ head or abdomen phenotype reproduced ; – /par, partially reproduced. Orthologs of related genes in *Drosophila* were given. Re-produced genes with head phenotypes were marked with an asterisk (*), and abdominal/leg defects with underline.

iB No.	*SB* × *SB*	Remarks	*Dm*_gene
***13007**	√	reproduced	*Maf-S*
15557	√	reproduced	-
14288	√	reproduced	CG13531
***15102**	√	reproduced	*Acp62F*
14257	-	off-target	CG7231
13206	-	off-target	*Gustatory receptor 64a*
15365	-	off-target	-
15350	-	off-target	-
14403	-	off-target	-
15175	-	off-target	-
15172	- / par	off-target par	-
13619	-	off-target	*Convoluted*
14792	-	off-target	-
13310	-	off-target	-

10 genes were discarded because the interesting phenotypic aspects were not reproduced while other phenotypic aspects were reproduced. For *IB_15102* and *IB_14288*, the phenotypes were reproduced but both showed high penetrance of empty

eggs and produced high portion of other unspecific phenotypes (“strong defects”; Fig 4.6). These two genes were not specific enough for following up. The same phenotypes with high penetrance were observed in the primary screen and the re-screen for two genes: *IB_13007* and *IB_15557*.

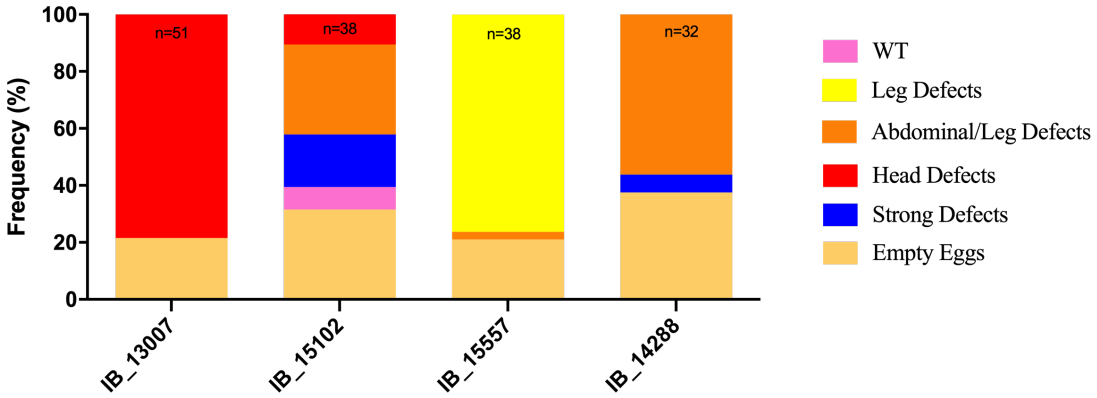

Figure 4.6 Four phenotypes were reproduced in the rescreen.

Highly penetrant head (78.43%) and leg (76.32%) defects were observed in *IB_13007* and *IB_15557* cuticles, respectively. The percentage of abdominal defects of *IB_14288* was lower in the rescreen (31.58%) compared with primary screen (50%). *IB_15102* showed strongly reduction of head defects between rescreen (3.45%) and primary screen (42.86%).

The phenotype of *IB_13007* showed a mandible transformation to maxilla, an absent labrum, and the number of maxillae was increased compared with wt (Fig 4.7 A & B). A phylogenetic tree was built based on an alignment of protein sequences. The targeted *Tribolium* gene TC015977 was revealed as the ortholog of the transcription factor *Drosophila Maf-S* (Fig 4.7 C). Previous studies had investigated the function of *Maf-S* in the *Drosophila* head, where it cooperates with *CncB* to suppress Deformed (*Dfd*) inducing mandible transformation (McGinnis et al., 1998). In *Tribolium*, it has been demonstrated that *Tc-cnc* and *Tc-Dfd* are necessary for patterning the mandibular and maxillary segments (Coulcher and Telford, 2012). My result showed that the phenotype of *Tc-Maf-S* was similar to the previously reported *Drosophila* phenotype with its function in head development. Therefore, this gene was not very interesting for further study.

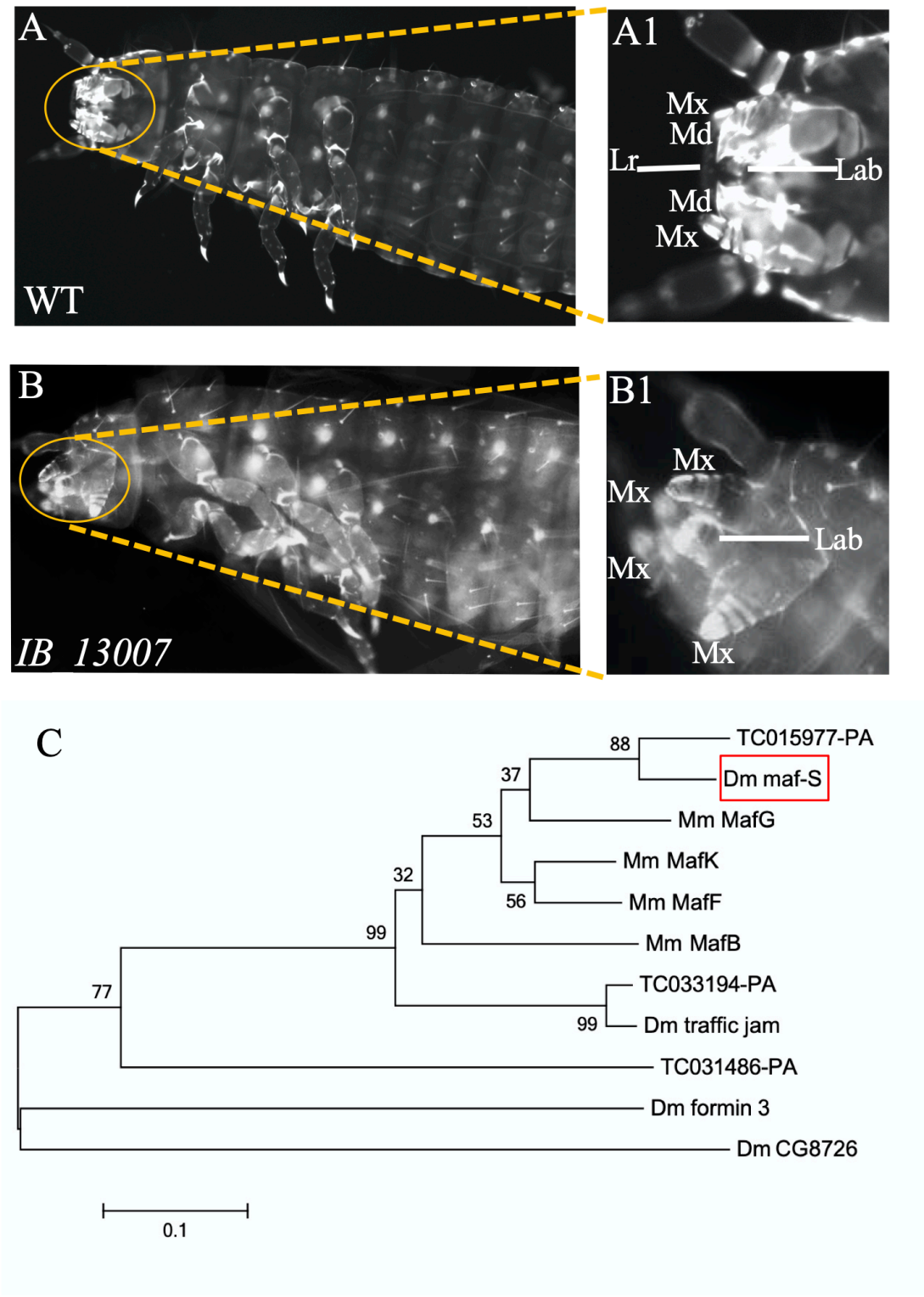

Figure 4.7 Cuticle phenotypes and phylogenetic tree of *IB_13007*.

Cuticles in ventral view. (A & A1) Larval heads were oriented with the anterior towards the left. Cuticles of wt have one pair of maxillae and mandibles and one labrum in the head region. (B & B1) Cuticles with *IB_13007* RNAi showed four maxillae, no labrum and no mandibles. This

phenotype indicated a transformation of mandibles to maxillae and a loss of the labrum. (C) A phylogenetic tree was constructed based on the Maximum likelihood method. The *IB_13007* fragment targets the gene TC015977 most closely related to *Maf-S* (marked with red box) in *Drosophila*. (A1 & B1) Close-ups of head appendages of wt and RNAi, respectively. Lr (Labrum); Mx (Maxillae); Md (Mandible); Lab (Labium). *Dm: Drosophila melanogaster; Mm: Mus musculus.*

Injection of the fragment *IB_15557* led to loss of abdominal segments and absent distal parts of the legs both in the primary screen and re-screen (Fig 4.8B). Orthology analysis revealed that this gene was orthologous to TC031047. I found that the genome position of *Tc-Pan (Tc-Pangolin)* was close to *IB_15557* in the *Tribolium* genome (Fig 4.9).

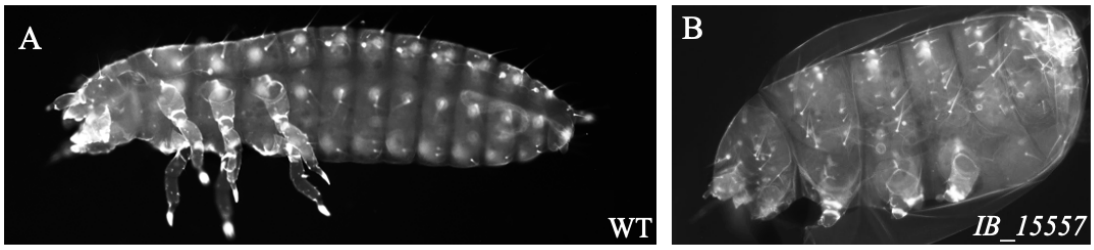

Figure 4.8 larval cuticle of *IB_15557* RNAi.

Cuticles in lateral view. (A) Wt larval contained three thoracic and eight abdominal segments. (B) Knockdown of *IB_15557* caused loss of abdominal segments and the distal parts of the legs were not present.

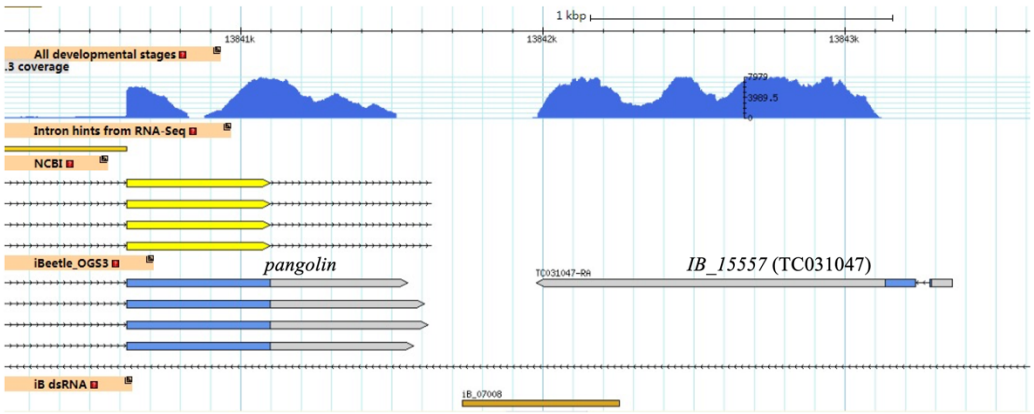

Figure 4.9 Position of *Tc-Pan* and *IB_15557* were annotated in the *Tribolium* genome.

TC031047 was annotated with a surprisingly short open reading frame (blue) on the opposite strand to *Tc-Pan*. However, on the same strand as *Tc-Pan*, 1141bp of sequences were identified to be identical between the published mRNA of *Tc-Pan* and the reverse complement of TC031047 (Fig 4.10). This opened the possibility that this gene was an erroneous annotation while in reality, this sequence was part of the *Tc-Pan* gene. Indeed, knockdown of *Tc-Pan* showed loss of distal parts of appendages and of posterior abdominal segments (Bolognesi et al., 2009). I found that TC031047 was expressed ubiquitously like *Tc-Pan*. Taken together, these data indicated that the sequence of TC031047 was actually a part of well-studied gene *Tc-Pan* but was erroneously annotated as another gene in *Tribolium* genome. Therefore, it was decided not to do research on this gene.

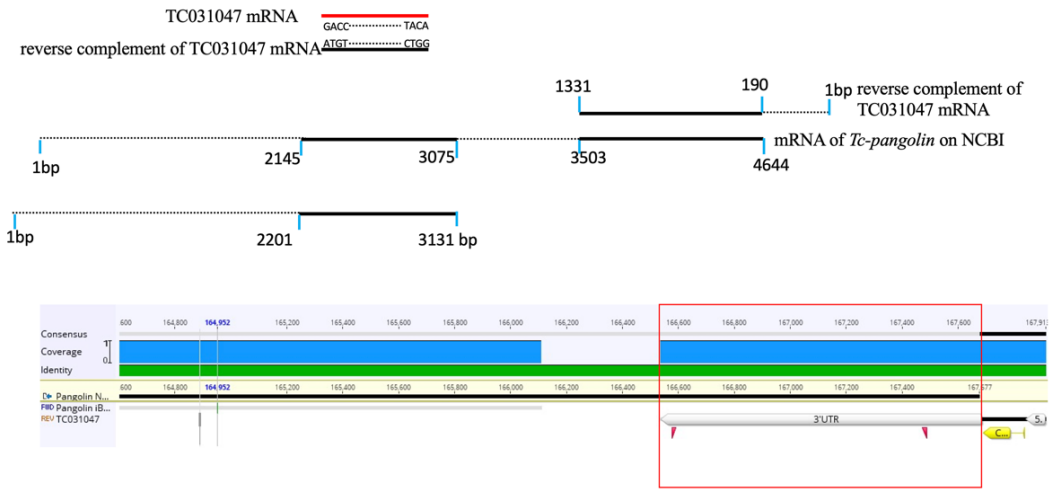

Figure 4.10 Alignment of mRNA sequence between *Tc-Pan* and *IB_15557*.

Reverse complement sequence of TC031047 mRNA was identical with sequence of *Tc-Pan* mRNA published in the *iBeetle*-database (red box).

In summary, the re-screen revealed that the phenotypes for several genes was too unspecific to be followed up and that the two with very specific and interesting phenotypes had targeted genes with known functions or with functions very similar to *Drosophila* data making them less interesting to follow up.

4.2 Two new genes affected maintenance of segment boundaries and appendages development

4.2.1 Identification of empty egg phenotypes *IB_02501* and *IB_00737*

A large number of phenotypes in the primary screen were empty egg phenotypes, where no recognizable cuticle structures were inside the egg shell. Empty egg phenotypes provided no cuticle for judging likely functions, because the embryo died before it developed into a larva. Usually, empty egg genes (i.e. genes that lead to empty egg phenotypes) were not expected to be of interest for understanding embryonic development. However, some of them such as *Tc-axin*, *Tc-otd*, and *Tc-cad* were identified affecting segmentation (Copf et al., 2004; Fu et al., 2012; Schröder, 2003). Therefore, a number of empty egg genes were re-screened and the development of the embryos after knockdown were observed. Some of them were followed up in the lab of Michael Schoppmeier (Erlangen). That work revealed two interesting empty egg gene fragments *IB_02501* and *IB_00737* that functions in same metabolic pathway. *IB_02501* and *IB_00737* targeted genes number TC015651 and TC004619 and phylogenetic trees done by M. Schoppmeier and by myself revealed that TC015651 was an ortholog of *Dm-GlyS* (*Glycogen synthase*; CG6904), and TC004619 was the ortholog of *Dm-AGBE* (*1,4-Alpha-Glucan Branching Enzyme*; CG33138) (Fig 4.11), both of which acted in the glycogen synthesis pathway. Based on this finding, I started a closer analysis.

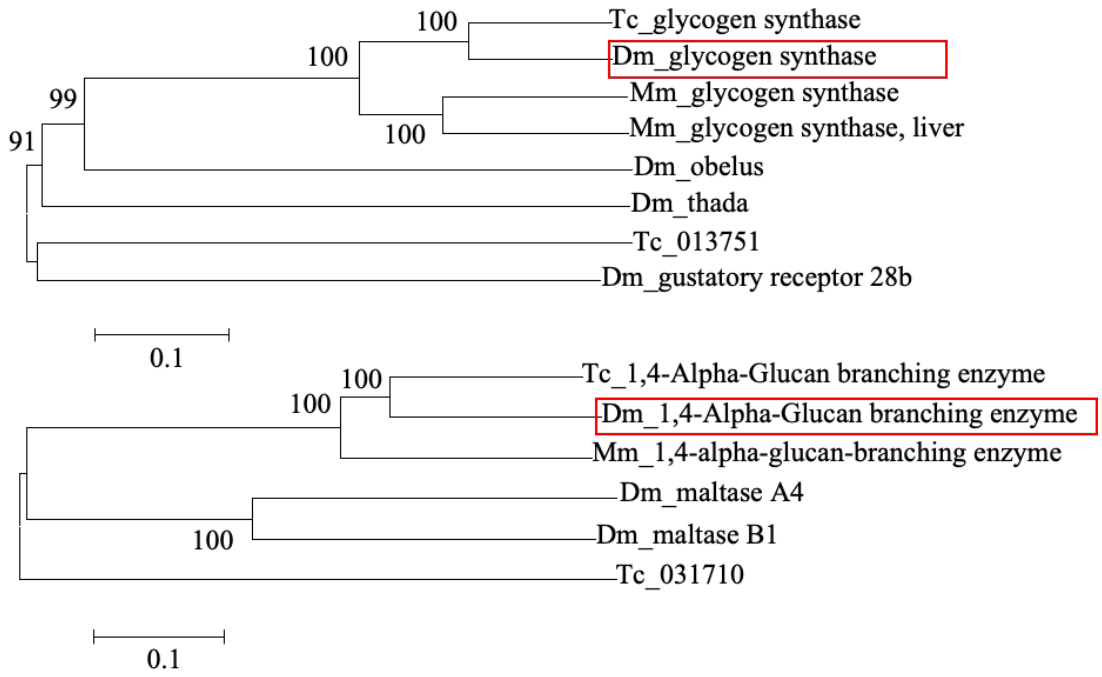

Figure 4.11 Phylogenetic tree of TC015651 and TC004619.

Sequences were downloaded from *iBeetle* database and aligned by ClustalW algorithm of Mega 6. The closest *Drosophila* orthologs of TC015651 and TC004619 were identified and marked with a red box. *Dm*: *Drosophila melanogaster*; *Mm*: *Mus musculus*.

To confirm whether the RNAi phenotypes could be reproduced and to exclude off-target effects, non-overlapping fragments were designed and synthesized. Each gene was targeted with non-overlapping fragment and *iBeetle* fragment by dsRNA injection into 10 female pupae. Knockdown of *Tc-GlyS* and *Tc-AGBE* with different dsRNA fragments produced similar empty egg phenotypes (Fig 4.12 B & C). Quantitative analysis of *Tc-GlyS* and *Tc-AGBE* RNAi cuticles showed higher penetrance of empty egg phenotypes injected with the original *iBeetle* fragments than non-overlapping fragments (Fig 4.12 D). Therefore, dsRNA of the original *iBeetle* fragments were used for follow-up experiments due to their higher RNAi efficiency.

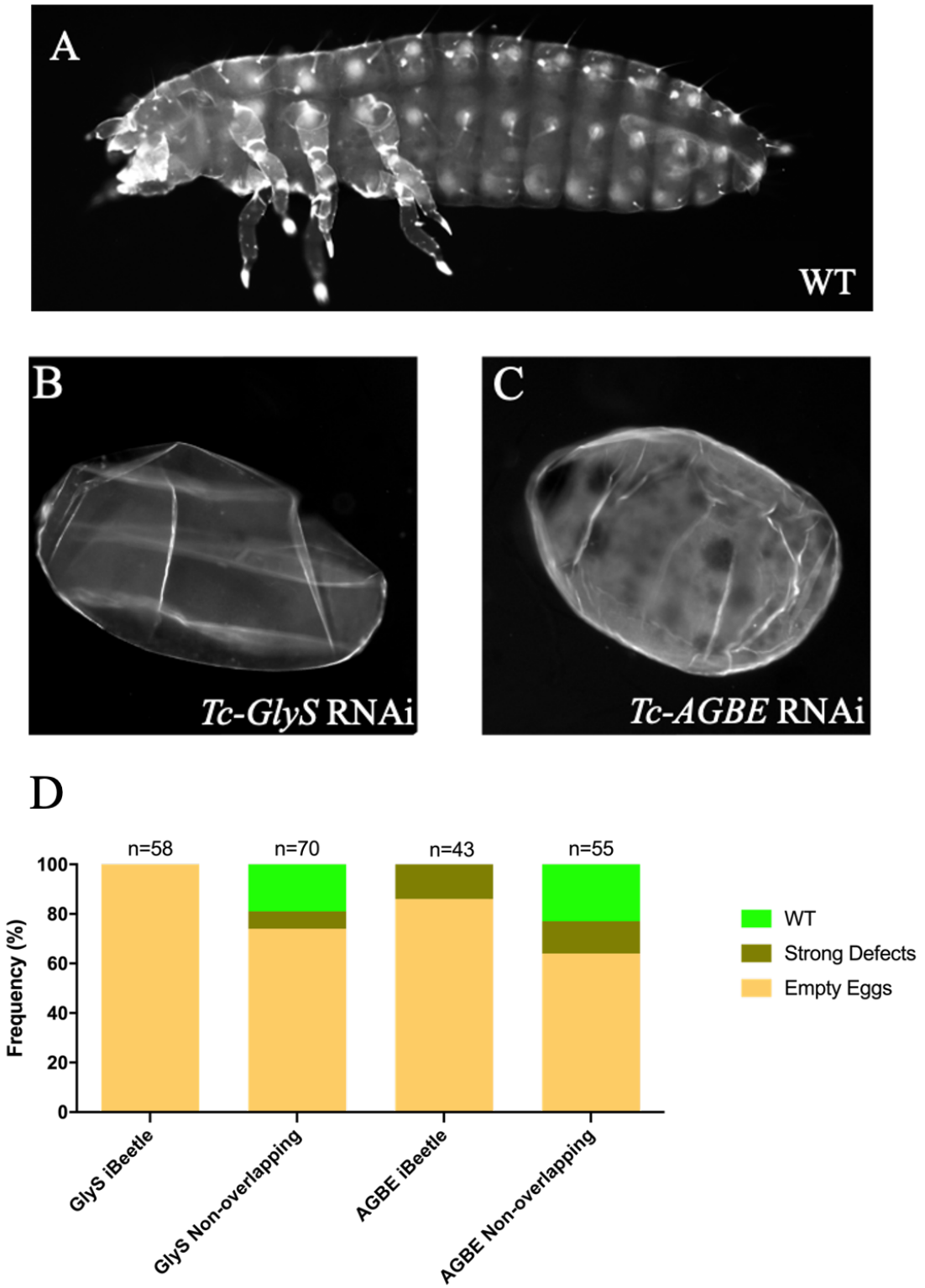

Figure 4.12 Cuticle phenotypes after *Tc-GlyS* and *Tc-AGBE* RNAi.

(A) WT larva. (B, C) knockdown of *Tc-GlyS* and *Tc-AGBE* with non-overlapping fragments. Anterior was toward the left. (D) 74% and 64% empty egg phenotypes were found in *Tc-GlyS* and *Tc-AGBE* RNAi with non-overlapping fragments, respectively. In contrast to non-overlapping fragments, 100% and 86% of empty egg phenotypes were produced by injection with *iBeetle*

fragments. “Strong defects” means cuticles with un-identifiable segments, cuticle remnants or inside-out phenotypes.

4.2.2 Expression of *Tc-GlyS* and *Tc-AGBE* mRNA at early stages

Tc-GlyS and *Tc-AGBE* transcripts were found predominantly at one of the poles and in randomly distributed lateral patterns before the staining became ubiquitous (A, B, C & H, I, G). At the time of blastoderm formation and differentiation, *Tc-GlyS* and *Tc-AGBE* were found to be expressed ubiquitously (D, K). During germ-band growth stages, *Tc-GlyS* and *Tc-AGBE* remained distributed ubiquitously throughout the entire embryos (E, F, G & L, M, N).

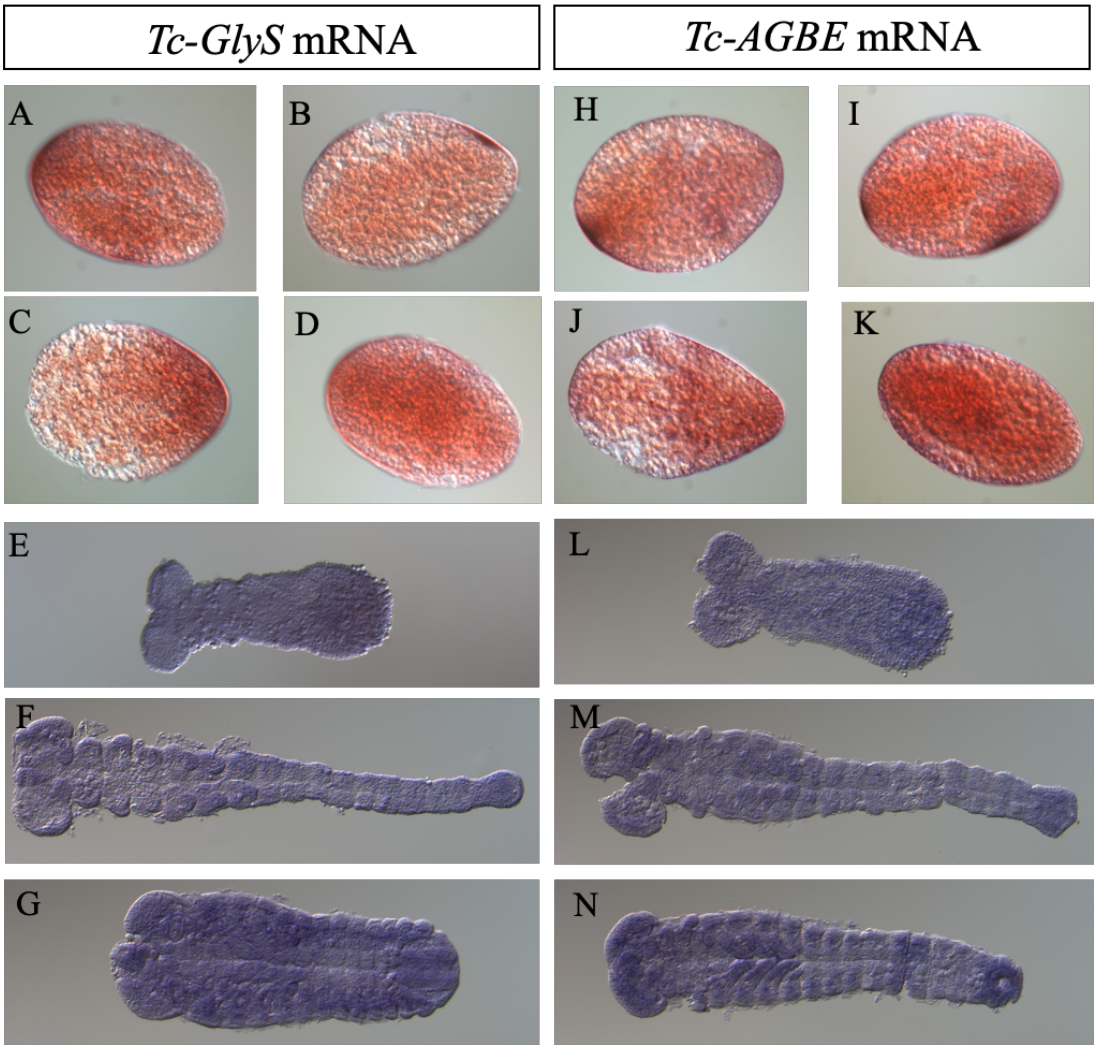

Figure 4.13 *Tc-GlyS* and *Tc-AGBE* showed ubiquitous expression during embryogenesis.

ISH marked *Tc-GlyS* and *Tc-AGBE* expression at different stages of embryo development including

early blastoderm stages (A-D & H-K) and germ-band growth stages (E-G & L-N). (A, B & H, I) *Tc-GlyS* and *Tc-AGBE* transcripts localized at the random poles and lateral sides. (C, D & J, K) The expression of both enzymes spread to most areas of the embryos. (E-G & L-N) *Tc-GlyS* and *Tc-AGBE* exhibited ubiquitous expression in the embryos in subsequent germ-band stages.

Both enzymes (*Tc-GlyS* and *Tc-AGBE*) catalyze glycogen synthesis in the glycolytic pathway affecting glycogen storage, which is essential for early *Tribolium* morphogenesis (Frame and Cohen, 2001). The content of glucose and glycogen are not stable at oogenesis and embryogenesis stages in insects (Jorge et al., 2007; Vital et al., 2010). To confirm the prerequisite for participation of both enzymes in early embryonic development, the expression levels of *Tc-GlyS* and *Tc-AGBE* in wt embryos were quantified using RT-PCR in 0-72 hours covering the entire embryogenesis. Among *Tribolium* tissues, highest expression level of *Tc-GlyS* and *Tc-AGBE* were detected at 0-5 hours, followed by 11-24 hours and 24-48 hours after oviposition (Fig 4.14). The amount of expression of *Tc-GlyS* and *Tc-AGBE* were extremely reduced at 11-72 hours compared with 0-5 hours after oviposition. Interestingly, *Tc-GlyS* levels continued to decline while the *Tc-AGBE* levels remained at a similar low after 11 hours.

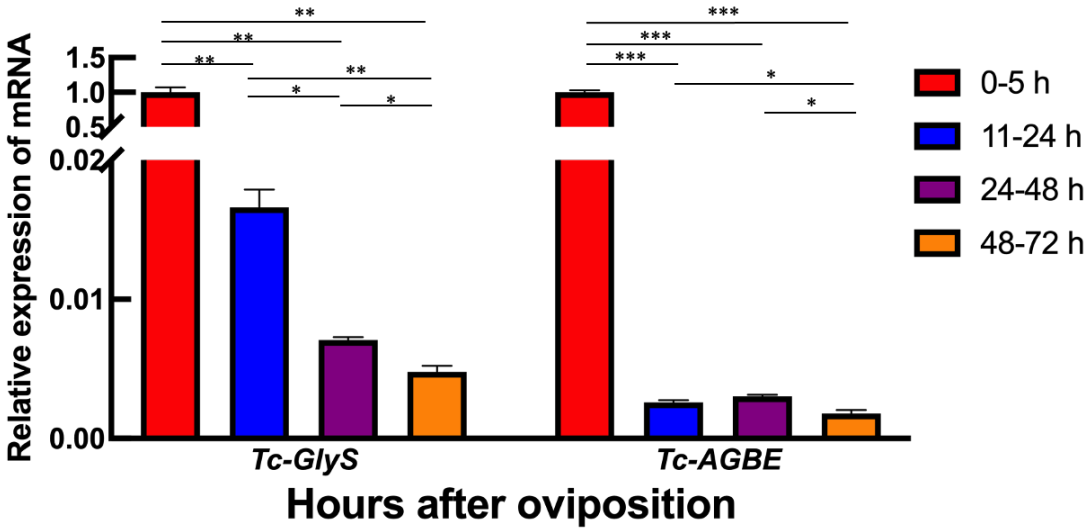

Figure 4.14 RT-PCR validation of *Tc-GlyS* and *Tc-AGBE* levels during 0-72 hours embryogenesis.

RPS and *GAPDH* as the reference genes were used for the normalization. The expression of *Tc-GlyS* and *Tc-AGBE* were highest in first 0-5 hours. A largely decrease of *Tc-GlyS* and *Tc-AGBE* levels were after 5 hours. Later, both enzymes maintained very low levels in embryos. Significant difference was calculated with t-test between groups (* $p < 0.05$; ** $p < 0.01$; *** $p < 0.001$; n=3).

4.2.3 Embryonic development prior to cuticle formation after *Tc-GlyS* and *Tc-AGBE* RNAi

To examine timing and nature of the embryonic defects by injection of *Tc-GlyS* and *Tc-AGBE* dsRNA during *Tribolium* embryogenesis, I observed the series of phenotypes between 0-72 hours with nuclear staining (DAPI). Analysis of early offspring of knock-down embryos revealed that blastoderm morphology and germ rudiments were not altered compared with normal embryogenesis (Fig 4.15 Aa-Ca & Ab-Cb). At germ-band extension stages, segments are added gradually from the posterior growth zone. At that stage, posterior abdominal segments appeared to be slightly bent (Fig 4.15 Bc-Cc & Bd-Cd). Later, segmental boundaries were irregular, leading to loss of visible segmental boundaries and grooves (Fig 4.15 Be, Ce). With time, the affected area covered all abdominal segments, but also limbs and gnathal appendages were affected. In severely affected phenotypes of a later stage, almost all segment boundaries were deranged including thoracic and head segments, resulting in a shortened A-P axis and a reduced number of anterior appendages. Segment disruption was stronger in the ventral region compared to the dorsal region. In less affected embryos, some head and thoracic segment boundaries formed dorsally and ventrally, but gnathal and distal limbs were malformed or partially absent (Fig 4.15 Bf, Cf). Normally, after complete germ-band retraction, the dorsal organ becomes internalized and dorsal closure occurs. However, no embryos of this stage were observed in RNAi both treatments (Fig 4.15 Ag). This indicated that after the previous shortening and truncation of segments the embryos stopped development and degenerated such that no cuticle was formed.

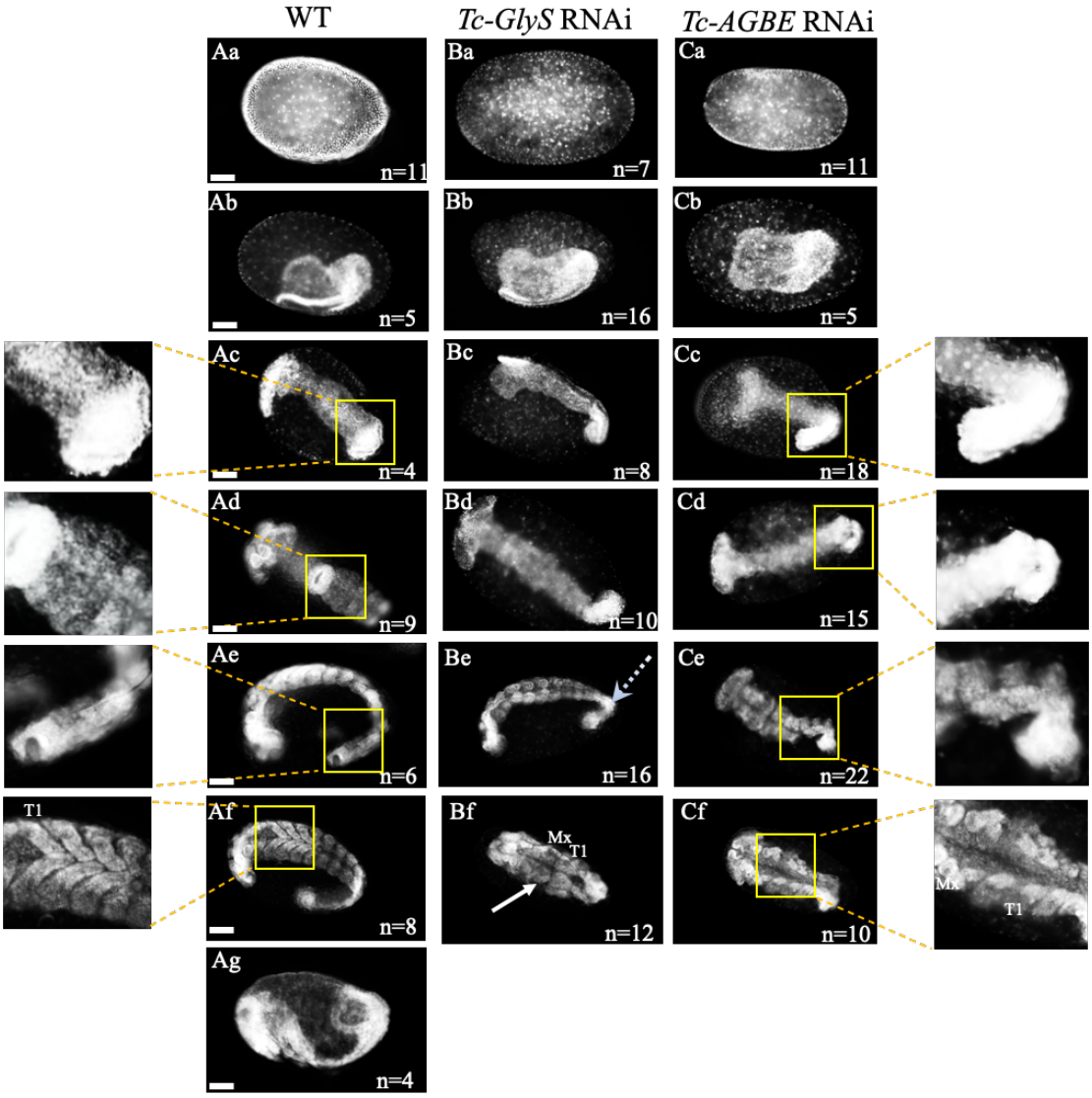

Figure 4.15 Embryonic phenotypes after *Tc-GlyS* and *Tc-AGBE* RNAi.

Embryo development during 0-72 hours with DAPI staining to visualize nuclei in fixed embryos (white). Scale bars, 100 μm. Mx (Maxilla); T1 (first thoracic segment). Panel Aa-g showed wt embryos as control. B & C represented knock-down embryos. (Aa-Ca & Ab-Cb) After *Tc-GlyS* and *Tc-AGBE* RNAi, the uniform blastoderm started to rearrange and differentiate resulting in the serosa and embryonic rudiment without visible defects. (Bc-Cc & Bd-Cd) Gnathal and thorax exhibited signs of segmentation and the boundaries became visible accompanied by germ-band extension. However, the posterior part of abdomen was affected and bent and segment boundaries were absent. Close-ups of the posterior region of abdominal segments were showed with yellow boxes on both sides. (Ae) Wt embryos reaching full germband extension. (Be, Ce) A wide range of segment boundaries were defect (yellow box) or completely missing (dotted arrow) in the ventral region.

(Af-Cf) Leg development reached maximum length at germ-band retraction stage in normal embryogenesis, whereas strongly disruption of segment boundaries was displayed in the shorten A-P axis covering the gnathal, thorax and abdomen region knock-down embryos (arrow). In less affected embryos, all limbs on the thoracic and gnathal segments stopped outgrowth, although segment boundaries were still present.

4.2.4 Silencing of *Tc-GlyS* and *Tc-AGBE* induces apoptosis in head and trunk

Based on DAPI staining it appeared that the embryo was degenerating at later stages. Therefore, we performed immunofluorescence staining to detect and localize apoptotic cells during different embryonic phases after RNAi. The number of apoptosis-positive cells on head and trunk were significantly increased compared with wt embryos at early germ-band stages (Fig 4.16 Ab-c and B, C). Most of dying cells were located along the ventral midline in a diffuse way. During germline expansion, most apoptotic cells were located in the trunk region, including thoracic and abdominal segments (Fig 4.16 Ae, f, B, C). No obvious alteration was observed in the anterior head region at fully elongation stages, although the region of specific cell apoptosis larger than the region where I found strong RNAi effects (Fig 4.16 Ah, i). The number of apoptotic cells was similar to that of wt in head and trunk region, but an influence of *Tc-GlyS* RNAi was found in the germ-band region (Fig 4.19 Ag, h, i). Furthermore, no significant difference of apoptosis was detected in growth zone both in untreated and RNAi embryos, which could be interpreted that this developmental process still functioned (Fig S7.5).

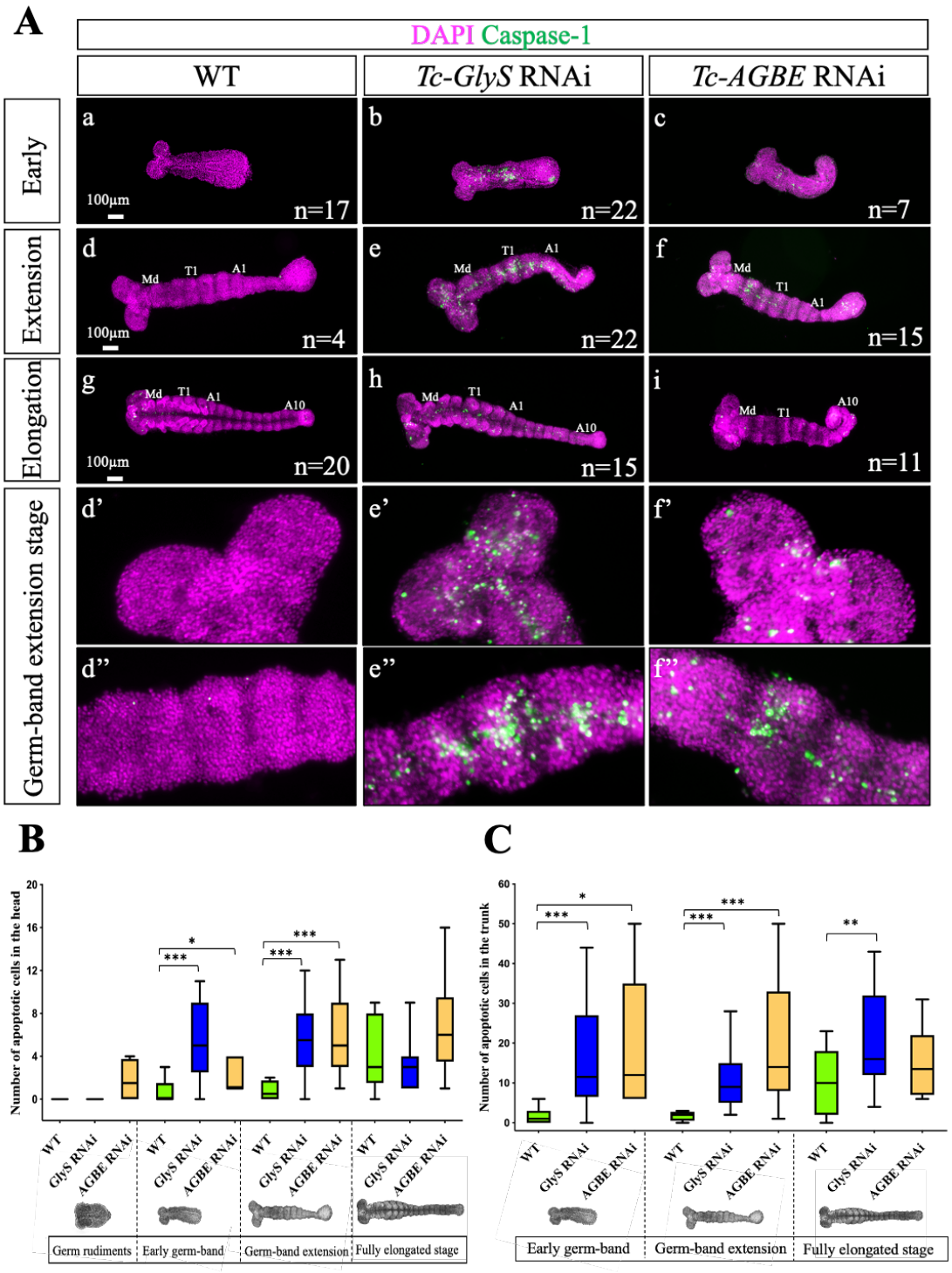

Figure 4.16 Cell apoptosis induced by *Tc-GlyS* and *Tc-AGBE* RNAi at different developmental stages.

Anterior to the left. Apoptotic cells were monitored with an antibody against *Drosophila* Caspase-1 (Dcp-1) (green) (Florentin and Arama, 2012). Md (Mandible); T1 (first thoracic segment); A1, A10 (first, 10th abdominal segment). Scale bars, 100 μm. (Aa, d, g) Not much cell death was detected in wt embryos at different stages. (Ab, c, e, f) During early germ-band and extension stages,

the number of apoptotic cells increased significantly in both head and germ-band region when treated with RNAi. (Ad'-f', d''-f'') Magnification of corresponding embryos in head and germ-band region at extension stages. (Ah, i) No significant increase of apoptotic cells was found in the head region at full elongation stages, but *Tc-GlyS* knock-down embryos still displayed more cell death in the trunk region. (B, C) Box plots were constructed to visualize the distribution of the numbers of apoptotic cells at four development stages. B showed the values for the head, C for the trunk. Significance was calculated with the t-test between groups (* $p < 0.05$; ** $p < 0.01$; *** $p < 0.001$; n>3).

4.2.5 *Tc-GlyS* and *Tc-AGBE* functions in appendages outgrowth

To test, in what way functions of *Tc-GlyS* and *Tc-AGBE* were involved in appendage outgrowth, I analyzed marker genes expression patterns of developing legs and gnathal appendages in both knock-down embryos. In wt embryos, *Tc-dac* expression domains were detected in the prominent sub-distal parts of appendages and antennae and in the head lobes (Fig 4.17 A) (Prpic et al., 2001). Additional weak expression was found in the proximal legs (black arrow in Fig 4.17 A). After *Tc-GlyS*/*Tc-AGBE* RNAi, the expression of *Tc-dac* in the proximal and distal domains of the limbs was strongly reduced, while gnathal appendages and head expression was not or much less affected. Moreover, an extremely weak expression appeared on the distal tip of legs in some *Tc-GlyS* knock-down embryos (white arrow in Fig 4.17 B). The wild-type expression pattern of *Tc-Dll* was in the distal part of all appendages including labrum and antennae except for the mandible (Fig 4.17 D) (Siemanowski et al., 2015). A similar expression domain of *Tc-Dll* was found in both RNAi treatments compared to the control, while the appendages appeared shortened (Fig 4.17 E & F). In fully elongated appendages of wt, *Tc-Sp8* was expressed in multiple ring-shaped patterns in gnathal, antennal appendages and walking legs (black arrows in G). Like the expression of *Tc-dac* and *Tc-Dll*, *Tc-Sp8* expression was more diffuse in the head lobes (Fig 4.17 G). After knockdown of *Tc-GlyS* and *Tc-AGBE*, the ring-shaped expression of *Tc-Sp8* of fully elongated embryos was reduced and replaced by one domain on the distal parts of the

shortened appendages. The development of limbs at young stages was normal after removing function of *Tc-GlyS*/*Tc-AGBE*, which seemed to indicate that appendage development stalled at a later stage and that they were not able to elongate. In contrast, *Tc-Sp8* expression in mandibles and antennae showed similar pattern to that of wt embryos (Fig 4.17 H & I). In summary, the distal parts of knock-down embryos were comparably normal (*Tc-Dll* and distal *Tc-Sp8* pattern) while the medial parts appeared to be affected (*Tc-dac*, lower *Tc-Sp8* ring), indicating the outgrowth of appendages except the mandible requires function of *Tc-GlyS* and *Tc-AGBE*.

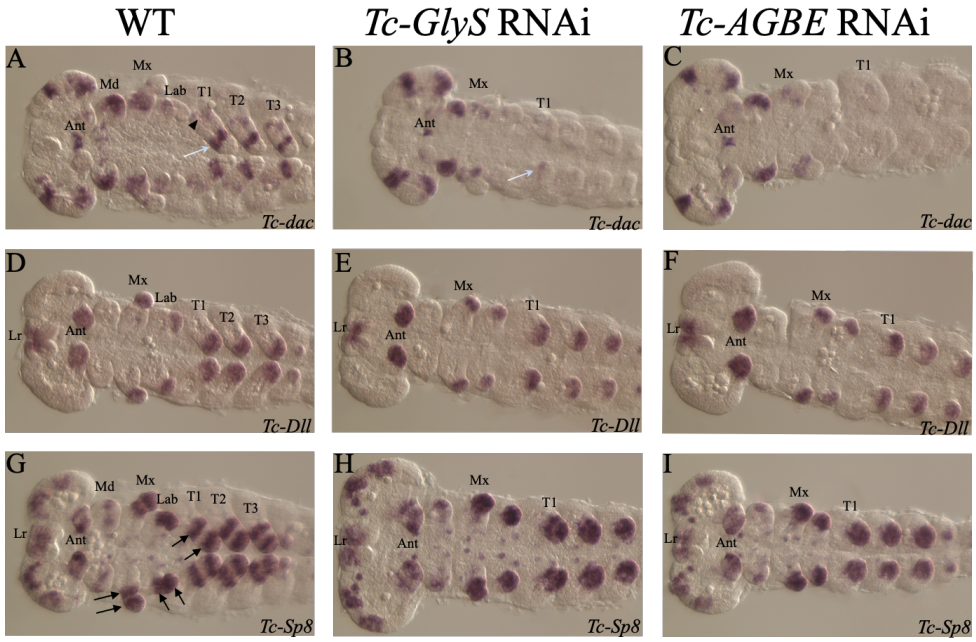

Figure 4.17 The expression of appendage patterning genes after *Tc-GlyS*/*Tc-AGBE* knock-down embryos.

(A, D, G) Wild-type; (B, E, H & C, F, I) *Tc-GlyS* and *Tc-AGBE* knock-down embryos shown at late elongation or early retraction stages. (A) In the wt embryos, strong expression domains of *Tc-dac* covered a subterminal domain in all walking legs. In contrast, to strong expression of *Tc-dac* in distal part of legs (white arrow), relatively weak expression was found in the proximal of legs (black arrowhead). (B, C) After depletion of *Tc-GlyS*/*Tc-AGBE*, *Tc-dac* expression was absent in all thoracic limbs, while some of *Tc-GlyS* RNAi embryos showed extremely weak expression in distal domain of leg segment (white arrow in B). (D) *Tc-Dll* was expressed in the labrum and the most distal parts of limbs, antennae, and gnathal segments except mandibles in wt embryos. (E , F) There was no difference of *Tc-Dll* expression found in both RNAi treatments. (G, H, I) Two ring-shaped

Tc-Sp8 expression domains were found in thoracic limbs, maxillae and labia (double black arrows), but the proximal ring was not detected after *Tc-GlyS*/*Tc-AGBE* RNAi. Instead, *Tc-Sp8* showed a distal expression on shortened appendages. (B, C, E, F, H, I) All knock-down embryos exhibited shortened maxillae, labia and thoracic limbs in comparison to those of wt embryos. Lr (Labrum); Ant (Antenna); Mx (Maxillae); Md (Mandible); Lab (Labium); T1-T3 (first-third thoracic segment).

4.2.6 *Tc-GlyS* and *Tc-AGBE* affect segment boundaries and head development

In order to explore segment formation before embryos decay and end up as empty eggs, I assessed the expression patterns of the segmentation genes *Tc-wingless* (*Tc-wg*) and *Tc-hedgehog* (*Tc-hh*) after knockdown of *Tc-GlyS* and *Tc-AGBE* during segmentation. The expression of *Tc-wg* and *Tc-hh* was analyzed at germ-band extension and elongation stages by double fluorescent in-situ hybridization (Fig 4.18 B1-B4). Irregular *Tc-wg* and *Tc-hh* expression was found in *Tc-GlyS* and *Tc-AGBE* knock-down embryos, where reduced gaps between *Tc-wg* or *Tc-hh* adjacent stripes and partially absent stripes were observed at early germ-band stages. The disordered stripes first appeared in the abdomen (white arrowheads in Fig 4.18 C1-C4 & E1-E4). Later, extremely malformed abdominal stripes were observed during the elongation, resulting in asymmetrical disruption of many abdominal segments. At the same time, abnormal patterning of gnathal and thoracic segments was found, indicating that the irregularities started in abdominal segments but affected almost all segments (white arrows in Fig 4.18 D1-D4 & F1-F4). Normally, the labrum has marked with two wedges of *Tc-wg* stripes along its proximodistal (P-D) axis, while the complete loss of the labrum was observed in strong RNAi affected embryos (*Tc-GlyS* RNAi, n=13, 62%; *Tc-AGBE* RNAi, n=11, 56%) (Fig S7.4). Interestingly, knock-down embryos had a bent abdomen, in which boundary grooves were not visible any more (Fig 4.16 D1, D2 & F1, F2). Hence, segmentation initially proceeded normally but segment boundaries appeared to decay (e.g. in the thorax) while later segment boundary maintenance may be affected after depletion of *Tc-GlyS* or *Tc-AGBE* function.

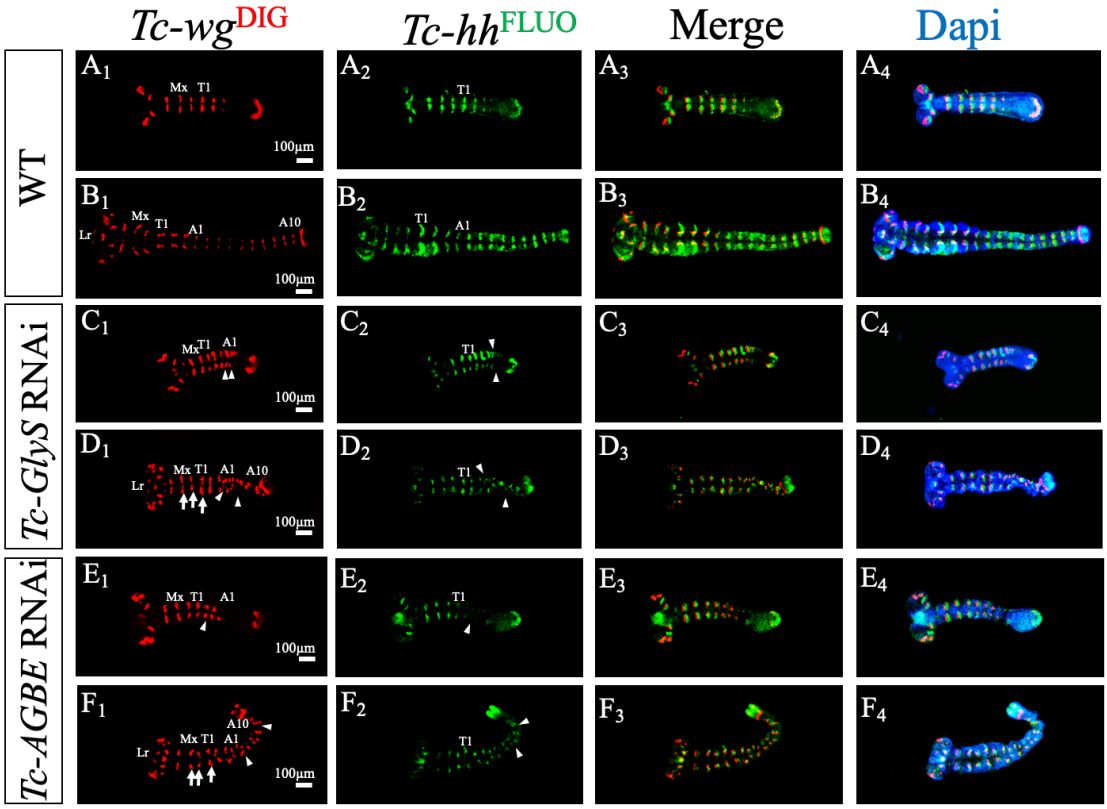

Figure 4.18 Expression of *Tc-wg* and *Tc-hh* on segmentation were repressed in *Tc-GlyS*/*Tc-AGBE* knock-down embryos.

(A-F) Double fluorescent in situ hybridization (FISH) in embryos to visualize *Tc-wg* and *Tc-hh* expression in wt and RNAi groups at both germ-band extension and elongation stages. Scale bars, 100 μm. Segment polarity genes *Tc-wg* and *Tc-hh* were marked red and green color, respectively. Lr (Labrum); Mx (Maxillae); T1 (first thoracic segment); A1, A10 (first, 10th abdominal segment). (A4-F4) DAPI staining (blue) was used for visualization of the nucleus. Anterior was towards the left. (A1-A4, B1-B4) *Tc-wg* and *Tc-hh* expression in wt embryos at different stage. (C1-C4, E1-E4) The distance between adjacent stripes of segments posterior to T1 was changed. Some stripes at one side were obviously missing. *Tc-GlyS* RNAi n= 27, 63%; *Tc-AGBE* RNAi n=21, 61% (white arrowheads) . (D1-D4, F1-F4) In fully elongated germ-bands, the range of irregular and missing stripes expanded towards anterior. The abnormal shape of *Tc-wg* expression was found in some head segments (e.g.in maxillary and labial segments), and thoracic segments were disordered (white arrows). The abdominal segments displayed a certain degree of bending. *Tc-GlyS* RNAi n=22, 100%; *Tc-AGBE* RNAi n=14, 93%.

To test, whether the interaction of segment polarity genes was maintained after depletion of *Tc-GlyS* and *Tc-AGBE*, we investigated *Tc-engrailed* (*Tc-en*) expression which is regulated by *Tc-wg* in adjacent cells. *Tc-en* is co-expressed with *Tc-hh* in same cells of the posterior segmental compartments (Lim and Choe, 2020; Peifer and Bejsovec, 1992). During early embryogenesis, *Tc-en* expression in stripes was similar to expression pattern of *Tc-hh*, except for the labrum, ocular segment (oc) and growth zone (Fig 4.19 A, D, G). In embryos with less than 4 or 5 stripes at early germ-band stage, *Tc-en* expression was not altered obviously after *Tc-GlyS* and *Tc-AGBE* RNAi (Fig 4.19 B, C), whereas at later stages segment boundaries showed irregular distance or orientation of *Tc-en* stripes (arrowheads in Fig 4.19 E, H, F, I). The severity of the impact gradually increased with the developmental age of embryos. Shrinkage and absence of *Tc-en* and *Tc-wg* stripes were both observed in multiple segments, where some abdominal segments were morphologically aberrant (arrows in Fig 4.19 H, I). In strong RNAi embryos, *Tc-wg* stripes on the labrum were almost completely deleted in the anterior head (asterisk showed in Fig 4.19 H, I). Taken together, these experiments showed that *Tc-GlyS* and *Tc-AGBE* were involved in maintaining the expression of the segment polarity genes *Tc-wg*, *Tc-hh*, and *Tc-en* at the parasegmental boundary while the formation appeared to be undisturbed (Choe et al., 2006; Ober and Jockusch, 2006).

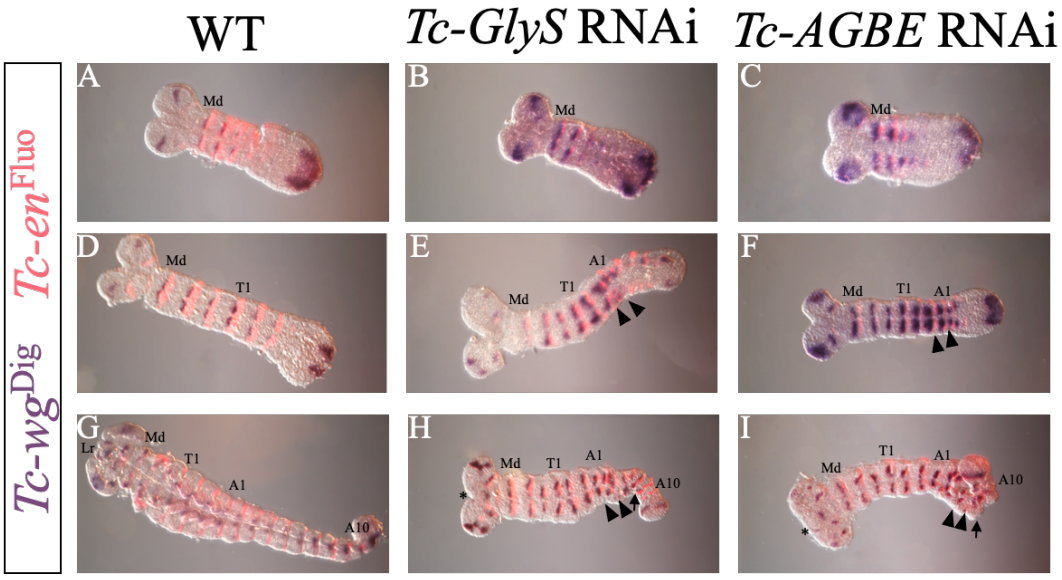

Figure 4.19 *Tc-en* and *Tc-wg* co-expression in *Tc-GlyS* and *Tc-AGBE* RNAi germ-bands.

Double ISH was used for visualization of *Tc-wg* and *Tc-en* expression and signals were labeled with

NBT/BCIP (blue) and TSA-Dylight555 (red), respectively. Lr (Labrum); Md (Mandible); Mx (Maxilla); T1 (first thoracic segment); A1, A10 (first, 10th abdominal segment). (A, D, G) *Tc-en* and *Tc-wg* were expressed in gnathal segments, three thoracic and eight abdominal segments in wt embryos. (B, C) No obvious changes were found in RNAi embryos at early germ-band stages until four or five segments were formed. (E, F) The gaps between adjacent stripes of abdominal segments were abnormal (arrowheads). (H, I) Irregularities and aberrant *Tc-en* and *Tc-wg* stripes were observed in the posterior trunk region, presenting a twisted abdomen during later stages (arrows).

4.2.7 *Tc-GlyS* and *Tc-AGBE* are not required for growth zone patterning

To determine whether the growth zone was affected after *Tc-GlyS* and *Tc-AGBE* RNAi, I analyzed the expression of the segmentation gene *Tc-even-skipped* (*Tc-eve*) and the posterior marker gene *Tc-caudal* (*Tc-cad*) during embryogenesis. In wildtype, *Tc-eve* expression is in a wide stripe in the pre-segment region and in the posterior growth zone. As the germ-band elongates, two broad stripes form from this domain, which determine a double segmental pattern in the growth zone (white bars). At the region of segment boundary formation, these stripes resolve into secondary stripes (arrowheads in Fig 4.20 A_2 & B_2) (O and Choe, 2020). In RNAi embryos, the *Tc-eve* expression showed a normal pattern as in control embryos both at early germ-band and extension stages suggesting that *Tc-GlyS* or *Tc-AGBE* did not participate in the regulation of the PSR (arrowheads in Fig 4.20 C_2-F_2). *Tc-cad* was expressed in the entire growth zone in young embryos in a similar way (Fig 4.20 C_1-F_1, C_3-F_3). Based on these results, I assumed that *Tc-GlyS* and *Tc-AGBE* were not required for the generation of posterior segments in the growth zone by *Tc-cad* and the primary pair-rule gene *Tc-eve*.

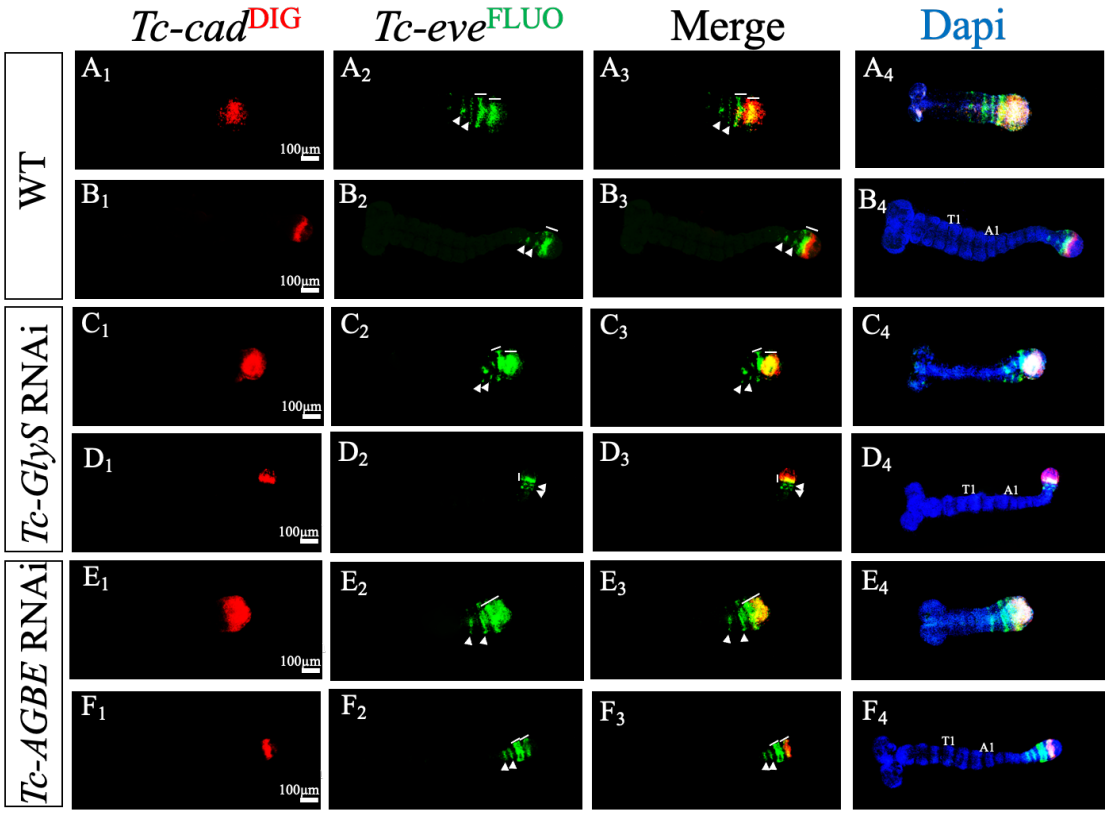

Figure 4.20 Expression of growth zone marker genes after *Tc-GlyS* and *Tc-AGBE* RNAi.

(A-F) Double ISH embryos were stained with the posterior marker gene *Tc-cad* (red color), and the segmentation gene *Tc-eve* (green color). DAPI staining (blue color) was used to visualize the shape of embryos. Scale bars, 100 μm. (A, C, E & B, D, F) The expression of *Tc-eve* and *Tc-cad* in wt and RNAi embryos at both early germ-band and extension stages, respectively. (A_1-A_4, B_1-B_4) *Tc-cad* expression covered the posterior growth zone. (C_1-F_1) Same *Tc-cad* expression pattern was observed in *Tc-GlyS* and *Tc-AGBE* RNAi embryos compared to the control. (A_2-F_2) Downregulation of *Tc-GlyS* and *Tc-AGBE*, *Tc-eve* expression was as in wt embryos. (A_3-F_3) Overlapping parts between *Tc-cad* and *Tc-eve* appeared in growth zone.

4.2.8 Testing whether *Tc-GlyS* and *Tc-AGBE* function via the Wnt and Hh pathways

Interestingly, the activity of *GlyS* is increased by inhibition of *GSK-3* which at the same time has a critical role in regulating Wnt/β-catenin and Hh signaling pathways (He et al., 1995; Jiang and Struhl, 1996). Given that *Tc-GlyS* has a segmentation phenotype

somewhat similar to segment polarity genes where stripes are formed but later degenerate, I hypothesized that the glycogen metabolism and segmentation might be linked via *Tc-GSK-3*. To test whether *Tc-GlyS* and *Tc-AGBE* RNAi may influence Wnt and Hh signaling, double RNAi with key components of both pathways and *Tc-GlyS* or *Tc-AGBE* were performed. For comparison, single RNAi experiments were added where *dsRed* dsRNA was added to reach comparable dsRNA concentrations as in the double injections. Double knockdown of the Wnt transcription factor *Tc-Pan* and *dsRed* exhibited phenotypes with reduced abdominal segments and distal parts of the legs (41%) (Fig 4.21 Ab & B) as previously described (Bolognesi et al., 2008). In 8% of the cuticles the abdominal and thoracic segments were completely missing. *Tc-Pan*/*dsRed* double RNAi also produced a certain percentage of empty egg phenotypes (38%) and wt cuticles (13%). Depletion of both *Tc-GlyS*/*Tc-Pan* or *Tc-AGBE*/*Tc-Pan* showed a much stronger phenotype with strongly truncated cuticles without any thoracic or abdominal segments besides some relics of the head being observed. A few cuticles of *Tc-AGBE*/*Tc-Pan* RNAi retained residual limbs of first thoracic segment (red asterisk in Fig 4.21 Ag, l) and a similar percentage of empty eggs was obtained. These results indicated that *Tc-GlyS* and *Tc-AGBE* did not function exclusively upstream of *Tc-Pan* (because then, a pan-like phenotype would have been expected). Rather, the two appear to act at least in part additively. A similar result occurred with double RNAi with the Wnt co-receptor *Tc-Arrow (Tc-Arr)*. *Tc-Arr*/*dsRed* displayed a shortened abdomen and a high percentage of empty eggs, which reflected the severity of *Tc-Arr* dsRNA effects (Fig 4.21 Ac & B) (Bolognesi et al., 2009). However, depletion of *Tc-GlyS*/*Tc-Arr* and *Tc-AGBE*/*Tc-Arr* resulted in much stronger phenotypes that lacked signs of segmentation, had limbless cuticles and showed only some identifiable head structures or only small spherical structures (Fig 4.21 Ah & m). Importantly, *Tc-Pan* and *Tc-Arr* RNAi in combination with *Tc-GlyS* or *Tc-AGBE* produced more severely truncated phenotypes than that by single RNAi alone. Cuticles showed a complete lack of segmentation and malformed anterior head appendages, that could be similar to *Tc-wg* and *Tc-wls* RNAi phenotypes (Bolognesi et al., 2008). It seemed to illustrate *Tc-GlyS* and *Tc-AGBE* functions were essential for body axis elongation. Given that interference

with *Tc-GlyS* and *Tc-AGBE* makes both Wnt pathway gene phenotypes stronger indicates that they do not act via the Wnt pathway alone.

A different concentration of dsRNA was used for *Tc-hh* RNAi (2 µg/µl) compared with injection of Wnt components (1 µg/µl) because lower concentration of *Tc-hh* RNAi did not produce strong phenotypes. The phenotypes after *Tc-hh*/*dsRed* double RNAi were classified into three groups: strong, intermediate and weak *Tc-hh* RNAi. Strong *Tc-hh* RNAi displayed a small head and partial absence of appendages. The boundary between the adjacent abdominal segments was not obvious, where some of the segments were reduced or fused. Despite the fact that the number of thoracic segments was normal, most of distal structure of legs was bent (Fig 4.21 Ad & C). Intermediate *Tc-hh* RNAi phenotypes showed similar cuticles to the strong effects, presenting a small head capsule and appendage defects. The abdomen was better developed with some absent or irregular bristles on the abdominal segments (Fig 4.21 Ai & C). The weakly affected cuticles produced a small head capsule where the antenna was completely missing (Fig 4.21 An & C). My analysis revealed that combination of RNAi targeting *Tc-GlyS*/*Tc-hh* or *Tc-AGBE*/*Tc-hh* functions led to great reduction of *Tc-hh* typical phenotypes but higher percentage of empty eggs compared with *Tc-hh*/*dsRed* RNAi (Fig 4.21 C, Af, k). Again, this indicated an additive effect and argued against *Tc-GlyS* or *Tc-AGBE* acting only via the Hh pathway. However, I cannot exclude that they acted via both pathways in parallel, which is not unlikely because *Tc-GSK-3* is involved in signal transduction of both (Jia et al., 2002).

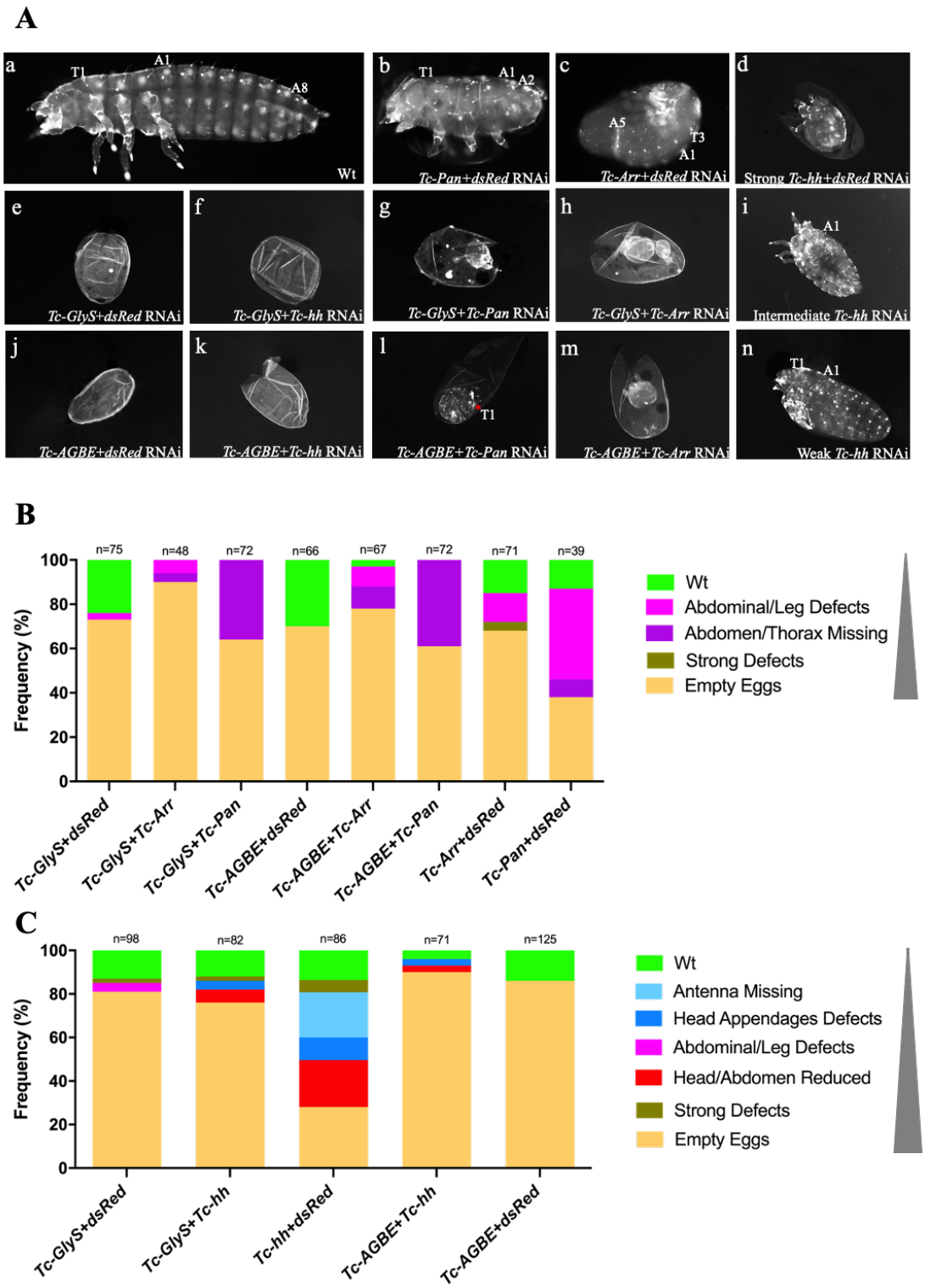

Figure 4.21 Cuticle analysis of double knockdown of Wnt and Hh key components combined with *Tc-GlyS* and *Tc-AGBE*.

(Aa) wild-type cuticle (anterior towards the left) contains head, three thoracic and eight abdominal segments. (Ab, g, l) *Tc-Pan* RNAi was performed in combination with *dsRed*, *Tc-GlyS* and *Tc-AGBE*. (Ac, h, m) *Tc-Arr* RNAi was combined with *dsRed*, *Tc-GlyS* and *Tc-AGBE*. (Ad, i, n) *Tc-hh*/*dsRed*

RNAi phenotypes from strong to weak. (Af, k) Phenotypes after *Tc-GlyS*/*Tc-hh* and *Tc-AGBE*/*Tc-hh* double RNAi. (Ae, j) Empty eggs phenotypes were showed after injection of *Tc-GlyS*/*dsRed* and *Tc-AGBE*/*dsRed* dsRNA (1 µg/µl and 2 µg/µl). (B & C) Phenotypic analysis of double RNAi combined with Wnt and Hh components, respectively. The effects of RNAi phenotypes were increased in turn from top to bottom labeled with grey triangle. Different colors represented corresponding phenotypes. Each dsRNA was used for injection with same concentration and volume. *dsRed* dsRNA was injected as the control. T1, T3: first, third thoracic segment. A1-A8: first-eighth abdominal segment. Red asterisk indicated impaired limbs.

4.2.9 High level of glucose disrupts segmentation formation

Next, I wanted to further elaborate whether glycogen metabolism has an effect on segmentation along the A-P axis. The strategy was through embryonic injection with different doses of glucose, which might influence the activity of *Tc-GlyS*, *Tc-AGBE* and *Tc-GSK-3* with potential effect on the pathways. The concentration of the glucose solution had been diluted with injection puffer and was injected early to influence all 72 hours of *Tribolium* embryogenesis (Fraga et al., 2013). In general, embryonic micro-injection of 2-3 hours after oviposition is often accompanied by high lethality of eggs, but it is effective as a prerequisite to assess stable and specific phenotypes. The injection puffer, as a negative control, expressed higher survival rate (33%) of cuticles in combination with glucose injections. In addition to the wt cuticles, other phenotypes with a lower proportion were discovered in the injections (3% head defects, 3% abdominal/thoracic defects) (Fig 4.22 B). Some specific defects were obtained after injection of 0.1 µg and 0.5 µg glucose, where some eggs developed normally although mortality of eggs increased. Apparently, a group of strong phenotypes (i.e. strong defects of the cuticle along the entire AP axis and only few identifiable segmental structures) were observed when treated with 1 µg glucose, which exhibited a high percentage of specific phenotypes among those developed cuticles (Fig 4.22 Ab-g). Most of cuticles showed a constriction within the abdominal or thoracic segments, where loss of at least one pair of adjacent body segments (arrows in Fig 4.22 Ac, d).

Cuticles with a slightly stronger phenotype had normal head, thorax, and twisted abdominal segments. The constricted phenotypes were only in posterior segments of collapsed regions, which was distinct from truncated phenotypes (Fig 4.22 Ac, d, g). Some cuticles developed into incomplete A-P axis, which resembled truncation phenotypes with fewer thoracic or abdominal segments. In some other severe phenotypes, only parts of gnathal segments remained intact (Fig 4.22 Ae, f). Instead of defects in posterior structures, larvae were characterized by absent head and one or two pairs of the thoracic segments compared with wt cuticles (Fig 4.22 Aa, b). Since glucose injection displayed deletions of neighbored contiguous segments, resembling a gap pattern in the A-P axis, which was highly consistent with phenotypes of *Lrp4* in *Tribolium* (Prühs et al., 2017). A series of phenotypes ranging from mild to severe, such as adjacent segments fused, distorted and missing, resulted in border disruption of cuticles segments when the amount of glucose in the body was about 10 times higher than normal (Fraga et al., 2013) (0.08 μg < normal content < 0.1 μg). Together, glucose injection did indeed influence patterning . However, the phenotypes were quite diverse and not unequivocally similar to *Tc-GlyS* or *Tc-AGBE* RNAi phenotypes. Therefore, no strong statements can be drawn from these results.

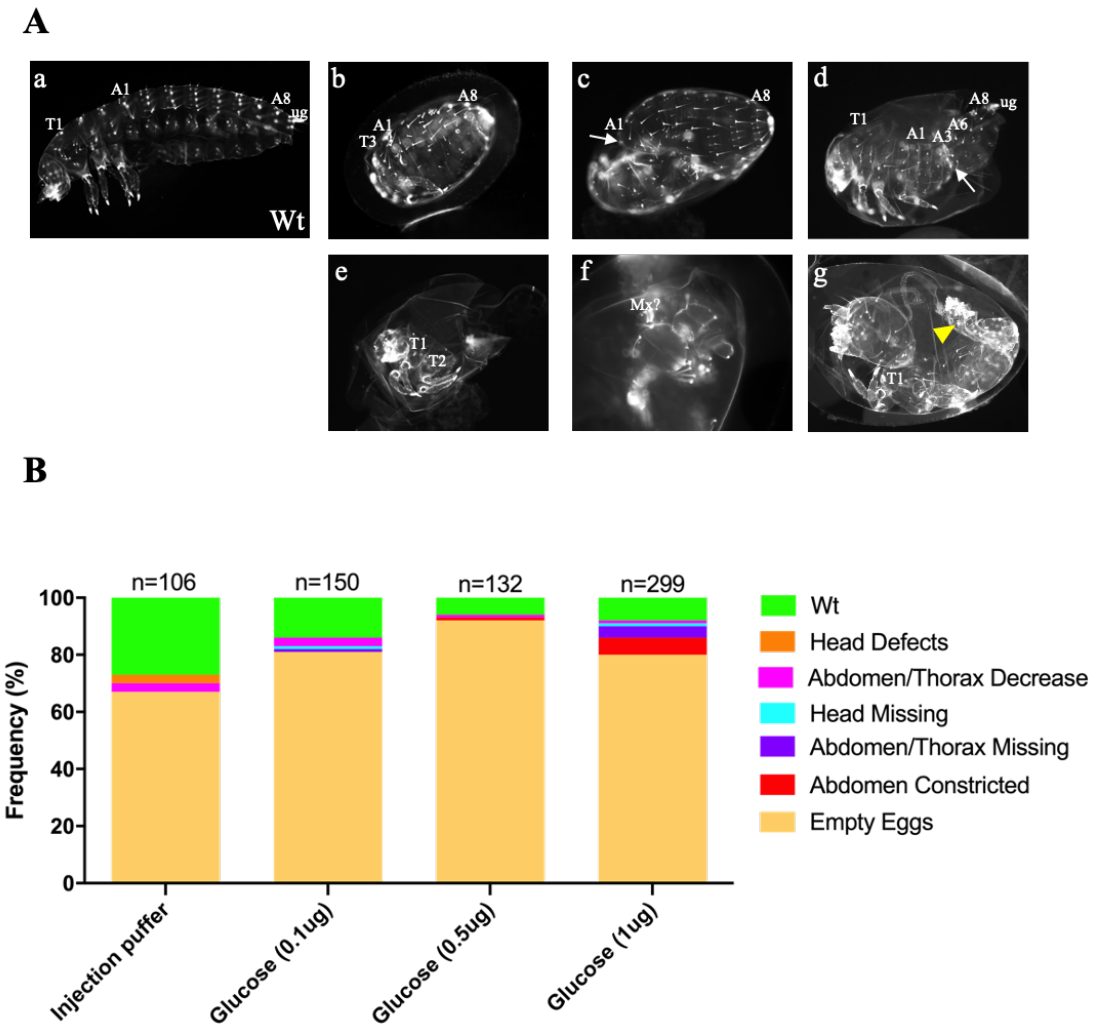

Figure 4.22 Cuticle analysis of embryos treated with increasing amounts of glucose.

(Ab-g) Cuticle phenotypes injected with 1 µg glucose. (Ab) Absence of complete head, but two pairs of thoracic segments, some abdominal segments and urogomphi were visible. (Ac, d, g) Several (6%) larvae had malformed cuticles with constricted thoracic or abdominal segments (yellow arrowhead indicated twisted posterior parts). (Ae, f) Truncated phenotypes with abolished posterior segments consisted of only gnathal-like structures or head and some thoracic segments. Mx (Maxillae); T1 (first thoracic segment); A1-A8 (first-eighth abdominal segment). Ug (Urogomphi). (B) Detailed analysis of cuticle phenotypes in wt and different doses of glucose diluted with injection puffer. Exogenous injection of large amounts of glucose increased embryonic mortality.

5 Discussion

5.1 Identification of new gene functions through phenotypic annotation in an RNAi screen

The large scale *iBeetle* RNAi screen was performed to overcome limitations of the candidate gene approach. Specifically, genes acting in beetles but not flies cannot be identified by the candidate gene approach. Indeed, the first and second screening phase showed that with respect to the same developmental processes in *Drosophila,* a number of novel *Tribolium* candidate genes were found with unexpected functions (Hakeemi et al., 2022; Schmitt-Engel et al., 2015). I screened the third phase of *iBeetle* screen, where less conserved and less highly expressed genes were included. In comparison to the traditional candidate gene approach, systematic bias towards conservation and technical restrictions are greatly decreased through an unbiased genetic screen (Schmitt-Engel et al., 2015). Because it is a "first pass screen", for most of the genes annotated with the phenotypes "labrum, leg and abdomen" in the primary screen, the phenotypes were not reproduced. Normally, the rate of reproducibility is depending on annotated penetrance. Phenotypes with a penetrance > 50% were reproduced in around 60% of the cases in the former screens (Schmitt-Engel et al., 2015). However, in my rescreening, only 4 of 14 (28.6%) phenotypes were re-produced, including two candidate genes related to head development and two genes involved in segmentation. The reasons for lower reproducibility could be several fold. First, most of the candidate genes selected for re-screening displayed moderate penetrance of phenotypes (around 50%, only one gene > 90%). Second, in previous phases of the screen, the genes to be tested were prioritized based on GO terms and conservation. Hence, I predominantly worked on a gene set that was less conserved.

Knockdown of *Tc-Maf-S* showed a specific function resulting in a mandible to maxilla transformation and a missing labrum (Fig 4.7). The *Drosophila* ortholog of

transcription factor *Maf-S* is contributed maternally in eggs, and is then distributed in nearly all embryonic cells (Blank and Andrews, 1997). *Maf-S* has an indispensable role in promoting the interaction of Cap'n'collar (Cnc) protein and DNA to specify the identity of the mandibular structure (Igarashi et al., 1994; Kobayashi et al., 1999). These studies of *Maf-S* are consistent with our finding, in that they describe the duplications of mouth hooks, which are derived from maxillae. In summary, in *Drosophila* the interaction between *Maf-S* and *Cnc* is essential for specifying the identity of the mandibular segment of head (Veraksa et al., 2000). In line with our initial findings with respect to *Tc-Maf-S,* previous work in *Tribolium* points to suppression of *Deformed* (*Dfd*) by *Cnc* (Coulcher and Telford, 2012; McGinnis et al., 1998). Together, these results indicate that *Tc-Maf-S* and *Tc-cnc* have a similar function in specifying the identity of the mandible. Given the high likelihood of a conserved function, I did not follow-up this gene in detailed analyses.

Given that I did find no novel genes with respect to head development, I searched for other ways mining the *iBeetle*-Base. As a very common phenotypic class, “empty egg” phenotypes are caused by embryonic death before cuticles formation, which do not allow analyzing the cuticle phenotypes. They can be elicited either by patterning genes with strong effects (e. g. *Tc-otd*, *Tc-axin* and *Tc-cad*) or by rather general cellular factors that are not related to pattern formation. For instance, maternal-zygotic transition (MZT) occurs during early embryonic development, accompanied by degradation of corresponding maternal RNAs and activation of zygotic genome (ZGA) (John and Kirschner, 1982; Schultz Richard M, 2002; Tadros and Lipshitz, 2005). In case that the regulation mechanism of RNA synthesis and degradation is disrupted, it would lead to embryonic lethality during embryogenesis before cuticle secretion (Anupama et al., 1999; Fu et al., 2012). Because it cannot be determined from empty egg phenotypes, what kind of mechanism produces this phenotype, further exploration of empty egg phenotypes will provide an efficient strategy towards identification of novel gene functions. Such an “empty-egg screen” has been performed by others and my follow-up work showed that very interesting new things can be found.

5.2 The roles of *Tc-GlyS* and *Tc-AGBE* in development pattern anterior-posterior compartment boundary

Prior studies have noted the importance of glycogen synthesis in physiological aging, iron homeostasis, and metabolism disease in *Drosophila* development. It is governed by cooperative action of the evolutionarily conserved enzymes *GlyS* and *AGBE* (Bruno et al., 2004; Huynh et al., 2019; Sinadinos et al., 2014; Tay et al., 2004; Vilchez et al., 2007). In this study, my first discovery demonstrated that *Tc-GlyS* and *Tc-AGBE* functions were involved in segment boundary maintenance and appendage development in the short germ-band beetle *Tribolium*. I revealed that the maintenance of segment boundaries along A-P axis was affected by downregulation of *Tc-GlyS* and *Tc-AGBE*. Being a general feature of a segmented organism, segmental boundaries define repeated units through allowing population of cells to grow and develop in separate compartments (Basler and Struhl, 1994; Lawrence and Struhl, 1996). The segment boundaries are established in early embryogenesis by adjacent expression of the segment polarity genes *wg*, *hh* and *en*. *hh* is responsible for signal transmission from posterior *en* expressing cells across the boundary to anterior *wg* secreting cells, maintaining transcription of *wg* (Peifer and Bejsovec, 1992; Vincent and O'Farrell, 1992). Hence, expression of these genes reflects the segment boundary very well. Analysis of the morphological changes of *Tc-GlyS* and *Tc-AGBE* RNAi during embryogenesis determined that the disruption of segmental organization appeared first during elongation stages in the posterior abdomen and subsequently extended to the thorax. However, the SAZ appeared to be not affected. Additionally, the development of appendages was affected at the stage before dorsal closure. Knockdown of *Tc-GlyS* and *Tc-AGBE,* the segmental marker gene expression of *Tc-wg*, *Tc-hh*, and *Tc-en* reflected the observation of a start in the posterior abdomen and extension towards anterior. Remarkably, the phenotypes of *Tc-GlyS* and *Tc-AGBE* RNAi strongly resembled the phenotypes observed in *wg* mutants and RNAi knock-down embryos with respect to loss of segment boundaries, loss of parts of gnathal and thoracic appendages and shortened A-P axis both in *Drosophila* and *Tribolium*, suggesting a

close correspondence between their functions on segment boundary maintenance, axis elongation, and appendage allocation (Kubota et al., 2003; Ober and Jockusch, 2006; Simcox et al., 1989). Degrading segment boundaries are also occurred after depletion of *Tc-en* and *Tc-hh*, displaying similar compact segmental remnants as observed after knockdown of *Tc-wg.* The stripes marked by *Tc-en* in *Tc-hh* RNAi embryos are absent in the more anterior segments during elongation stage and irregular *Tc-en* expression along ventral midline is visible when the germ-band has been completely retracted (Bolognesi et al., 2008; Farzana and Brown, 2008; Lim and Choe, 2020). Particularly, in loss of *Tc-hh* function enbryis, the abnormalities of *Tc-en* stripes appears evident during retraction, which is different in comparison with *Tc-GlyS* and *Tc-AGBE* RNAi embryos. In extending germ-bands, *Tc-wg* expression showed severe disruption in the head and entire trunk after *Tc-en* RNAi, i.e. the RNAi effects is much stronger than that of *Tc-GlyS* and *Tc-AGBE* (Lim and Choe, 2020). Embryo mutants for a series of conserved segment polarity genes such as *fused*, *armadillo*, and *disheveled* generate similar embryonic segment polarity phenotypes to that of *wg*. It is also proposed that loss of functions of those genes results in cell death of posterior compartments, whereas the cells of anterior compartments are responsible for the rearrangement of positional information within segments (Limbourg-Bouchon et al., 1991; Peifer et al., 1991; Perrimon and Mahowald, 1987). Therefore, I assumed that disordered boundaries along A-P axis may be attributed to an influence of the downregulation of *Tc-GlyS* or *Tc-AGBE* on the segment polarity genes network. However, it's still unclear how exactly segment polarity genes expression is affected by the presence of *Tc-GlyS* or *Tc-AGBE*. It is probably via upregulation of the Wnt pathway, because the knockdown of the Wnt antagonist *Tc-axin* produces a similar pattern. Here, the fused and degrading *Tc-wg* stripe patterns in trunk region is observed after depletion of *Tc-axin* (Fu et al., 2012). Like *Tc-axin*, *GSK-3* is also inhibiting Wnt activity and *sgg* (ortholog of *GSK-3*) RNAi is able to disrupt *Tribolium* and *Oncopeltus* segment boundaries (Fu et al., 2012; Lev and Chipman, 2021). Taken together, the RNAi data pointed to a requirement for *Tc-GlyS* and *Tc-AGBE* in the maintenance of segment boundaries by segment polarity genes and in appendage development.

5.3 *Tc-GlyS* and *Tc-AGBE* are required for leg outgrowth

In *Drosophila*, organization of legs along P-D axis is maintained by the antagonistic repression between Wg and Dpp morphogens which induce activation of target genes such as *Distalless* (*Dll*) and *dachshund* (*dac*) (Campbell et al., 1993; Diaz-Benjumea et al., 1994; Mardon et al., 1994). However, the expression of target gene *Tc-Dll* is not affected by *Tc-Dpp* in *Tribolium* limb development, suggesting that the regulation of corresponding target genes in leg patterning depends on other signals, as well (Grossmann et al., 2009; Ober and Jockusch, 2006). As a functionally conserved gene in insects and vertebrates, *wg* can establish positional information and specify developmental fates of adjacent ventral leg cells (Heuvel et al., 1989; Martinez Arias et al., 1988). Mutations or RNA interference with *wg* leads to loss of morphological structures of legs, gnathal and lateral head lobes observed in *Drosophila* and *Tribolium* (Baker, 1988; Couso et al., 1993; Ober and Jockusch, 2006). Our data showed that *Tc-GlyS* and *Tc-AGBE* activity led to shortened legs along the P-D axis and malformed head appendages (arrows in Fig 4.18 B1, D1, F1). We had identified that *Tc-wg* expression was partially absent in gnathal and legs, reflecting that the limbs failed to finish normal outgrowth in *Tc-GlyS* and *Tc-AGBE* RNAi embryos. I speculated that the response of proximal-distal leg patterning might depend on an interaction between neighboring cells dominated by *Tc-wg* and *Tc-GlyS* and *Tc-AGBE* function.

The effects for shortening of legs and gnathal appendages induced by knock-down *Tc-GlyS*/*Tc-AGBE* are reflected in the phenotypes of *Sp8* RNAi in *Tribolium* and milkweed bug *Oncopeltus fasciatus* (Beermann et al., 2004; ND et al., 2009). As mentioned in the previous studies, *Sp1* (ortholog of *Sp8*) is upstream of *Dll*, is also initially activated in response to *wg* in *Drosophila* (Estella and Mann, 2010; Estella et al., 2003). In *Triboluim*, *Tc-Sp8* is also thought to be a possible target gene of *Tc-Dll*, contributing to limb outgrowth (Beermann et al., 2004; Estella and Mann, 2010). In *Tribolium*, the expression of *Tc-dac*, *Tc-Dll*, *Tc-Sp8* and *Tc-wg* exhibits partial overlap from proximal to the distal domain of legs at fully elongation stages (Beermann et al., 2004;

Siemanowski et al., 2015). Our analysis found that *Tc-dac* expression was lost from the limbs, while *Tc-dac* expression of antennae and gnathal segments was retained after *Tc-GlyS* and *Tc-AGBE* RNAi treatments. On the contrary, *Tc-Dll* expression in the most distal parts of appendages of RNAi embryos showed no difference in comparison to wt embryos. Equally, *Tc-Sp8* lost the ring-shaped expression pattern of medial parts on thoracic limbs, maxillae and labia after depletion of *Tc-GlyS*/*Tc-AGBE*. Moreover, downregulation of *Tc-GlyS* and *Tc-AGBE* resulting in residual expression of *Tc-Sp8* at the distal tips of appendages revealed young bud growths, which were severely compromised so that they were unable to develop into final length. Remarkably, extremely shortened legs and gnathal appendages were found after knockdown, together with expression pattern of *Tc-dac*, *Tc-Dll*, *Tc-Sp8* and *Tc-wg*, which suggested *Tc-GlyS*/*Tc-AGBE* RNAi was required for the development of the parts of the appendages between proximal and distal. The RNAi embryos lacked *Tc-dac* expression in legs and reduced expression of *Tc-wg* and *Tc-Sp8*. What remains unclear is how *Tc-GlyS* and *Tc-AGBE* exactly participate in signaling to reduce *Tc-wg*, *Tc-Sp8* and *Tc-dac* transcription to control appendage development. Overall, this evidence strongly suggested that the functions of *Tc-GlyS* and *Tc-AGBE* were different with respect to A-P and P-D axes of embryos.

5.4 Transduction of Wnt and Hh signaling mediated by *Tc-GlyS* and *Tc-AGBE*

Previous studies elaborate on the crucial roles of Wnt and Hh signaling for axis elongation and limb morphogenesis in embryonic development (Diaz-Benjumea et al., 1994; Geetha-Loganathan et al., 2008; Yamaguchi, 2001). It is now generally implicated that canonical Wnt signaling regulates posterior germ-band elongation along A-P axis, whose inhibition promotes anterior normal development in early *Tribolium* embryogenesis (Bolognesi et al., 2008; Fu et al., 2012). Depletion of Wnt signaling alters posterior morphology, resulting in formation of truncated phenotypes with lacking abdominal segments (Bolognesi et al., 2009). The present evidence has been

confirmed that the coordinated regulation between of Wnt and Hh signaling pathway contribute to anterior head, limb formation and growth zone. Wnt signaling acts downstream of Hh signaling in head and thoracic segments, while the activation of *hh* requires upstream Wnt signaling in the posterior growth zone (Oberhofer et al., 2014; Singh et al., 2012; Tu et al., 2020). In my study, embryos treated with *Tc-GlyS*/*Tc-AGBE* RNAi exhibited extremely shortened A-P axis at later stages, producing disrupted or utterly lost segment boundaries might be associated with segment polarity network. On the other hand, insulin via its receptor regulates Akt, which in turn phosphorylates and inactivates-GSK-3 (Frame and Cohen, 2001) which is involved in multiple signaling pathways such as Wnt, Hh and Notch (Foltz et al., 2002; He et al., 1995; Jia et al., 2002). Double depletion of *Tc-GlyS*/*Tc-AGBE* and *Tc-hh* showed stronger phenotypes, i.e. a substantial reduction of Hh phenotypes and high percentage of empty egg phenotypes. Previous studies showed the crucial roles of *Tc-Arr* and *Tc-Pan* are involved in generation of posterior patterning and formation of distal limbs driven by Wnt signaling in *Tribolium* (Beermann et al., 2011; Bolognesi et al., 2009; Fu et al., 2012). Obviously, even more strongly truncated phenotypes were observed when we performed *Tc-GlyS*/*Tc-AGBE* double RNAi in combination with the Wnt receptor *Tc-Arr* or the transcription factor *Tc-Pan*, resulting in small spheres of cuticles without any thoracic or abdominal segments. Importantly, the truncated effects with small limbless structure of *Tc-Pan* and *Tc-Arr* were enhanced greatly by additional interference of *Tc-GlyS*/*Tc-AGBE.* Hence, *Tc-GlyS* and *Tc-AGBE* could not act exclusively upstream of Wnt or hh signaling. Additionally, most of *Tc-GlyS*/*Tc-AGBE* RNAi embryos showed an relatively normal body plan before fully elongated stages (Fig 4.15 Bc-Be & Cc-Ce), which does not resemble the truncated embryos of *Tc-Pan* or *Tc-Arr* (Bolognesi et al., 2008; Bolognesi et al., 2009). Extremely truncated phenotypes lacking all segments only retaining relics of head structures by depletion of both *Tc-GlyS*/*Tc-AGBE* and Wnt key components resembled the cuticles of *Tc-wg* and *Tc-wls* (*Tc-Wntless*) alone whose functions are not responsible for posterior growth zone. Knockdown of them (*Tc-GlyS*/*Tc-AGBE* or *Tc-wg* and *Tc-wls*) produce similar high percentage of empty eggs, but *Tc-wg* or *Tc-wls* RNAi display specific small

spherical cuticles that could be attributed to different concentration of dsRNA injection (Bolognesi et al., 2008). Further, we saw no change of *Tc-eve* nor *Tc-cad* in the growth zone. Together, these results appeared to indicate that *Tc-GlyS*/*Tc-AGBE* acted later than those genes and may not be involved in Wnt signaling in the growth zone. In contrast, the A-P axis of the embryos obtained after *Tc-GlyS*/*Tc-AGBE* RNAi became shortened and eventually deleted only after the germ-band retraction stage. Nevertheless, reduced maintenance of segment boundaries by segment polarity genes such as *Tc-wg* and *Tc-hh* occurred after loss of *Tc-GlyS*/*Tc-AGBE*, suggesting *Tc-GlyS*/*Tc-AGBE* may be required for one aspect of this network. We hypothesized, that glycogen metabolism may influence GSK-3 activity, which in turn in known to affect both Hh and Wnt signaling. We could speculate that *Tc-GlyS*/*Tc-AGBE* RNAi act via *Tc-GSK-3* on both pathways to result in breakdown of the segment polarity network. However, the presented experiments did not test this hypothesis.

5.5 Ubiquitously expressed *Tc-GlyS* and *Tc-AGBE* but localized effects on apoptosis

I found that loss of *Tc-GlyS* and *Tc-AGBE* led to increased apoptosis occurring in head and trunk tissues at early developmental stages, while cells in posterior growth zone were not affected, although both genes shared ubiquitous expression throughout embryogenesis. In *Tc-GlyS* and *Tc-AGBE* RNAi embryos, most apoptosis-positive cells were distributed within the areas where defects were observed on the level of segment boundaries and outgrowth of appendages. Apoptosis of cells of the anterior head correlate with the absence of labrum and other tissues, while it remains unclear why apoptosis rate recovered to normal levels at later stages. Apparently, cells in the trunk were more sensitive than the head region to depletion of *Tc-GlyS*/*Tc-AGBE* function. It could be that those tissues that need most active cell division activity are the first tissues where the lack of the enzymes leads to a phenotype. Testing this hypothesis requires comparing the rates of apoptosis that I found with the rate of cell division in normal embryogenesis.

5.6 Maternal contribution of *Tc-GlyS* and *Tc-AGBE* and glycogen metabolism in early embryogenesis

In this study, I demonstrated that *Tc-GlyS* and *Tc-AGBE* have hitherto undiscovered roles in maintenance of segment boundaries and outgrowth of appendages. As we expected, *Tc-GlyS* and *Tc-AGBE* showed ubiquitous expression. Similar expression pattern of *Tc-GlyS* and *Tc-AGBE* were found in *Drosophila* and mouse, being involved in functions such as controlling lifespan and affecting larval growth and survival (Bai et al., 2013; Duran et al., 2012; Yamada et al., 2019). Interestingly, *Tc-GlyS* and *Tc-AGBE* displayed much higher levels in freshly laid eggs (0-5 hours) than at the other time points (11-24, 24-48, 48-72). Hence, the high levels of mRNA mainly reflect maternal contribution. It has been shown before that in *Tribolium,* the level of glucose is low in freshly laid eggs but then increases after 20 hours of development. In contrast, high glycogen levels are found in freshly laid eggs, which drop to an intermediate level within the first 8 hours and then drop further between 24 and 48 hours (Fraga et al., 2013; Jorge et al., 2007). Hence, glycogen is supplied maternally and is consumed subsequently (Arrese and Soulages, 2010). Taken together, a possible explanation for the high levels of *Tc-GlyS* and *Tc-AGBE* during early embryogenesis is that the activity of both enzymes is required in the oocyte to produce the observed high glycogen levels. The high amounts of mRNAs found in the freshly laid eggs may still reflect their function during oogenesis and the dramatic drop after 5 hours would be in line with that. During embryogenesis, energy is consumed such that glycogen synthesis seems unnecessary – the slowly fading expression of glycogen synthesis enzymes could be one reason that glucose starts accumulating only after 20 hours or so. Hence, our results revealed the expression levels of *Tc-GlyS* and *Tc-AGBE* may reflect maternal function and correlate with the previously described levels of glucose and glycogen during early embryonic development.

6 Reference

Abzhanov, A. and Kaufman, T. C. (2000). Homologs of Drosophila appendage genes in the patterning of arthropod limbs. *Dev. Biol.* **227**, 673–689.

Angelini, D. R. and Kaufman, T. C. (2004). Functional analyses in the hemipteran Oncopeltus fasciatus reveal conserved and derived aspects of appendage patterning in insects. *Dev. Biol.* **271**, 306–321.

Angelini, D. R. and Kaufman, T. C. (2005a). Functional analyses in the milkweed bug Oncopeltus fasciatus (Hemiptera) support a role for Wnt signaling in body segmentation but not appendage development. *Dev. Biol.* **283**, 409–423.

Angelini, D. R. and Kaufman, T. C. (2005b). Insect appendages and comparative ontogenetics. *Dev. Biol.* **286**, 57–77.

Angelini, D. R., Smith, F. W., Aspiras, A. C., Kikuchi, M. and Jockusch, E. L. (2012). Patterning of the adult mandibulate mouthparts in the red flour beetle, Tribolium castaneum. *Genetics* **190**, 639–654.

Ansari, S., Troelenberg, N., Dao, V. A., Richter, T., Bucher, G. and Klingler, M. (2018). Double abdomen in a short-germ insect: Zygotic control of axis formation revealed in the beetle Tribolium castaneum. *Proc. Natl. Acad. Sci. U. S. A.* **115**, 1819–1824.

Anupama, D., Walker, J. A. and Wharton, R. P. (1999). Smaug, a novel RNA-binding protein that operates a translational switch in Drosophila. *Mol. Cell* **4**, 209–218.

Arrese, E. L. and Soulages, J. L. (2010). Insect fat body: Energy, metabolism, and regulation. *Annu. Rev. Entomol.* **55**, 207–225.

Bai, H., Kang, P., Hernandez, A. M. and Tatar, M. (2013). Activin Signaling Targeted by Insulin/dFOXO Regulates Aging and Muscle Proteostasis in Drosophila. *PLOS Genet.* **9**, doi: 10.1371/journal.pgen.1003941.

Baker, N. E. (1988). Transcription of the segment-polarity gene wingless in the imaginal discs of Drosophila, and the phenotype of a pupal-lethal wg mutation. *Development* **102**, 489–497.

Basler, K. and Struhl, G. (1994). Compartment boundaries and the control of Drosophila limb pattern by hedgehog protein. *Nature* **368**, 208–214.

Beermann, A., Jay, D. G., Beeman, R. W., Hülskamp, M., Tautz, D. and Jürgens, G. (2001). The Short antennae gene of Tribolium is required for limb development and encodes the orthologue of the Drosophila distal-less protein. *Development* **128**, 287–297.

Beermann, A., Aranda, M. and Schröder, R. (2004). The Sp8 zinc-finger transcription factor is involved in allometric growth of the limbs in the beetle Tribolium castaneum. *Development* **131**, 733–742.

Beermann, A., Prühs, R., Lutz, R. and Schröder, R. (2011). A context-dependent combination of Wnt receptors controls axis elongation and leg development in a short germ insect. *Development* **138**, 2793–2805.

Bejsovec, A. and Arias, A. M. (1991). Roles of wingless in patterning the larval epidermis of Drosophila. *Development* **113**, 471–485.

Berghammer, A. J., Klingler, M. and A. Wimmer, E. (1999). A universal marker for transgenic insects. *Nature* **402**, 370–371.

Blank, V. and Andrews, N. C. (1997). The Maf transcription factors: regulators of differentiation. *Trends Biochem. Sci.* **22**, 437–441.

Bolognesi, R., Farzana, L., Fischer, T. D. and Brown, S. J. (2008). Multiple Wnt Genes Are Required for Segmentation in the Short-Germ Embryo of Tribolium castaneum. *Curr. Biol.* **18**, 1624–1629.

Bolognesi, R., Fischer, T. D. and Brown, S. J. (2009). Loss of Tc-arrow and canonical Wnt signaling alters posterior morphology and pair-rule gene expression in the short-germ insect, Tribolium castaneum. *Dev. Genes Evol.* **219**, 369–375.

Boxshall, G. A. (2004). The evolution of arthropod limbs. *Biol. Rev. Camb. Philos. Soc.* **79**, 253–300.

Brook, W. J. and Cohen, S. M. (1996). Antagonistic interactions between wingless and decapentaplegic responsible for dorsal-ventral pattern in the Drosophila leg. *Science.* **273**, 1373–1377.

Brown, S. J., Shippy, T. D., Miller, S., Bolognesi, R., Beeman, R. W., Lorenzen, M. D., Bucher, G., Wimmer, E. A. and Klingler, M. (2009). The red flour beetle, Tribolium castaneum (Coleoptera): A model for studies of development and pest biology. *Cold Spring Harb. Protoc.* **4**, doi: 10.1101/pdb.emo126.

Bruno, C., van Diggelen, O., Cassandrini, D., Gimpelev, M., Giuffrè, B., Donati, M., Introvini, P., Alegria, A., Assereto, S., Morandi, L., et al. (2004). Clinical and genetic heterogeneity of branching enzyme deficiency (glycogenosis type IV). *Neurology* **63**, 1053–1058.

Campbell, G., Weaver, T. and Tomlinson, A. (1993). Axis specification in the developing Drosophila appendage: The role of wingless, decapentaplegic, and the homeobox gene aristaless. *Cell* **74**, 1113–1123.

Capdevila, J., Estrada, M. P., Sanchez-Herrero, E. and Guerrero, I. (1994). The Drosophila segment polarity gene patched interacts with decapentaplegic in wing development. *EMBO J.* **13**, 71–82.

Cappellini, M. D., Brancaleoni, V., Graziadei, G., Tavazzi, D. and Di Pierro, E. (2010). Porphyrias at a glance: Diagnosis and treatment. *Intern. Emerg. Med.* **5**, 73–80.

Choe, C. P., Miller, S. C. and Brown, S. J. (2006). A pair-rule gene circuit defines segments sequentially in the short-germ insect Tribolium castaneum. *Proc. Natl. Acad. Sci.* **103**, 6560–6564.

Church, V. L. and Francis-West, P. (2004). Wnt signalling during limb development. *Int. J. Dev. Biol.* **46**, 927–936.

Clark, E. and Peel, A. D. (2018). Evidence for the temporal regulation of insect segmentation by a conserved sequence of transcription factors. *Dev.* **145**, doi: 10.1242/dev.155580.

Cohen, S. M. (1990). Specification of limb development in the Drosophila embryo by positional cues from segmentation genes. *Nature* **343**, 173–177.

Conlon, R. A., Reaume, A. G. and Rossant, J. (1995). Notch1 is required for the coordinate segmentation of somites. *Development* **121**, 1533–1545.

Copf, T., Schröder, R. and Averof, M. (2004). Ancestral role of caudal genes in

axis elongation and segmentation. *Proc. Natl. Acad. Sci. U. S. A.* **101**, 17711–17715.

Córdoba, S., Requena, D., Jory, A., Saiz, A. and Estella, C. (2016). The evolutionarily conserved transcription factor Sp1 controls appendage growth through Notch signaling. *Dev.* **143**, 3623–3631.

Coulcher, J. F. and Telford, M. J. (2012). Cap'n'collar differentiates the mandible from the maxilla in the beetle Tribolium castaneum. *EvoDevo 2012 31* **3**, 1–16.

Couso, J. and González-Gaitán, M. (1993). Embryonic limb development in Drosophila. *Trends Genet.* **9**, 371–373.

Couso, J. P., Bate, M. and Martínez-Arias, A. (1993). A wingless-dependent polar coordinate system in Drosophila imaginal discs. *Science.* **259**, 484–489.

Cummins, M., Pueyo, J. I., Greig, S. A. and Couso, J. P. (2003). Comparative analysis of leg and antenna development in wild-type and homeotic Drosophila melanogaster. *Dev. Genes Evol.* **213**, 319–327.

Da Rocha Fernandes, M., Martins, R., Pessoa Costa, E., Casagrande Pacidoniô, E., Araujo De Abreu, L., Da Silva Vaz, I., Moreira, L. A., Nunes Da Fonseca, R. and Logullo, C. (2014). The modulation of the symbiont/host interaction between Wolbachia pipientis and Aedes fluviatilis embryos by glycogen metabolism. *PLoS One* **9**, doi: 10.1371/journal.pone.0098966.

Dahanukar, A. and Wharton, R. P. (1996). The Nanos gradient in Drosophila embryos is generated by translational regulation. *Genes Dev.* **10**, 2610–2621.

Dahmann, C., Basler, K., Dahmann, C. and Basler, K. (1999). Compartment boundaries: at the edge of development. *Trends Genet.* **15**, 320–326.

Davis, G. K. and Patel, N. H. (2002). Short, long, and beyond: Molecular and embryological approaches to insect segmentation. *Annu. Rev. Entomol.* **47**, 669–699.

Demoulin, V. (1979). Protein and nucleic acid sequence data and phytogeny. *Science.* **205**, 1036–1039.

Diaz-Benjumea, F. J. and Cohen, S. M. (1993). Interaction between dorsal and ventral cells in the imaginal disc directs wing development in Drosophila. *Cell*

75, 741–752.

Diaz-Benjumea, F. J., Cohen, B. and Cohen, S. M. (1994). Cell interaction between compartments establishes the proximal-distal axis of Drosophila legs. *Nature* **372**, 175–179.

Diaz-Benjumen, F. J. and Cohen, S. M. (1994). Wingless acts through the shaggy/zeste-white 3 kinase to direct dorsal-ventral axis formation in the Drosophila leg. *Development* **120**, 1661–1670.

Dönitz, J., Schmitt-Engel, C., Grossmann, D., Gerischer, L., Tech, M., Schoppmeier, M., Klingler, M. and Bucher, G. (2015). iBeetle-Base: a database for RNAi phenotypes in the red flour beetle Tribolium castaneum. *Nucleic Acids Res.* **43**, D720–D725.

Driever, W. and Nüsslein-Volhard, C. (1988). The bicoid protein determines position in the Drosophila embryo in a concentration-dependent manner. *Cell* **54**, 95–104.

Duran, J., Tevy, M. F., Garcia-Rocha, M., Calbó, J., Milán, M. and Guinovart, J. J. (2012). Deleterious effects of neuronal accumulation of glycogen in flies and mice. *EMBO Mol. Med.* **4**, 719–729.

El-Sherif, E., Zhu, X., Fu, J. and Brown, S. J. (2014). Caudal Regulates the Spatiotemporal Dynamics of Pair-Rule Waves in Tribolium. *PLoS Genet.* **10**, doi: 10.1371/journal.pgen.1004677.

Embi, N., Rylatt, D. B. and Cohen, P. (1980). Glycogen synthase kinase-3 from rabbit skeletal muscle. Separation from cyclic-AMP-dependent protein kinase and phosphorylase kinase. *Eur J Biochem* **107**, 519–527.

Estella, C. and Mann, R. S. (2008). Logic of Wg and Dpp induction of distal and medial fates in the Drosophila leg. *Development* **135**, 627–636.

Estella, C. and Mann, R. S. (2010). Non-redundant selector and growth-promoting functions of two sister genes, buttonhead and Sp1, in Drosophila leg development. *PLoS Genet.* **6**, 1–13.

Estella, C., Rieckhof, G., Calleja, M. and Morata, G. (2003). The role of buttonhead and Sp1 in the development of the ventral imaginal discs of

Drosophila. *Development* **130**, 5929–5941.

Farzana, L. and Brown, S. J. (2008). Hedgehog signaling pathway function conserved in Tribolium segmentation. *Dev. Genes Evol.* **218**, 181–192.

Felsenstein, J. (1985). Confidence Limits on Phylogenies: An Approach Using the Bootstrap. *Evolution (N. Y).* **39**, 783–791.

Florentin, A. and Arama, E. (2012). Caspase levels and execution efficiencies determine the apoptotic potential of the cell. *J. Cell Biol.* **196**, 513–527.

Foltz, D. R., Santiago, M. C., Berechid, B. E. and Nye, J. S. (2002). Glycogen synthase kinase-3β modulates notch signaling and stability. *Curr. Biol.* **12**, 1006–1011.

Fraga, A., Ribeiro, L., Lobato, M., Santos, V., Silva, J. R., Gomes, H., Moraes, J. L. da C., Menezes, J. de S., Oliveira, C. J. L. de, Campos, E., et al. (2013). Glycogen and Glucose Metabolism Are Essential for Early Embryonic Development of the Red Flour Beetle Tribolium castaneum. *PLoS One* **8**, doi: 10.1371/journal.pone.0065125.

Frame, S. and Cohen, P. (2001). GSK3 takes centre stage more than 20 years after its discovery. *Biochem. J.* **359**, 1–16.

Fu, J., Posnien, N., Bolognesi, R., Fischer, T. D., Rayl, P., Oberhofer, G., Kitzmann, P., Brown, S. J. and Bucher, G. (2012). Asymmetrically expressed axin required for anterior development in Tribolium. *Proc. Natl. Acad. Sci.* **109**, 7782–7786.

Galindo, M. I., Bishop, S. A., Greig, S. and Couso, J. P. (2002). Leg patterning driven by proximal-distal interactions and EGFR signaling. *Science.* **297**, 256–259.

Gallitano-Mendel, A. and Finkelstein, R. (1997). Novel segment polarity gene interactions during embryonic head development in Drosophila. *Dev. Biol.* **192**, 599–613.

Garcia-Bellido, A., Ripoll, P. and Morata, G. (1973). Developmental compartmentalisation of the wing disk of drosophila. *Nat. New Biol.* **245**, 251–253.

Geetha-Loganathan, P., Nimmagadda, S. and Scaal, M. (2008). Wnt signaling in limb organogenesis. *Organogenesis* **4**, doi: 10.4161/org.4.2.5857.

Gilbert, S. F. (2003). Developmental Biology. 7th ed. *Sinauer Assoc. Inc*.

Gilbert, S. F. (2006). Developmental biology.8th ed. *Sinauer Assoc. Inc*.

González, F., Swales, L., Bejsovec, A., Skaer, H. and Arias, A. M. (1991). Secretion and movement of wingless protein in the epidermis of the Drosophila embryo. *Mech. Dev.* **35**, 43–54.

Gotoh, H., Zinna, R. A., Ishikawa, Y., Miyakawa, H., Ishikawa, A., Sugime, Y., Emlen, D. J., Lavine, L. C. and Miura, T. (2017). The function of appendage patterning genes in mandible development of the sexually dimorphic stag beetle. *Dev. Biol.* **422**, 24–32.

Greene, H. L., Brown, B. I., McClenathan, D. T., Agostini, R. M. and Taylor, S. R. (1988). A new variant of type IV glycogenosis: deficiency of branching enzyme activity without apparent progressive liver disease. *Hepatology* **8**, 302–306.

Grossmann, D. and Prpic, N. M. (2012). Egfr signaling regulates distal as well as medial fate in the embryonic leg of Tribolium castaneum. *Dev. Biol.* **370**, 264–272.

Grossmann, D., Scholten, J. and Prpic, N.-M. (2009). Separable functions of wingless in distal and ventral patterning of the Tribolium leg. *Dev. Genes Evol.* **219**, 469–479.

Hakeemi, M. S., Ansari, S., Teuscher, M., Weißkopf, M., Großmann, D., Kessel, T., Dönitz, J., Siemanowski, J., Wan, X., Schultheis, D., et al. (2022). Screens in fly and beetle reveal vastly divergent gene sets required for developmental processes. *BMC Biol.* **20**, 38.

Hannibal, R. L. and Patel, N. H. (2013). What is a segment? *Evodevo* **4**, doi: 10.1186/2041-9139-4-35.

He, X., Saint-Jeannet, J. P., Woodgett, J. R., Varmus, H. E. and Dawid, I. B. (1995). Glycogen synthase kinase-3 and dorsoventral patterning in Xenopus embryos. *Nature* **374**, 617–622.

Heslip, T. R., Theisen, H., Walker, H. and Marsh, J. L. (1997). Shaggy and dishevelled exert opposite effects on wingless and decapentaplegic expression and on positional identity in imaginal discs. *Development* **124**, 1069–1078.

Heuvel, M. van den, Nusse, R., Johnston, P. and Lawrence, P. A. (1989). Distribution of the wingless gene product in drosophila embryos: A protein involved in cell-cell communication. *Cell* **59**, 739–749.

Hülskamp, M., Pfeifle, C. and Tautz, D. (1990). A morphogenetic gradient of hunchback protein organizes the expression of the gap genes Krüppel and knirps in the early Drosophila embryo. *Nature* **346**, 577–580.

Huynh, N., Ou, Q., Cox, P., Lill, R. and King-Jones, K. (2019). Glycogen branching enzyme controls cellular iron homeostasis via Iron Regulatory Protein 1 and mitoNEET. *Nat. Commun.* **10**, doi: 10.1038/s41467-019-13237-8.

Igarashi, K., Kohsuke, K., Itoh ken, Hayashi, N., Makoto, N. and Yamamoto (1994). Regulation of transcription by dimerization of erythroid factor NF-E2 p45 with small Maf proteins. *Nature* **367**, 568–572.

Ing, T., Tseng, A., Sustar, A. and Schubiger, G. (2013). Sp1 modifies leg-to-wing transdetermination in Drosophila. *Dev. Biol.* **373**, 290–299.

Jaynes, J. B. and Fujioka, M. (2004). Drawing lines in the sand: even skipped et al. and parasegment boundaries. *Dev. Biol.* **269**, doi: 10.1016/j.ydbio.2004.03.001.

Jia, J., Amanai, K., Wang, G., Tang, J., Wang, B. and Jiang, J. (2002). Shaggy/GSK3 antagonizes hedgehog signalling by regulating Cubitus interruptus. *Nature* **416**, 548–552.

Jiang, J. and Struhl, G. (1996). Complementary and mutually exclusive activities of decapentaplegic and wingless organize axial patterning during Drosophila leg development. *Cell* **86**, 401–409.

John, N. and Kirschner, M. (1982). A major developmental transition in early Xenopus embryos: I. characterization and timing of cellular changes at the midblastula stage. *Cell* **30**, 675–686.

Johnston, D. S. and Nüsslein-Volhard, C. (1992). The origin of pattern and polarity in the Drosophila embryo. *Cell* **68**, 201–219.

Johnston, L. A. and Schubiger, G. (1996). Ectopic expression of wingless in imaginal discs interferes with decapentaplegic expression and alters cell determination. *Development* **122**, 3519–3529.

Jorge, M., Galina Antônio, H, A. P., Lazzaro, R. G., Masuda Aoi, Vaz, da S. I. and Logullo Carlos (2007). Glucose metabolism during embryogenesis of the hard tick Boophilus microplus. *Comp. Biochem. Physiol. A. Mol. Integr. Physiol.* **146**, 528–533.

Kimelman, D. and Martin, B. L. (2012). Anterior-posterior patterning in early development: three strategies. *Wiley Interdiscip. Rev. Dev. Biol.* **1**, 253–266.

Kobayashi, A., Ito, E., Toki, T., Kogame, K., Takahashi, S., Igarashi, K., Hayashi, N. and Yamamoto, M. (1999). Molecular Cloning and Functional Characterization of a New Cap'n' Collar Family Transcription Factor Nrf3 *. *J. Biol. Chem.* **274**, 6443–6452.

Kojima, T. (2004). The mechanism of Drosophila leg development along the proximodistal axis. *Dev. Growth Differ.* **46**, 115–129.

Kubota, K., Goto, S. and Hayashi, S. (2003). The role of Wg signaling in the patterning of embryonic leg primordium in Drosophila. *Dev. Biol.* **257**, 117–126.

Larsen, C. W., Hirst, E., Alexandre, C. and Vincent, J.-P. (2003). Segment boundary formation in Drosophila embryos. *Development* **130**, 5625–5635.

Lawrence, P. A. and Struhl, G. (1996). Morphogens, compartments, and pattern: lessons from drosophila? *Cell* **85**, 951–961.

Lecuit, T. and Cohen, S. M. (1997). Proximal-distal axis formation in the drosophila leg. *Nature* **388**, 139–145.

Lee, J. J., von Kessler, D. P., Parks, S. and Beachy, P. A. (1992). Secretion and localized transcription suggest a role in positional signaling for products of the segmentation gene hedgehog. *Cell* **71**, 33–50.

Lee, H. C., Tsai, J. N., Liao, P. Y., Tsai, W. Y., Lin, K. Y., Chuang, C. C., Sun, C. K., Chang, W. C. and Tsai, H. J. (2007). Glycogen synthase kinase 3α and 3β have distinct functions during cardiogenesis of zebrafish embryo. *BMC Dev. Biol.* **7**, 1–15.

Lev, O. and Chipman, A. D. (2021). Development of the Pre-gnathal Segments in the Milkweed Bug Oncopeltus fasciatus Suggests They Are Not Serial Homologs of Trunk Segments. *Front. Cell Dev. Biol.* **9**, doi: 10.3389/fcell.2021.695135.

Li, S. C., Chen, C. M., Goldstein, J. L., Wu, J. Y., Lemyre, E., Burrow, T. A., Kang, P. B., Chen, Y. T. and Bali, D. S. (2010). Glycogen storage disease type IV: novel mutations and molecular characterization of a heterogeneous disorder. *Inherit. Metab. Dis.* **33**, S83-90.

Lim, J. and Choe, C. P. (2020). Functional analysis of engrailed in Tribolium segmentation. *Mech. Dev.* **161**, doi: 10.1016/j.mod.2019.103594.

Limbourg-Bouchon, B., Busson, D. and Lamour-Isnard, C. (1991). Interactions between fused, a segment-polarity gene in Drosophila, and other segmentation genes. *Development* **112**, 417–429.

Liu, P. Z. and Kaufman, T. C. (2005). Short and long germ segmentation: unanswered questions in the evolution of a developmental mode. *Evol. Dev.* **7**, 629–646.

Lorenzen, M. D., Berghammer, A. J., Brown, S. J., Denell, R. E., Klingler, M. and Beeman, R. W. (2003). piggyBac-mediated germline transformation in the beetle Tribolium castaneum. *Insect Mol. Biol.* **12**, 433–440.

Macdonald, P. M. and Struhl, G. (1986). A molecular gradient in early Drosophila embryos and its role in specifying the body pattern. *Nature* **324**, 537–545.

Mardon, G., Solomon, N. M. and Rubin, G. M. (1994). dachshund encodes a nuclear protein required for normal eye and leg development in Drosophila. *Development* **120**, 3473–3486.

Martinez Arias, A., Baker, N. E. and Ingham, P. W. (1988). Role of segment polarity genes in the definition and maintenance of cell states in the Drosophila embryo. *Development* **103**, 157–170.

McGinnis, N., Ragnhildstveit, E., Veraksa, A. and McGinnis, W. (1998). A cap ‘n’ collar protein isoform contains a selective Hox repressor function. *Development* **125**, 4553–4564.

Méthot, N. and Basler, K. (1999). Hedgehog controls limb development by regulating the activities of distinct transcriptional activator and repressor forms of cubitus interruptus. *Cell* **96**, 819–831.

Miyawaki, K., Mito, T., Sarashina, I., Zhang, H., Shinmyo, Y., Ohuchi, H. and Noji, S. (2004). Involvement of Wingless/Armadillo signaling in the posterior sequential segmentation in the cricket, Gryllus bimaculatus (Orthoptera), as revealed by RNAi analysis. *Mech. Dev.* **121**, 119–130.

Morimura, S., Maves, L., Chen, Y. and Hoffmann, F. M. (1996). decapentaplegic overexpression affects Drosophila wing and leg imaginal disc development and wingless expression. *Dev. Biol.* **177**, 136–151.

ND, S., NM, P. and EA, W. (2009). A conserved function of the zinc finger transcription factor Sp8/9 in allometric appendage growth in the milkweed bug Oncopeltus fasciatus. *Dev. Genes Evol.* **219**, 427–435.

Neumann, C. and Cohen, S. (1997). Morphogens and pattern formation. *Bioessays* **19**, 721–729.

Niswander, L. (2004). Interplay between the molecular signals that control vertebrate limb development. *Int. J. Dev. Biol.* **46**, 877–881.

Nusse, R. and Varmus, H. E. (1992). Wnt genes. *Cell* **69**, 1073–1087.

O, J. and Choe, C. P. (2020). even-skipped acts as a pair-rule gene in germ band stages of Tribolium development. *Dev. Biol.* **462**, 1–6.

Ober, K. A. and Jockusch, E. L. (2006). The roles of wingless and decapentaplegic in axis and appendage development in the red flour beetle, Tribolium castaneum. *Dev. Biol.* **294**, 391–405.

Oberhofer, G., Grossmann, D., Siemanowski, J. L., Beissbarth, T. and Bucher, G. (2014). Wnt/β-catenin signaling integrates patterning and metabolism of the insect growth zone. *Development* **141**, 4740–4750.

Onishi, K. and Zou, Y. (2017). Sonic hedgehog switches on Wnt/planar cell polarity signaling in commissural axon growth cones by reducing levels of Shisa2. *Elife* **6**, doi: 10.7554/eLife.25269.

Ozbudak, E. M. and Pourquié, O. (2008). The vertebrate segmentation clock: the

tip of the iceberg. *Curr. Opin. Genet. Dev.* **18**, 317–323.

Paik, D., Jang, Y. G., Lee, Y. E., Lee, Y. N., Yamamoto, R., Gee, H. Y., Yoo, S., Bae, E., Min, K. J., Tatar, M., et al. (2012). Misexpression screen delineates novel genes controlling Drosophila lifespan. *Mech. Ageing Dev.* **133**, 234–245.

Palmeirim, I., Henrique, D., Ish-Horowicz, D. and Pourquié, O. (1997). Avian hairy Gene Expression Identifies a Molecular Clock Linked to Vertebrate Segmentation and Somitogenesis. *Cell* **91**, 639–648.

Panganiban, G., Irvine, S. M., Lowe, C., Roehl, H., Corley, L. S., Sherbon, B., Grenier, J. K., Fallon, J. F., Kimble, J., Walker, M., et al. (1997). The origin and evolution of animal appendages. *Proc. Natl. Acad. Sci. U. S. A.* **94**, 5162–5166.

Pankratz, M. J., Busch, M., Hoch, M., Seifert, E. and Jäckle, H. (1992). Spatial control of the gap gene knirps in the Drosophila embryo by posterior morphogen system. *Science.* **255**, 986–989.

Parody, T. R. and Muskavitch, M. A. T. (1993). The pleiotropic function of Delta during postembryonic development of Drosophila melanogaster. *Genetics* **135**, 527–539.

Peifer, M. and Bejsovec, A. (1992). Knowing your neighbors: Cell interactions determine intrasegmental patterning in Drosophila. *Trends Genet.* **8**, 243–249.

Peifer, M., Rauskolb, C., Williams, M., Riggleman, B. and Wieschaus, E. (1991). The segment polarity gene armadillo interacts with the wingless signaling pathway in both embryonic and adult pattern formation. *Development* **111**, 1029–1043.

Perrimon, N. and Mahowald, A. P. (1987). Multiple functions of segment polarity genes in Drosophila. *Dev. Biol.* **119**, 587–600.

Petersen, C. P. and Reddien, P. W. (2009). Wnt Signaling and the Polarity of the Primary Body Axis. *Cell* **139**, 1056–1068.

Prpic, N. M., Wigand, B., Damen, W. G. and Klingler, M. (2001). Expression of dachshund in wild-type and Distal-less mutant Tribolium corroborates serial homologies in insect appendages. *Dev. Genes Evol.* **211**, 467–477.

Prühs, R., Beermann, A. and Schröder, R. (2017). The Roles of the Wnt-Antagonists Axin and Lrp4 during Embryogenesis of the Red Flour Beetle Tribolium castaneum. *J. Dev. Biol.* **5**, doi: 10.3390/jdb5040010.

Pueyo, J. I. and Couso, J. P. (2005). Parallels between the proximal-distal development of vertebrate and arthropod appendages: Homology without an ancestor? *Curr. Opin. Genet. Dev.* **15**, 439–446.

Rosenberg, M., Lynch, J. and Desplan, C. (2009). Heads and Tails: Evolution of Antero-Posterior Patterning in Insects. *Biochim. Biophys. Acta* **1789**, doi: 10.1016/j.bbagrm.2008.09.007.

Rudolf, H., Zellner, C. and El-Sherif, E. (2020). Speeding up anterior-posterior patterning of insects by differential initialization of the gap gene cascade. *Dev. Biol.* **460**, 20–31.

Ruel, L., Bourouis, M., Heitzler, P., Pantesco, V. and Simpson, P. (1993). Drosophila shaggy kinase and rat glycogen synthase kinase-3 have conserved activities and act downstream of Notch. *Nature* **362**, 557–560.

Sarrazin, A. F., Peel, A. D. and Averof, M. (2012). A segmentation clock with two-segment periodicity in insects. *Science* **336**, 338–341.

Schinko, J., Posnien, N., Kittelmann, S., Koniszewski, N. and Bucher, G. (2009). Single and double whole-mount in situ hybridization in red flour beetle (Tribolium) embryos. *Cold Spring Harb. Protoc.* **2009**, doi: 10.1101/pdb.prot5258.

Schinko, J. B., Hillebrand, K. and Bucher, G. (2012). Heat shock-mediated misexpression of genes in the beetle Tribolium castaneum. *Dev. Genes Evol.* **222**, 287–298.

Schmitt-Engel, C., Schultheis, D., Schwirz, J., Ströhlein, N., Troelenberg, N., Majumdar, U., Dao, V. A., Grossmann, D., Richter, T., Tech, M., et al. (2015). The iBeetle large-scale RNAi screen reveals gene functions for insect development and physiology. *Nat. Commun.* **6**, 1–10.

Schmittgen, T. D. and Livak, K. J. (2008). Analyzing real-time PCR data by the comparative CT method. *Nat. Protoc.* **3**, 1101–1108.

Schoppmeier, M. and Damen, W. G. M. (2001). Double-stranded RNA interference in the spider Cupiennius salei: The role of Distal-less is evolutionarily conserved in arthropod appendage formation. *Dev. Genes Evol.* **211**, 76–82.

Schröder, R. (2003). The genes orthodenticle and hunchback substitute for bicoid in the beetle Tribolium. *Nature* **422**, 621–625.

Schultz Richard M (2002). The molecular foundations of the maternal to zygotic transition in the preimplantation embryo. *Hum. Reprod. Update* **8**, 323–331.

Shubin, N., Tabin, C. and Carroll, S. (1997). Fossils, genes and the evolution of animal limbs. *Nature* **388**, 639–648.

Shvartsman, S. Y., Coppey, M. and Berezhkovskii, A. M. (2008). Dynamics of maternal morphogen gradients in the Drosophila embryo. *Curr. Opin. Genet. Dev.* **18**, doi: 10.1016/j.gde.2008.06.002.

Siegfried, E., Chou, T.-B. and Perrimon, N. (1992). wingless signaling acts through zeste-white 3, the Drosophila homolog of glycogen synthase kinase-3, to regulate engrailed and establish cell fate. *Cell* **71**, 1167–1179.

Siemanowski, J., Richter, T., Dao, V. A. and Bucher, G. (2015). Notch signaling induces cell proliferation in the labrum in a regulatory network different from the thoracic legs. *Dev. Biol.* **408**, 164–177.

Simcox, A. A., Wurst, G., Hersperger, E. and Shearn, A. (1987). The defective dorsal discs gene of Drosophila is required for the growth of specific imaginal discs. *Dev. Biol.* **122**, 559–567.

Simcox, A. A., Roberts, I. J. H., Hersperger, E., Clare Gribbin, M., Shearn, A., Robert, J. and Whittle, S. (1989). Imaginal discs can be recovered from cultured embryos mutant for the segment-polarity genes engrailed, naked and patched but not from wingless. *Development* **107**, 715–722.

Sinadinos, C., Valles-Ortega, J., Boulan, L., Solsona, E., Tevy, M. F., Marquez, M., Duran, J., Lopez-Iglesias, C., Calbó, J., Blasco, E., et al. (2014). Neuronal glycogen synthesis contributes to physiological aging. *Aging Cell* **13**, 935–945.

Singh, B. N., Doyle, M. J., Weaver, C. V, Koyano-Nakagawa, N. and Garry, D. J. (2012). Hedgehog and Wnt coordinate signaling in myogenic progenitors and

regulate limb regeneration. *Dev. Biol.* **371**, 23–34.

Sokoloff, A., Slatis, H. M. and Stanley, J. (1960). The black mutation in tribolium castaneum. *J. Hered.* **51**, 131–135.

Swarup, S. and Verheyen, E. M. (2012). Wnt/Wingless signaling in Drosophila. *Cold Spring Harb. Perspect. Biol.* **4**, 1–15.

Tabata, E. and Takei, Y. (2004). Morphogens, their identification and regulation. *Development* **131**, 703–712.

Tadros, W. and Lipshitz, H. D. (2005). Setting the stage for development: mRNA translation and stability during oocyte maturation and egg activation in Drosophila. *Dev. Dyn.* **232**, 593–608.

Tamura, K., Stecher, G., Peterson, D., Filipski, A. and Kumar, S. (2013). MEGA6: Molecular evolutionary genetics analysis version 6.0. *Mol. Biol. Evol.* **30**, 2725–2729.

Tay, S. K. H., Akman, H. O., Chung, W. K., Pike, M. G., Muntoni, F., Hays, A. P., Shanske, S., Valberg, S. J., Mickelson, J. R., Tanji, K., et al. (2004). Fatal infantile neuromuscular presentation of glycogen storage disease type IV. *Neuromuscul. Disord.* **14**, 253–260.

Theisen, H., Purcell, J., Bennett, M., Kansagara, D., Syed, A. and Marsh, J. L. (1994). Dishevelled is required during wingless signaling to establish both cell polarity and cell identity. *Development* **120**, 347–360.

Tu, R., Duan, B., Song, X. and Xie, T. (2020). Dlp-mediated Hh and Wnt signaling interdependence is critical in the niche for germline stem cell progeny differentiation. *Sci. Adv.* **6**, doi: 10.1126/sciadv.aaz0480.

Varjosalo, M., Li, S. P. and Taipale, J. (2006). Divergence of hedgehog signal transduction mechanism between Drosophila and mammals. *Dev. Cell* **10**, 177–186.

Veraksa, A., McGinnis, N., Li, X., Mohler, J. and McGinnis, W. (2000). Cap ‘n’ collar B cooperates with a small Maf subunit to specify pharyngeal development and suppress deformed homeotic function in the Drosophila head. *Development* **127**, 4023–4037.

Vilchez, D., Ros, S., Cifuentes, D., Pujadas, L., Vallès, J., García-Fojeda, B., Criado-García, O., Fernández-Sánchez, E., Medraño-Fernández, I., Domínguez, J., et al. (2007). Mechanism suppressing glycogen synthesis in neurons and its demise in progressive myoclonus epilepsy. *Nat. Neurosci.* **10**, 1407–1413.

Vincent, J.-P. and O'Farrell, P. H. (1992). The state of engrailed expression is not clonally transmitted during early Drosophila development. *Cell* **68**, 923–931.

Vital, W., Rezende, G. L., Abreu, L., Moraes, J., Lemos, F. J., Vaz, I. D. S. and Logullo, C. (2010). Germ band retraction as a landmark in glucose metabolism during Aedes aegypti embryogenesis. *BMC Dev. Biol.* **10**, doi: 10.1186/1471-213X-10-25.

Wohlfrom, H., Schinko, J. B., Klingler, M. and Bucher, G. (2006). Maintenance of segment and appendage primordia by the Tribolium gene knödel. *Mech. Dev.* **123**, 430–439.

Woodgett, J. R. (1990). Molecular cloning and expression of glycogen synthase kinase-3/Factor A. *EMBO J.* **9**, DOI:10.1002/j.1460-2075.1990.tb07419.x.

Woodgett, J. R. and Cohen, P. (1984). Multisite phosphorylation of glycogen synthase. Molecular basis for the substrate specificity of glycogen synthease kinase-3 and casein kinase-II (glycogen synthase kinase-5). *Biochim. Biophys. Acta (BBA)/Protein Struct. Mol.* **788**, 339–347.

Wu, D. and Pan, W. (2010). GSK3: a multifaceted kinase in Wnt signaling. *Trends Biochem. Sci.* **35**, doi: 10.1016/j.tibs.2009.10.002.

Yamada, T., Habara, O., Yoshii, Y., Matsushita, R., Kubo, H., Nojima, Y. and Nishimura, T. (2019). The role of glycogen in development and adult fitness in Drosophila. *Dev.* **146**, doi: 10.1242/dev.176149.

Yamaguchi, T. P. (2001). Heads or tails: Wnts and anterior-posterior patterning. *Curr. Biol.* **11**, R713–R724.

Yoon, Y., Klomp, J., Martin-Martin, I., Criscione, F., Calvo, E., Ribeiro, J. and Schmidt-Ott, U. (2019). Embryo polarity in moth flies and mosquitoes relies on distinct old genes with localized transcript isoforms. *Elife* **8**, doi:

10.7554/eLife.46711.

Zheng, L. and Conner, S. D. (2018). Glycogen synthase kinase 3β inhibition enhances Notch1 recycling. *Mol. Biol. Cell* **29**, 385–395.

Zhu, X., Zhu, H., Zhang, L., Huang, S., Cao, J., Ma, G., Feng, G., He, L., Yang, Y. and Guo, X. (2012). Wls-mediated Wnts differentially regulate distal limb patterning and tissue morphogenesis. *Dev. Biol.* **365**, 328–338.

7 Appendix

7.1 Abbreviations

GlyS/GS	*Glycogen synthase*
HK	Hexokinase
AGBE	*1,4-Alpha-Glucan Branching Enzyme*
Bcd	Bicoid
Hb	Hunchback
Nos	Nanos
Cad	Caudal
otd	*orthodenticle*
en	*engrailed*
hh	*hedgehog*
ci	*cubitus interruptus*
gsb	*gooseberry*
smo	*smoothened*
fu	*fused*
arm	*armadillo*
dsh	*disheveled*
proc	*porcupine*
sgg/zw3	*shaggy/zeste-white 3*
arr	*arrow*
pan	*pangolin*
wls	*wntless*
Ptc	Patched
Dll	*Distalless*
dac	*dachshund*
fz1	*frizzled-1*
al	*aristaless*
B	*Bar*
rn	*rotund*
Vn	Vein
Spi	Spitz

eve	*even-skipped*
Cnc	*cap 'n' collar*
wg	*wingless*
dpp	*decapentaplegic*
Dfd	*Deformed*
A-P	Anterior-Posterior
D-V	Dorsal-Ventral
P-D	Proximal-Distal
FGF	Fibroblast Growth Factor
SB	*San Berndardino*
pBA-19	*Pig-19*
IP	Injection Puffer
ISH	In situ Hybridization
NBT	Nitro Blue Tetrazolium
BCIP	5-Bromo-4-chloro-3-indolyl Phosphate
TSA	Tyramide Signal Amplification
qRT-PCR	Quantitative Real-time PCR
Lr	Labrum
Vt	Vertex triplet
At	Antenna
Md	Mandible
Mx	Maxilla
Lab	Labium
Ab	Abdomen
Uro	Urogomphi
Pygo	Pygopods
oc	ocular segment
Dcp-1	*Drosophila* caspase-1
MZT	Maternal-zygotic Transition
ZGA	Zygotic Genome Activation
Wt	Wildtype

7.2 Primer sequences

Table S7.1 Gene specific primers

Gene Name (Tc_ No.)	Primer ID	Sequence	Purpose
Tc-GlyS (TC015651)	iBeetle_Fw	TCCGGCGGTGTAATTTATTC	dsRNA
Tc-GlyS (TC015651)	iBeetle_Rv	AAGTCGCGATACCATTGTCC	dsRNA
Tc-GlyS (TC015651)	Non-overlapping_Fw	TGGACGCAAAAGTTCGGTTT	dsRNA/in situ probe
Tc-GlyS (TC015651)	Non-overlapping_Rv	CGTGGACTTGAGGTAGTGGT	dsRNA/in situ probe
Tc-GlyS (TC015651)	Fw_1	ACAGTGTCGGATATTACAGGCTT	qPCR
Tc-GlyS (TC015651)	Rv_1	AATTCGTGCAAGGCGGAGA	qPCR
Tc-GlyS (TC015651)	Fw_2	GGGCCCCTAGGTTCGGA	qPCR
Tc-GlyS (TC015651)	Rv_2	GGATTCCCATCGACAAGCCA	qPCR
Tc-AGBE (TC004619)	iBeetle_Fw	ACGTCCAGCCAGACAACAC	dsRNA
Tc-AGBE (TC004619)	iBeetle_Rv	TATGCGTGCTCCATTATTGC	dsRNA
Tc-AGBE (TC004619)	Non-overlapping_Fw	ACACCCGAACAACTGAAACG	dsRNA/in situ probe
Tc-AGBE (TC004619)	Non-overlapping_Rv	TCTCCTCCCGCAGAAACTTT	dsRNA/in situ probe
Tc-AGBE (TC004619)	Fw_1	CCCGCCAAACTCAGAGAAGT	qPCR
Tc-AGBE (TC004619)	Rv_1	ACTTTCAGTTCAGACGTGGCT	qPCR
Tc-AGBE (TC004619)	Fw_2	AGGAAATCCGTCGCCGATATG	qPCR
Tc-AGBE (TC004619)	Rv_2	ACCCTTGGGTGAAACTGTCC	qPCR
Arrow (TC008151)	Fw	CGCAATCACTCCTGTTCTCA	dsRNA
Arrow (TC008151)	Rv	GTTTTGGTTGCATCGGACTT	dsRNA

Table S7.2 General gene primers

Primer Name	Sequence	Purpose
pJET_Fw_T7	GAATTGTAATACGACTCACTATAGGCGACT CACTATAGGGAGAGC	dsRNA Template synthesis
pJET_Rv_T7	GAATTGTAATACGACTCACTATAGGAAGAA CATCGATTTTCCATG	dsRNA Template synthesis
T7	GAATTGTAATACGACTCACTATAGG	dsRNA Template synthesis
T7-SP6	TAATACGACTCACTATAGGATTTAGGTGAC ACTATAGA	dsRNA Template synthesis
*RPS3.3*_Fw	AGGGTGTGCTGGGAATTAAAG	normalization for qPCR
*RPS3.3*_Rv	GGGTAGGCAGGCAAAATCTC	normalization for qPCR
*GAPDH3*_Fw	CGTTTCCGTTGTGGATTTGAC	normalization for qPCR
*GAPDH3*_Rv	AACGACCTCTTCCTCCGTGTA	normalization for qPCR

Table S7.3 Plasmids for dsRNA synthesis

Plasmid	Sense	Anti-sense	Size	Purpose
Tc-GlyS-pJET1.2-XW	pJET_FwT7	pJET_RvT7	513bp	dsRNA
Tc-AGBE-pJET1.2-XW	pJET_FwT7	pJET_RvT7	511bp	dsRNA
Tc-Arrow-pJET1.2-XW	pJET_FwT7	pJET_RvT7	652bp	dsRNA
Tc-Pangolin-pJET1.2-SA	pJET_FwT7	pJET_RvT7	385bp	dsRNA
dsRed-pDsRed-NH	T7	SP6-T7	896bp	dsRNA
Tc-Hedgehog-pCRII-EN	T7	SP6-T7	1148bp	dsRNA

7.3 Vector maps

Pjet1.2 vector was used as the PCR template for dsRNA and probes synthesis of *Tc-GlyS* and *Tc-AGBE*. Vectors cloned by *iBeetle* fragments of both genes were showed in (Fig S7.1 A & B).

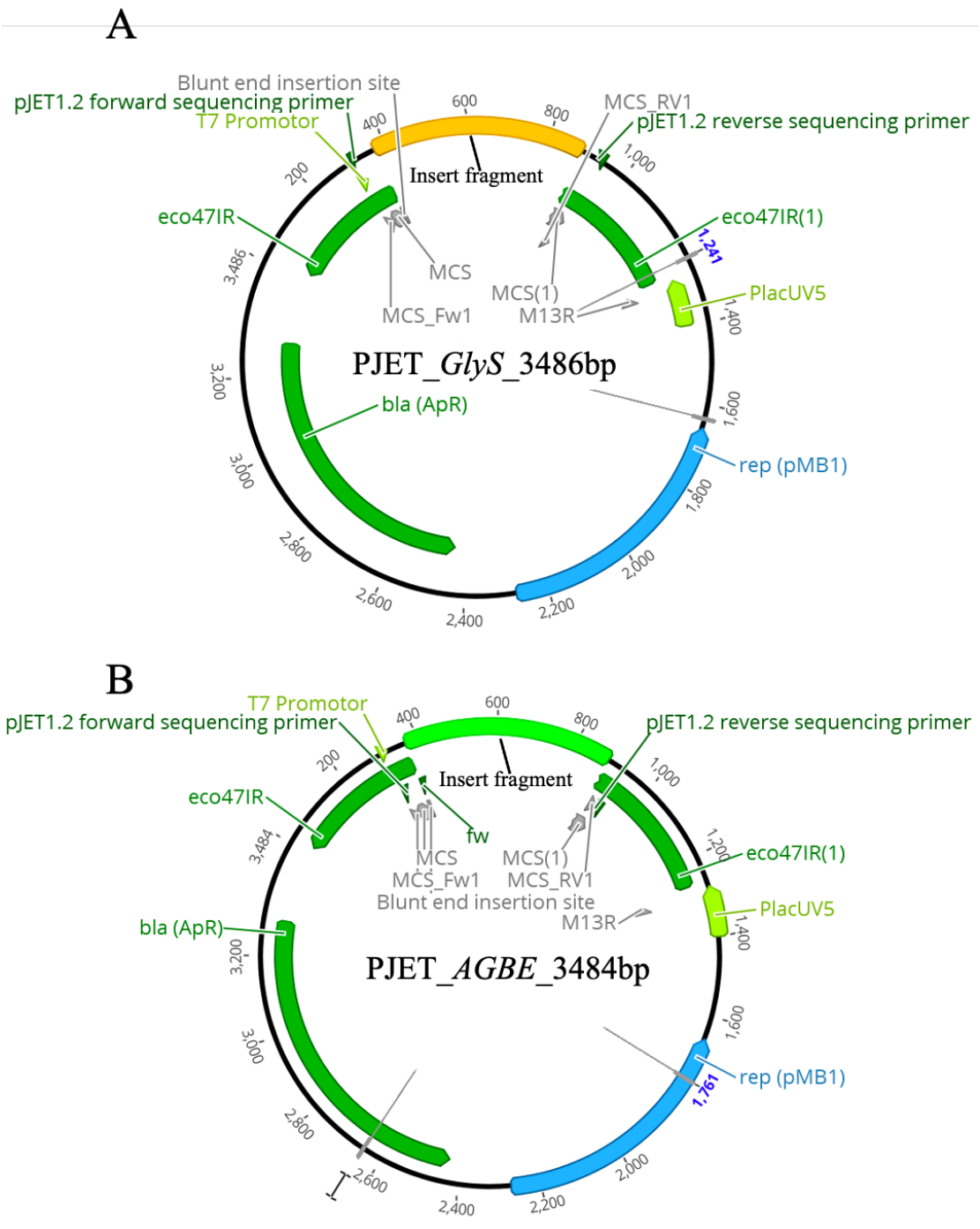

Figure S7.1 Vector maps of *Tc-GlyS* and *Tc-AGBE*.

(A & B) Recombined pJET1.2 blunt vectors contained 513bp of *Tc-GlyS* and 511bp of *Tc-AGBE*, respectively.

7.4 The absence of labrum caused by depletion of *Tc-GlyS* and *Tc-AGBE*

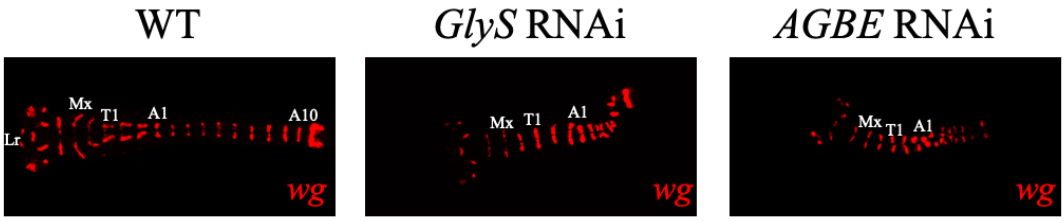

Figure S7.2 Labrum was absent in *Tc-GlyS* and *Tc-AGBE* strong RNAi embryos.

Mx (Maxilla); T1 (first thoracic segment); A1, A10 (first, 10th abdominal segment).

7.5 Apoptotic cells of growth zone in *Tc-GlyS*/*Tc-AGBE* RNAi embryos

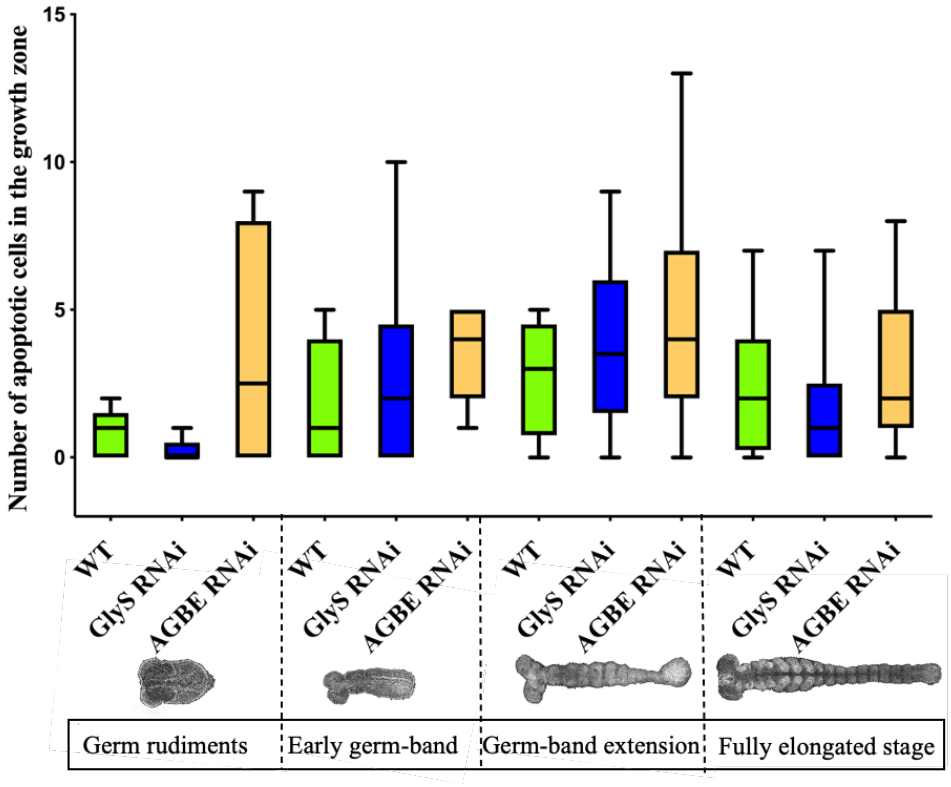

Figure S7.3 Cell apoptosis in growth zone region after knockdown of *Tc-GlyS*/*Tc-AGBE*.

Box plots were constructed to visualize the distribution of the cell apoptotic values at four development stages. The number of apoptotic cells in RNAi embryos showed no difference compared with wt embryos.

7.6 Candidate genes from screening

Table S7.4 Head genes during the screen

ID-number	Tc-number	Screen annotation (Partially)
IB_06502	TC032115	Size of head capsule decreased; antenna/labrum not present (50-80%)
IB_06626	TC031568	Size of head capsule decreased (50-80%)
IB_13872	TC002145	Size of head capsule decreased (50-80%)
IB_14403	TC010707	Size of head capsule decreased; labrum/antenna not present (30-50%)
IB_06502	TC032115	Antenna/labrum not present; size of head capsule decreased (50-80%)
IB_13007	TC015977	Labrum transform to maxillae (>80%)
IB_13206	TC031155	Antenna/labrum not present (>80%)
IB_13594	TC000638	Labrum not present (50-80%)
IB_13619	TC005085	Head appendages not present; labrum irregular (30-50%)
IB_13872	TC002145	Size of head capsule decreased; head appendages not present (50-80%)
IB_14403	TC010707	Head appendages not present; size of head capsule decreased (50-80%)
IB_14792	TC030404	Labrum not present (50-80)
IB_14602	TC013757	labrum not present (30-50%), empty eggs (50-80%)
IB_14864	TC031249	Labrum not present (50-80%)
IB_15102	TC033045	Antenna and labrum not present; abdomen decreased (50-80%)
IB_15172	TC033625	Labrum not present (30-50%)
IB_15175	TC033669	Labrum and antenna not present (50-80%)
IB_15290	TC034207	Labrum and antenna not present (50-80%)
IB_15349	TC034660	Labrum not present (50-80%)
IB_15350	TC034664	Labrum and antenna not present (50-80%)
IB_15365	TC034715	Labrum and antenna not present; vertex triplet not present (50-80%)
IB_15774	TC031123	Labrum not present (50-80%)
IB_15788	TC002104	Labrum and antenna not present (50-80%)
IB_07127	TC007674	Position of vertex triplet irregular (30-50%),
IB_12344	TC007752	Head bristle irregular; shape/size of head capsule irregular (30-50%)
IB_14083	TC005730	Vertex triplet not present; antenna/labrum not present (30-50%)

Table S7.5 Leg candidate genes from the screening

ID-number	Tc-number	Screen annotation (Partially)
IB_09187	TC009351	Legs segment not present; size/shape of legs irregular (50-80%)
IB_10325	TC013293	Legs, antenna irregular; size of head/thorax decreased (50-80%)
IB_12148	TC004669	Legs segment distal irregular (50-80%)
IB_12332	TC007631	Legs segment irregular; legs distal not present (50-80)
IB_12787	TC013313	Number of legs decreased (>80%)
IB_12805	TC013402	Legs swollen; head appendages not present (50-80%)
IB_13568	TC034761	Number of legs increased; abdomen decreased (50-80%)
IB_14355	TC009922	Coxa of legs swollen (>80%)
IB_14698	TC015169	Number of legs decreased (50-80%)
IB_14657	TC014619	Number of legs decreased (50-80%)
IB_14288	TC008718	Thorax and abdomen bent; legs tibiotarsus fused (50-80)
IB_15071	TC032880	Number of legs decreased (50-80%)
IB_14871	TC031274	Number of legs decreased (50-80%)
IB_15345	TC034646	Number of legs decreased (50-80%)
IB_15557	TC031047	Femur and tibiotarsus of legs not present (50-80%)
IB_15809	TC013901	Number of legs decreased (50-80%)
IB_14640	TC014411	Number of legs decreased (50-80%)

Table S7.6 Abdomen candidate genes list

ID-number	Tc-number	Screen annotation (Partially)
IB_07886	TC000385	Abdominal segments decreased (50-80%)
IB_07991	TC000077	Abdominal segments decreased (50-80%)
IB_09072	TC014104	Abdominal segments decreased (50-80%)
IB_12101	TC002465	Abdominal segments decreased (50-80%)
IB_13285	TC032057	Abdominal segments decreased (50-80%)
IB_13310	TC032284	Abdominal segments decreased (>80%)
IB_13568	TC034761	Abdominal segments decreased; number of legs increased (50-80%)
IB_14257	TC008416	Abdominal segments decreased (50-80%)
IB_14288	TC008718	Thorax & abdomen segment bent (50-80%)
IB_14638	TC014367	Abdominal segments decreased (50-80%)
IB_14924	TC031643	Abdominal segments decreased (50-80%)
IB_15102	TC033045	Abdominal segments decreased; head appendages not present (50-80%)
IB_06639	TC008565	Terminus of abdomen irregular; size of pygopods decreased (50-80%)
IB_15354	TC034673	Abdominal segments decreased (50-80%)
IB_15523	TC000139	Abdominal segments decreased (50-80%)
IB_15557	TC031047	Femur and tibiotarsus not present; abdomen decreased (50-80%)
IB_15685	TC032200	Abdominal segments decreased (50-80%)